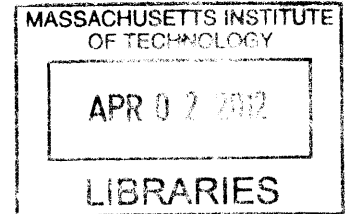# Engineering a Single Cell Microarray Platform
for High Throughput
DNA Damage and Repair Analysis

by

David McGregor Weingeist

B.S., Washington University in St. Louis (2005)
M.Phil., University of Cambridge (2006)

Submitted to the Department of Biological Engineering
in partial fulfillment of the requirements for the degree of

Doctor of Philosophy

at the

MASSACHUSETTS INSTITUTE OF TECHNOLOGY

February 2012

© David McGregor Weingeist, MMXII. All rights reserved.

Author . . .
Department of Biological Engineering
September 15, 2011
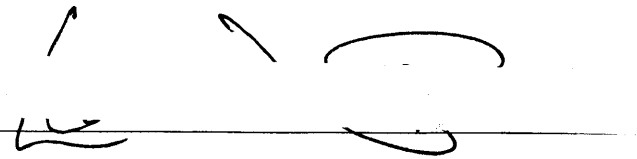
Certified by.
Bevin P. Engelward
Associate Professor
Thesis Supervisor
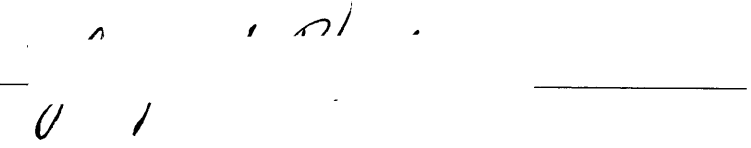
Accepted by
Forest M. White
Chairman, Department Committee on Graduate Theses

This doctoral thesis has been examined by a committee of the Department of Biological Engineering as follows:

Professor Leona D. Samson _____

Committee Chair

Professor Bevin P. Engelward _____

Thesis Supervisor

Professor Sangeeta N. Bhatia _____

Dedicated to my loving parents,

Dr. Thomas and Catherine Weingeist.

Thank you for everything.

Preface

The work described herein was accomplished through collaboration with many talented, hardworking individuals from MIT and beyond. I am extremely grateful for their contributions, guidance, and encouragement. I am especially thankful to Dr. Bevin Engelward and the extraordinary members of her lab, both past and present. Much of this work was done as a joint effort with Dr. Sangeeta N. Bhatia, and I am forever appreciative of the collaboration, mentorship, and friendship of Dr. David K. Wood from her Laboratory of Multiscale Regenerative Technologies.

Chapter II was published in *Proceedings of the National Academy of Sciences* in May of 2010. Initiation of the project was completed by the author as well as James Mutamba and Sukant Mittal. The development of the high throughput assay for analyzing DNA damage and repair and the collection of the published data was done in collaboration with Dr. David K. Wood from the Laboratory of Dr. Sangeeta N. Bhatia. Support with radiation was provided by Dwight Chambers and Dr. Jacquelyn C. Yanch with guidance from Deying Sun, Bob Kirby, and others at MIT Environmental Health Science. I would also like to acknowledge Laura Trudel for her help with culturing TK6 lymphoblastoid cells. Lastly, assistance with microfabrication was provided by Kurt Broderick and others from the MIT Microsystems Technology Laboratory.

Chapter III, while unpublished at the time of writing, represents the combined efforts of several individuals. Somsak Prasongtanakij performed the H_2O_2, MMS, and MNNG experiments. I would like to acknowledge the generosity and support of everyone at the Chulabhorn Research Institute in Thailand, especially Dr. Mathuros Ruchirawat and Dr. Panida Navasumrit. Dr. Robert Sobol from the University of Pittsburgh generously provided glioblastoma cell lines with differential base excision repair capacities. Chinese hamster ovary (CHO) cells were kindly gifted by Dr. Larry Thompson. Adebanke Fagbemin from the Laboratory of Dr. Orlando Schärer helped

to initiate the nucleotide excision repair project. Experiments involving 4NQO were conducted with support from Patrizia Mazzucato. All other data were generated by the author.

At the time of writing, Chapter IV had been drafted as a manuscript for submission. The project was initiated by the author with technical support from Dwight Chambers. The gamma-H2AX assay was conducted by Dr. Scott Floyd from the Laboratory of Dr. Michael Yaffe. IRS-20 CHO cells were a kind gift from Dr. Joel Bedford from Colorado State University. All other CHO cells were kindly provided by Dr. Larry Thompson. A Western blot to confirm the genotype of XRS-6 CHO cells was performed by James Mutamba. Dr. Aprotim Mazumder from the Laboratory of Professor Mark Bathe was incredibly patient while teaching us to use the Cellomics imaging platform provided by the MIT Center for Environmental Health Science. All other data were collected by the author with technical support from undergraduate researcher, Elizabeth Rowland.

Acknowledgments

First, I would like to thank the Department of Biological Engineering, under the leadership of Professor Doug Lauffenburger, for giving me the opportunity to pursue cutting edge research in a nurturing environment among the world's most talented and brightest scientists. It is with utmost sincerity and admiration that I thank my advisor, Professor Bevin P. Engelward, for her extraordinary guidance and support. She provided me every opportunity to develop scientifically, to travel and collaborate, and mature professionally, inspiring me at every step with her infectious optimism and rigorous pursuit of knowledge. Above all, she has instilled in me great patience and a deep rooted belief that you truly can achieve anything to which you passionately devote your mind and energy. I feel privileged to have worked under her direction and will take her global awareness and ability to lead through compassion with me wherever I go.

I would also like to thank the other members of my thesis committee: Professors Leona D. Samson and Sangeeta N. Bhatia. As chair of my committee, Leona generously shared her wisdom and expertise in the field of DNA damage and repair. She set high scientific standards, always challenging me to develop further as a biologist. Sangeeta provided invaluable technical insight and continues to inspire me with her ability to elegantly solve any problem with efficiency and composure.

I would also like to thank all of the former and current members of the Engelward Team, including Kathy Reposa, who is always cheerful and willing to help. Thank you to Dr. Dominika Wiktor-Brown, Dr. Werner Olipitz, Dr. Rebecca Rugo, and Dr. Yoon Sung Nam for welcoming me into the lab and showing me the way. Thank you to Dr. David "T-bone" Wood, Dr. James Mutamba, Dr. Orsolya Kiraly, Michelle Sukup-Jackson, Somsak "Tong" Prasongtanakij, Jing Ge, Dwight Chambers, Marcus Parrish, and Patrizia Mazzucato for creating a fun and collaborative environment to learn, grow, and do science. Their insights, encouragement, and generosity made all

6

the difference. I will miss working with you, but know that we will always remain friends. Lastly, thank you to the many UROPs who humbled me with their sharp intellect and inspired me with their youthful enthusiasm. They taught me to be patient by being patient with me. They taught me to be a leader by trusting me to lead. Together we persevered and accomplished a lot along the way. Thank you especially to Saja A. Fakhraldeen, Aline Thomas, Yunji Wu, Margaret A. Wangeline, Jeffrey Quinn, Kelly Schulte, Jie-Yoon Yang, and Elizabeth Rowland.

Most of all, thank you to my family. I am forever in debt to my loving parents for instilling in me a thirst for knowledge, for encouraging me to follow my dreams, for providing me every opportunity to succeed, for giving me the independence and confidence to explore, and for supporting and loving me unconditionally. I love you both so much! Also big thanks to my siblings, Rachel and Aaron, for paving the way, setting examples of the fulfilling life I am striving to achieve. And thanks to my brother, Rob, for literally standing by my side each and every day. Love you, man. I only see things getting better and better.

Engineering a Single Cell Microarray Platform

for High Throughput

DNA Damage and Repair Analysis

by

David McGregor Weingeist

Submitted to the Department of Biological Engineering
on September 15, 2011, in partial fulfillment of the
requirements for the degree of
Doctor of Philosophy

Abstract

DNA damage contributes to cancer, aging, and heritable diseases. Ironically, DNA damaging agents are also commonly used in current cancer treatment. We therefore need robust, high throughput, and inexpensive tools for objective, quantitative DNA damage analysis. The single cell gel electrophoresis (comet) assay has become a standard method for DNA damage analysis, however, it is not well suited for use in clinical and epidemiological settings due to issues of low throughput, poor reproducibility, and a laborious image analysis requirement. To overcome these limitations, we applied microfabrication techniques to engineer an arrayed cell comet platform that maximizes the number of analyzable cells and provides spatial encoding for automated imaging and analysis. Additionally, we developed complementary software that eliminates the inherent bias of manual analysis by automatically selecting comets from the defined array. In its 96-well format, the so-called CometChip integrates with high throughput screening technologies, further increasing throughput and removing user error. This improved approach enables multiple cell types, chemical conditions, and repair time points to be assayed in a single gel with improved reproducibility and processing speed, while maintaining the simple protocol and versatility of the comet assay to assess a wide range of DNA damage. Using the CometChip, we evaluated a variety of DNA damaging agents, revealing repair profiles that can be used to gain insight into biological mechanisms of damage sensitivities. We confirmed the ability of the CometChip to identify deficiencies in four major DNA repair pathways, supporting the use of the assay in determining pathway sensitivities that may be useful in guiding treatment strategies that more selectively target cancerous cells and reduce side-effects. We also used the platform to evaluate potential inhibitors of DNA repair, which are emerging as promising adjuvants in cancer management. Taken together, the CometChip enables high throughput genotoxic evaluation of chemical exposures, discovery of novel chemotherapeutic strategies, and measurement of DNA repair kinetics for identification of susceptible populations and disease prevention.

The CometChip is a significant advancement in DNA damage and repair technology, providing high throughput, objective, and quantitative measurements that have the potential to become a new standard in DNA damage analysis.

Thesis Supervisor: Bevin P. Engelward
Title: Associate Professor

Contents

13

List of Figures

List of Abbreviations

4NQO	4-Nitroquinoline 1-oxide
5′dRP	5′ deoxyribose-5-phosphate
AAG	Alkyladenine DNA glycosylase
AP	Apurinic/apyrimidinic
APE	Apurinic/apyrimidinic endonuclease
ATM	Ataxia telangiectasia mutated
BER	Base excision repair
bp	base pairs
BrdU	Bromodeoxyuridine
CA	Chromosomal aberration
CHO	Chinese hamster ovary
CV	Coefficient of variance
DMEM	Dulbecco's modified eagle medium
DMSO	Dimethyl sulfoxide

DNA	Deoxyribonucleic acid
DNA-PK	DNA-dependent protein kinase
DNA-PKcs	DNA-dependent protein kinase catalytic subunit
DOPA	6-hydroxy-DL-DOPA
FBS	Fetal bovine serum
FDA	Food and Drug Administration
H_2O_2	Hydrogen peroxide
HR	Homologous recombination
HT	High throughput
HTS	High throughput screening
ICL	Interstrand crosslink
ICLR	Interstrand crosslink repair
IR	Ionizing radiation
IWGT	International Workshop of Genotoxicity Testing
KD	Knocked-down

MGMT	0^6-methylguanine methyl-transferase
MMEJ	Microhomology-mediated end joining
MMS	Methyl methanesulfonate
MNNG	N-methyl-N'-nitro-N-nitrosoguanidine
mTOR	Mammalian target of rapamycin
MYR	Myricetin
NCA	7-nitro-1H-indole-2-carboxylic acid
NER	Nucleotide excision repair
NHEJ	Non-homologous end joining
NM	Nitrogen mustard
OE	Over-expressed
OGG1	8-Oxoguanine glycosylase
PBS	Phosphate buffered saline
PDMS	Polydimethylsiloxane
PFGE	Pulsed-field gel electrophoresis

PI3K	Phosphatidylinositol 3-kinase
PI3KK	Phosphoinositide 3-kinase related kinases
PolβB	Polymerase beta
SCE	Sister chromatid exchange
SSB	Single strand break
UDS	Unscheduled DNA synthesis
UV	Ultraviolet
XP	Xeroderma Pigmentosum

Chapter 1

Introduction

DNA damage promotes cancers, aging, neurological disorders and heritable diseases [1]. Unfortunately, exposure to genotoxins is unavoidable, as cells are continuously exposed to inflammatory chemicals, reactive byproducts of metabolism, adverse heat and pH, mechanical stress, exogenous chemicals, radiation, and other agents that damage DNA through formation of base lesions, crosslinks, and strand breaks. These lesions interfere with transcription and replication and can lead to mutations that can alter protein function and gene regulation, thus potentially disrupting critical cellular processes. To protect the genome from these deleterious effects, cells have evolved a complex network of coordinated DNA repair pathways, each having specificity for a subclass of DNA damage [2]. Imbalances in these pathways can allow cells to accumulate mutations that drive carcinogenesis through promotion of selective advantages such as unregulated cell growth [3]. This excessive cell division makes cancer cells especially vulnerable to DNA damaging agents, thus providing the basis for the frontline therapeutic strategies of radio- and chemotherapy [4, 5]. The study of DNA damage is therefore important in understanding mechanisms of disease, identifying harmful exposures, mitigating risk to susceptible populations, and guiding treatment strategies; however, there has been minimal improvement made to methods of DNA damage analysis in the past two decades. Available tools are limited in throughput and reproducibility, their range of DNA lesion detection, and their capacity to measure both DNA damage and repair in a variety of cell types. We overcame these

limitations by applying microfabrication techniques to engineer a high throughput platform for measurement of the integrated DNA damage response that is useful in both a variety of clinical and research settings.

1.1   Cancer

The World Health Organization lists cancer as the leading cause of global mortality, with an estimated 8 million deaths and nearly 13 million new cases diagnosed each year [6]. Cancer is a large, heterogeneous class of disease states that results from the accumulation of heritable modifications in tumor suppressor genes and oncogenes that promote phenotypic evolution by providing cancerous cells with a selective advantage to dominate local tissue through clonal expansion [3]. It is now well established that mutations that effect proteins involved in the many pathways of DNA repair are critical to carcinogenesis, as they promote mutagenesis through genomic instability [7]. Carcinogenesis describes the multi-stage succession of clonal expansions in which cells acquire traits that enable them to become immortal, grow uncontrollably, evading cell cycle checkpoints and apoptotic signaling, form tumors with their own blood vessel networks, evade immune responses, colonize surrounding normal tissue, and finally infiltrate the bloodstream and metastasize [8].

Although some single-nucleotide polymorphisms in oncogenes and tumor suppressor genes have been shown to increase susceptibility, the promotion and rapid progression of 95% of cancers is thought to be the consequence of environmental factors rather than genetic predisposition [9]. More than a quarter of cancer deaths involve the use of tobacco, another third are related to diet and lifestyle, and as much as a fifth are attributed to infections [10]. The remaining cases stem from exposures to environmental pollutants and radiation. The carcinogenicity of these agents is derived from their ability to both damage DNA and create mico-environments that promote proliferation and provide selective advantages to evolving tumor cells. For example, cigarette smoke contains over 4,000 chemicals, many of which damage DNA (e.g. formaldehyde, arsenic, etc.), but also elicits an inflammatory response, which

may advance carcinogenesis through the production of reactive oxygen species and activation of survival signaling cascades that promote cellular growth and transformation [11]. A deep understanding of both exogenous and endogenous sources of DNA damage is therefore critical in evaluating the effects and carcinogenic potential of environmental exposures.

DNA damage is also an important mechanism in cancer therapy. The uncontrolled, rapid proliferation of cancer cells makes them sensitive to compounds that are mutagenic or interfere with cell cycle progression [2]. This will be discussed in greater detail in *Section 1.3* once the context of DNA repair and its role in genomic stability and cancer resistance is established.

1.2 DNA Repair

In response to DNA damage, cells maintain genomic integrity by initiating complex responses, including the recruitment of DNA repair proteins, which can be grouped according to the DNA lesions they repair. The four major pathways that are most relevant to the aims of this thesis are: 1) base excision repair (BER), 2) nucleotide excision repair (NER), 3) interstrand crosslink (ICL) repair (ICLR), and 4) non-homologous end joining (NHEJ). Other mechanisms exist and continue to be discovered, including homologous recombination (HR), direct reversal, mismatch repair (MMR), and microhomology mediated end joining (MMEJ). Knowledge of these repair mechanisms and the specific proteins involved is important for predicting the consequences of genotoxic exposures, evaluating cancer susceptibilities, diagnosing heritable disease, revealing sources of tumor resistance, identifying drug targets, and developing novel treatment strategies. To develop an assay that is specific enough to detect subtle deficiencies in DNA repair, but general enough to be useful in a variety of applications, a comprehensive understanding of DNA repair is required. Here, an overview of BER, NER, ICLR, and NHEJ is provided.

1.2.1 Base Excision Repair

It is estimated that the BER pathway is utilized over 10,000 times per cell per day in order to service the endogenous nucleotide lesion burden [12]. BER targets small chemical alterations of bases (e.g. deamination, oxidation, alkylation) that can interfere with transcription or replication, or contribute to mutagenesis through nucleotide mispairing. While the DNA damage itself can be problematic, removal of such aberrant bases also leads to potentially dangerous repair intermediates, such as single strand breaks (SSBs), which are toxic if not repaired efficiently by downstream BER [13, 14, 15, 16]. Polymorphisms in such proteins have been linked to increased cancer susceptibility [17], indicating that even subtle imbalances in DNA repair have important implications regarding genomic stability. Indeed, deficiencies in proteins from all stages of the BER pathway have been linked to carcinogenesis [18, 19, 20].

One of the core aims of this project is to develop better ways of monitoring BER and of testing the impact of BER proteins on repair kinetics. BER involves over a dozen proteins and is initiated by lesion-specific DNA glycosylases that identify and cleave the N-glycosyl bonds of improper bases to generate apurinic/apyrimidinic (AP) sites [21]. Glycosylases are either monofunctional, removing only the nucleotide base, or bifunctional, possessing both glycosylase activity and the ability to cleave the DNA backbone 3' to the resulting AP site [22]. AP sites also frequently result from spontaneous hydrolysis [23, 24]. For monofunctional glycosylase initiated repair (Figure 1-1), the AP lyase activity is performed by an AP Endonuclease (APE) [25]. In mammalian cells, APE-1 is the sole endonuclease responsible for nicking the phosphodiester backbone to generate a free 3'OH on the normal nucleotide and a 5' deoxyribose phosphate (5'dRP) blocking terminus on the abasic site [26]. The resulting SSB can be processed by either short-patch BER, which replaces only the aberrant nucleotide, or long-patch BER, which replaces 2-10 bases from the damaged DNA strand [27]. For the sake of brevity, only the short patch BER pathway will be discussed in detail. Polymerase beta (Polβ) is responsible for the rate-limiting removal of the 5'dRP blocking lesion and also gap filling [28]. In cases where 3'

terminal processing is required, such as frank SSBs, additional gap tailoring proteins are available (e.g. polynucleotide kinase-3'-phosphatase (PNKP)) [29]. To complete the BER process, the 3'-OH and 5'-phosphate nick are sealed by a ligase (i.e. Ligase I or Ligase III) in an ATP-dependent manner [30]. These are the basic steps in BER, which has many points of entry and sophisticated subpathways for processing a wide range of lesions.

1.2.2 Nucleotide Excision Repair

While BER removes specific base lesions, NER recognizes helical distortions resulting from bulky lesions that may involve multiple nucleotide bases (e.g. pyrimidine dimers). NER was first observed in mammalian cells as unscheduled DNA synthesis (UDS) in response to X-ray irradiation, i.e. incorporation of nucleotides in cells not undergoing DNA synthesis [31]. Shortly after, cells from human patients suffering from the sunlight-sensitive and skin cancer-prone hereditary disease, xeroderma pigmentosum (XP), were shown to have diminished capacity for UDS [32]. This lead to the discovery of seven key NER proteins named XPA through XPG after the XP disease. NER capacity has since been associated with other diseases (e.g. Cockayne's syndrome and trichothyodystrophy) and susceptibility to numerous cancer types [33, 34, 35]. The repair pathway has also been implicated as a mechanism of tumor drug resistance [36, 37]. As such, the study of NER offers insight into genomic stability, cancer progression, and potential drug targets.

NER is divided into two subpathways, global genome NER (GG-NER) and transcription-coupled NER (TC-NER), which differ in their mechanism of lesion detection. GG-NER is initiated by the helix distortion recognition complex, XPC-Rad23B, while TC-NER, as its name suggests, is initiated by blockage of the RNA Polymerase II during transcription [38]. As shown in Figure 1-2, Both subpathways proceed similarly, by unwinding the DNA at the site of damage with the XPD and XPB helicase containing transcription/repair complex, transcription factor II H (TFIIH). This allows XPA, RPA and XPG to join the complex and engage ERCC1-XPF for initiating excision 5' of the DNA lesion. The resulting 3'-OH group acts as

25

a substrate for DNA polymerase and other factors, which fill in the 24-32 nucleotide gap resulting from 3' excision by XPG. The nick is sealed by a ligase to restore the original DNA sequence [39].

1.2.3 Interstrand Crosslink Repair

The use of DNA damaging chemotherapies was initiated by the success of the ICL agent, nitrogen mustard (NM), after World War II (described in *Section 1.3*) [40]. Today, crosslinking agents such as cisplatin are still routinely used in the management of numerous cancers; however, although highly successful upon administration, they are ultimately limited by tumor resistance [41]. Mechanisms of resistance are largely unknown due partially to an unavailability of assays to detect crosslinking lesions [42]. We aim to provide an analysis platform with the utility to both classify ICL agents and detect deficiencies in their repair.

ICLs, adducts that covalently bridge both DNA strands, are formed endogenously by agents such as products of lipid peroxidation [43]. They are extremely cytotoxic, disrupting replication and transcription, and causing strand breaks, chromosomal aberrations, or cell cycle arrest [44]. Figure 1-4a is an example of a NM induced crosslink formed between two guanine residues. The structure of ICLs can vary significantly depending on the source of damage and the local sequence context of the affected nucleotide bases. As a result, initiation of ICLR occurs through a variety of mechanisms, including encounters with transcriptional machinery, collision with replication forks (Figure 1-4b), or recognition of helix deformation [45]. This diversity of response demands coordination of multiple repair pathways in complicated processes that are still largely unknown. Deficiencies in both NER and HR have been shown to sensitize cells to ICLs [46, 47], implying a scenario in which HR repairs the DSB resulting from the excision, or "unhooking," of each opposing lesion by NER. In support of this model, people suffering from Fanconia anemia (FA), a disease resulting from mutations in genes including the critical HR gene, BRCA2, are hypersensitive to crosslinking agents [48]. Furthermore, XP patients with deficiencies in XPF, one of the two incision proteins of NER, have been shown to have defective "unhooking"

of ICLs [49]. A more complete understanding of ICLR and the coordination of the many pathways involved is still required to manage treatment of ICLR related heritable diseases such as FA [50]. In addition, crosslinking agents have become invaluable in cancer treatment over the past 30 years, but their efficacy is often limited by ICLR [51]. A better understanding of this complex mechanism will surely lead to new drug targets and strategies to overcome tumor ICL resistance.

1.2.4 Non-homologous End Joining

In addition to excision repair, which will be explored in Chapters II and III, we also aimed to improve methods for studying double strand break (DSB) repair. There are two major DSB repair pathways: HR, which uses the sister chromatid as a template to accurately resynthesize damaged DNA, and the more predominant, error-prone pathway, NHEJ, which directly ligates severed DNA ends [2]. NHEJ is active in all phases of the cell cycle and operates with a kinetic half-life of less than 30 min [52, 53]. If NHEJ is deactivated, blunt ended DSBs can be resected to reveal short microhomologies that guide ligation in a process known as MMEJ [52, 54]. MMEJ and other 'alternative end joining' processes are unfavorable due to the required loss of genetic material associated with resection [55, 56]. These back-up pathways operate with slower kinetics ($t_{1/2} > 2$ hr) and are thereby dominated by the faster NHEJ pathway [52, 57, 53].

An initiating step in NHEJ is recognition of the DSB by the Ku70/Ku80 heterodimer (Figure 1-3). The Ku heterodimer forms a ring-like structure that protects the DSB ends from degradation [58, 59] and inhibits the initiation of alternate repair pathways [52]. Multiple Ku proteins bind to a single DNA molecule and recruit the catalytic subunit, DNA-PKcs, forming the DNA-dependent protein kinase (DNA-PK) complex, which promotes strand alignment through trans-autophosphorylation [60, 61, 62]. The activated DNA-PK undergoes a conformational change that facilitates accessibility, recruitment, and activation of ligation and processing factors (i.e. XRCC4/Ligase IV complex and Artemis), as well as its subsequent release from the DNA end [63, 64]. Deficiencies in DNA-PK lead to extreme radiosensitivity [65],

which has recently brought it attention as a potential target for adjuvant cancer treatment. Chapter IV will explore the development of a DSB repair assay for evaluating such treatment strategies.

1.3   DNA Damage and Repair in Cancer Therapy

Information concerning DNA damage and repair is not only important in the study of cancer formation, but also in developing treatment strategies and understanding mechanisms of resistance. There have been many recent advances in biotechnology, but the three pillars of cancer treatment nevertheless remain: radiotherapy, surgery, and chemotherapy. Ionizing radiation therapy has been employed for over a century to combat cancer through direct collision with DNA or indirectly through the formation of free radicals that damage DNA [4]. In the United States, radiotherapy is given to nearly two-thirds of all cancer patients [66]. The main mechanism of action is formation of toxic DSBs by direct induction or through endogenous cellular processes such as DNA repair and replication, which are overactive in rapidly dividing cancer cells [2]. Side-effects to healthy tissue are reduced through localized exposure and by delivering radiotherapy in fractionated doses. For example, small doses may be given every six hours, enabling normal tissue to repair, while rapidly dividing tumors accumulate damage. Concurrent administration of chemotherapy treatment is effective in radiosensitizing tumors, and novel small molecule inhibitors of DNA repair are emerging to further enhance the efficacy of radiotherapy [4].

Cancer cells are also preferentially sensitive to the cytotoxic effects of chemical compounds that damage DNA or interfere with replication machinery. The success of NM in the treatment of leukemia after World War II initiated the field of anti-cancer chemotherapy and the evolution of three distinct categories of drugs: alkylating agents, antimetabolites, and antineoplastic antibiotics [40]. Nitrogen mustards are bifunctional alkylating agents that form DNA crosslinks through affinity for the N7 position of guanine residues (Figure 1-5), which has relatively high nucleophilic potential due to its relatively accessible position in the major groove of the double helix

[67]. DNA crosslinks are extremely cytotoxic because they block metabolic processes such as replication and transcription [45]. Mono-alkylating agents such as methyl methanesulfonate (MMS) and N-methyl-N'-nitro-N-nitrosoguanidine (MNNG) create N^7-methylguanine, N^3-methyladenine, and O^6-methylguanine lesions (Figure 1-5). The mutagenic potential of O^6-methylguanine to mispair with thymidine is one mechanism of alkylation toxicity. Interestingly, its toxicity is thought to result in part through a process in which mismatch repair removes the mispaired thymidine in an iterative and futile turnover of the daughter strand [68]. Direct removal of the lesion by O^6-methylguanine methyltransferase (MGMT) therefore provides a route of tumor resistance [69]. N^7-methylguanine and N^3-methyladenine also contribute to alkylation toxicity, evidenced by the potency of MMS, in which less than 1% of the lesion burden is O^6-methylguanine. N^7-methylguanine is relatively innocuous compared to N^3-methyladenine, which interferes with replication [67]. Both adducts additionally destabilize the N-glycosidic bond, potentiating abasic site formation through hydrolysis. Furthermore, their processing by BER forms SSB repair intermediates, which if not repaired efficiently, are preferentially toxic to rapidly dividing cancer cells [70]. So while proficient BER acts as a mechanism of resistance to certain levels of alkylation, imbalances in the pathway can lead to accumulation of BER intermediates and hypersensitivity to alkylation damage [71, 13, 14, 15, 16]. This was further illustrated by Sobol, et al. who demonstrated that cells could be sensitized to alkylation damage through accumulation of BER intermediates resulting from either overexpression of the initiating glycosylase (i.e. alkyladenine glycosylase (AAG)) or inhibition of the rate limiting polymerase step by $Pol\beta$ [14, 70]. The role of $Pol\beta$ in protecting against toxicity associated with accumulation of BER intermediates makes it an effective target to increase sensitivity of tumors to alkylation damage [15, 72, 73, 74]. Similarly, small molecule inhibitors of upstream APE-1 activity have also been shown to result in accumulation of toxic AP sites [75, 76, 77, 78]. Thus, a better understanding of the role of DNA repair in tumorigenic resistance can guide treatment strategies and help identify new targets of tumor susceptibility.

The use of inhibitors of DNA repair proteins is not limited to BER, but is

rather an emerging approach in cancer management to sensitize tumors to radio-
and chemotherapeutic approaches [79, 80, 81, 5]. Another compelling strategy is to
sensitize cells to DSBs through the inhibition of DNA-PK in NHEJ repair. This is
supported by studies demonstrating that cells lacking either subunit of the protein
kinase (i.e. Ku70/Ku80 heterodimer and DNA-PKcs) have increased radiosensitivity,
significant increases in chromosomal aberrations, and more MMEJ associated misjoin-
ing [82, 83, 84]. Such misrepairing is difficult to measure, as standard mammalian
assays provide information about residual DNA damage, but offer little insight into
mode of action and actual lesion burden. Indeed, whole-cell screening platforms to
identify small molecule inhibitors of NHEJ will be increasingly valuable to the phar-
maceutical industry as more companies add inhibitors of DNA-PK and other DNA
repair proteins into their preclinical pipelines [81].

1.4   Methods to Detect DNA Damage

Although effective methods for assessing DNA damage levels have been available
for decades, and it is well established that information about DNA damage levels
is highly useful both in the clinic and in population studies, measurements of DNA
damage and repair in human cells are far from routine. Currently available assays
are limited in throughput and often provide information about residual DNA damage
(e.g. chromosomal aberrations or mutations), but offer little insight into the actual
lesion burden or kinetics of repair. This section describes the strengths and limitations
of assays commonly used to evaluate DNA damage and repair, including unscheduled
DNA synthesis test (UDS), pulse field gel electrophoresis (PFGE), gamma-H2AX
assay, the chromosomal aberration (CA) test, sister chromatid exchange (SCE) assay,
and micronucleus (MN) assay. The single cell gel electrophoresis (comet) assay will
be described in detail in *Section 1.5*. Better genotoxicity tools that directly measure
DNA damage must be developed in order to perform epidemiological studies that
both reveal the impact of variations in DNA repair capacity and guide development
of valuable biomarkers of cancer susceptibility. In addition, the United States Food

and Drug Administration (FDA) is searching for new strategies that can provide greater detail concerning mechanism of genotoxicity at early stages of drug discovery to eliminate the cost and requirement of rodent models in later stages of development [85].

1.4.1 Unscheduled DNA Synthesis Test

Unscheduled DNA synthesis (UDS) refers to the replication of DNA during NER. By culturing cells in the presence of radionucleotides, the amount of UDS resulting from an exposure of interest can be quantified as an indicator of DNA damage. Scintillation counters cannot discriminate semi-conservative replication from UDS in a cell suspension, so autoradiography is required to visually quantify the extent of UDS, excluding cells undergoing synthesis based on their high radionucleotide content. This process is extremely laborious and neither directly nor selectively measures the removal of a specific type of damage. However, at this time, the UDS test is the only functional test to directly measure NER activity on the entire genome without the use of antibodies [86]. It has therefore been adopted by the FDA as a supplementary *in vivo* test in rats to evaluate the extent of liver genotoxicity [85].

1.4.2 Pulsed Field Gel Electrophoresis

Constant field gel electrophoresis is an invaluable technique in molecular biology to separate DNA fragments based on their size, but is limited to the range of 100 base pairs (bp) to 50 Kbp. PFGE was developed to measure large fragments of DNA resulting from DSBs. By periodically changing the direction of the electric field, fragments as long as 10 Mbp can be separated. The concept behind PFGE is that larger molecules take longer to reorient in the alternating electric field and can therefore be separated from shorter fragments that are able to more quickly change direction. Pulse times are optimized so that DNA molecules of a targeted size spend most of their time reorienting. At the end of the long electrophoresis process (>30 hr), the fragments of DNA that have migrated into the gel are stained, cut from

the gel, and quantified using scintillation counting. This radiation requirement limits the applications of PFGE, because cells must be pre-incubated for 24 hr to allow incorporation of radiolabeled nucleotides into their genome. Other limitations of the assay include a 17 hr lysis, in addition to the 30 hr electrophoresis, which significantly reduces throughput [87].

1.4.3   Gamma-H2AX Assay

Phosphorylation of histone variant H2AX is an early signaling event in response to DSB induction, and detection of γ-H2AX has emerged as a sensitive indicator for DSB quantification [88, 89, 90, 91]. The formation and disappearance of γ-H2AX has been shown to correlate linearly with DSBs induced by radiation doses as low as 1 mGy [92]. The sensitivity and low cell requirement of the γ-H2AX assay are favorable for use in biodosimetry and cancer staging, and higher throughput versions of the assay are emerging for the evaluation of novel cancer therapies [93, 94, 95, 96]. However, as an indirect and non-specific marker of DSB repair, the γ-H2AX assay is inappropriate for precise analysis of repair kinetics [89]. For example, the γ-H2AX assay is inaccurate for measurement of NHEJ inhibition, because H2AX phosphorylation is dependent on the activity of DNA-PK and other phosphatidylinositol 3-kinase (PI3K) related kinases (PI3KKs) [97]. Furthermore, the disappearance of the γ-H2AX signal may not correlate precisely with DSB repair [98, 89, 99]. One hypothesis is that γ-H2AX continues to mark DSBs after completion of NHEJ in order to signal further processing and chromatin remodeling [100]. Other explanations are that the dephosphorylation of γ-H2AX is simply limited by the concentration and activity of the phosphatase (i.e. PP2A) [101]. What is clear is that as an indirect marker of DSB disappearance, γ-H2AX is limited in its utility for precise analysis of repair kinetics.

1.4.4 Chromosomal Aberration Test and Sister Chromatid Exchange Assay

Chromosomal aberrations are a very severe form of DNA damage and are associated with heritable diseases and tumorigenesis. Improperly repaired DSBs can result in chromosomal breaks, gaps, fusions, deletions, translations, and inversions [2]. Although many of these structural aberrations cause cell death, they also serve as indicators of DNA damage in neighboring cells that may not be lethal, but may instead have profound genetic consequences. The FDA approves the chromosomal aberration (CA) test as the frontline method for determining carcinogenicity [85]. To analyze aberrations, cells are fixed in metaphase using a microtubule inhibitor such as colcemid. The cells are then harvested and added to a hypotonic solution in order to burst the cells open and enhance separation of the chromosomes. The chromosomes are then stained and evaluated under a microscope for easily identifiable aberrations such as dicentric and ring chromosomes, breaks, gaps, and aneuploidy [102]. The CA test is a direct marker of genotoxicity and a powerful predictor of carcinogenic potential [103], but does not provide mechanistic information and may not detect nonlethal exposures with mutagenic potential. Limitations in the assay include the requirement of *in vitro* cell cultivation, a laborious analysis process, and an inability to directly measure DNA repair.

Sister chromatid exchange (SCE) describes the process whereby genetic material is exchanged between two identical chromatids through HR during mitotic repair of DSBs [104]. SCEs are a biomarker for chromosomal recombination, but their frequency has not been shown to correlate with cancer risk [103]. The assay is time consuming, requiring two consecutive cell cycles to incorporate bromodeoxyuridine (BrdU), a mutagenic analogue of thymidine, for visualization of exchange events. Chromatids in which only one strand incorporated BrdU stain dark with Giemsa, while those with two rounds of synthesis stain lighter [105]. The SCE assay is limited by its requirement of two rounds of mitosis, detection of only damage repaired by HR, and manual image analysis requirement, which is labor intensive and subject to

bias. In addition, the endpoint is not accurate for ionizing radiation and some other damaging agents, because BrdU is highly reactive and can itself contribute to the formation of SCEs [106].

1.4.5   Micronucleus Test

Chromosomal breakage or spindle damage during the metaphase/anaphase transition of mitosis can result in improper chromosomal integration into the daughter nucleus. Chromosomal fragments that remain in the mother cell form micronuclei (MN) that can be visualized through fluorescent staining and counted as a measure of relative genotoxic activity. The assay can be performed *in vivo* on the erythrocytes of mice, which lack a nucleus, making identification of micronuclei straight forward [107]. This version of the assay is recommended by the FDA for genotoxicity screening, because it can detect a wide spectrum of changes in chromosomal integrity, including aneuploidy. For *in vitro* studies, most cell types can be assayed using an actin inhibitior (i.e. cytochalasin-B) to prevent cytokinesis in order to count micronuclei in bionucleated cells. The *in vitro* MN test is an indirect measure of DSBs with relevance only in mitotic cells. The assay has minimal quantitative capacity and provides no information concerning specific types of DNA damage or DNA repair. Furthermore, it requires a laborious imaging and analysis process [108].

1.5   Comet Assay

Over the past two and a half decades, the comet assay has become a standard method for detecting base lesions and DNA strand breaks with sensitivity down to spontaneous damage levels [109]. The comet assay is inexpensive, requires a relatively few number of cells, and has the versatility to measure a range of DNA lesions, in a variety of cell types [110]. In the traditional gel electrophoresis protocol (Figure 1-6), cells are embedded in agarose on a slide and a lysis solution is used to dissolve cell membranes and disrupt nucleosomes, leaving a nucleoid of negatively charged, supercoiled DNA. An alkaline electrophoresis buffer (pH > 13) is used to unwind the DNA and expose

SSBs and alkali-labile sites. An electrical current is then applied across the slide to pull relaxed loops and fragments of DNA toward the positive anode. The resulting morphology resembles a celestial comet when imaged using a fluorescent nucleic acid stain. Image processing software or manual analysis is used for DNA damage quantification under the governing principle that damaged DNA migrates more readily into the so-called "comet tail" than undamaged DNA, which remains tightly wound within the "comet head" [111].

While most genotoxicity assays probe a fairly specific repair process – e.g. γ-H2AX assay measures an early signal in DSB repair and UDS measures the incorporation of radionucleotides during NER – the comet assay directly measures DNA strand breaks, giving it the versatility to detect several different classes of DNA damage through simple modifications in protocol. The alkaline version of the assay detects SSBs, but also abasic and alkali labile sites, which have also been shown to be mutagenic [112]. DSBs can be quantified by using a neutral buffer [113, 111], ICLs can be detected as a decrease in comet tail length after radiation induced damage [114], and specific base lesions can be assessed using lesion specific glycosylases [115]. The comet assay also directly detects the disappearance of strand breaks, which can be used to precisely measure kinetics of the integrated DNA repair response to a given exposure [12, 116].

There are over 4,000 publications using the comet assay with diverse applications, including investigating DNA damage levels associated with cigarette smoke and other environmental genotoxins [117, 118, 119, 120], determining the roles of specific DNA repair proteins [82, 46, 121, 122, 20, 48] and the influence of their polymorphisms [123, 124, 125, 126, 127], predicting cancer susceptibility [128, 129, 116], establishing biomarkers for use in nutritional studies [130, 131], and understanding the connection between oxidative stress and disease [132, 133, 134, 135]. In addition, the assay is a strong candidate for clinical applications such as determining radiosensitivity of tumors [136], and evaluating chemotherapeutic options [137]. The comet assay requires relatively few cells and can performed in both *in vitro* and *in vivo* studies [138], making it an attractive option for preclinical pharmaceutical screening [139, 140, 141, 142, 143, 144].

Higher throughput detection of DNA damage is important in classification of chemicals, pharmaceutical screening and the development of novel cancer therapies. The FDA currently recommends the following standard three stage test battery for genotoxicity: 1) bacterial reverse mutation test (i.e. Ames test), 2) *in vitro* test for chromosomal aberration in mammalian cells (i.e. CA), and 3) *in vivo* test for chromosomal aberrations in rodent hematopoietic cells (i.e. CA or MN). At the 5th International Workshop on Genotoxicity Testing (IWGT) in 2009, the use of the comet assay as an *in vitro* test was discussed, because it does not require proliferation and measures a wide range of DNA damage [145]. Furthermore, the comet assay has been shown to have similar sensitivity to the MN Test, while providing more specific information on mode of action [146, 147, 148]. The comet assay may be used in combination with the MN Test to eliminate false negatives from the Ames Test and eliminate unnecessary, costly *in vivo* rodent studies [149]. The FDA has recommend the *in vivo* comet assay as a follow-up test [143, 85] and it has been shown that the comet assay can be effectively combined in the same animal with the *in vivo* MN Test to provide additional safety testing on critical target organs [150].

As a stand-alone test, issues relating to specificity and sensitivity of the comet assay need to be addressed before it is accepted by the regulatory framework [137]. One issue in terms of its utility as a standard gentoxicity assay is that the comet assay does not detect aneugenic effects and epigenetic mechanisms of DNA damage such as effects on cell-cycle checkpoints [110]. Other limitations include low throughput, slide-to-slide variability, limited parameter control, and image processing and analysis that are laborious, time consuming, and often biased [151, 152].

Many researchers have attempted to overcome these weaknesses in order to unlock the true potential of the comet assay as a high throughput, robust technique for measure of the integrated DNA damage response. Their approaches, however, have focused on improving a single variable rather than providing a complete solution. For example, Trevigen Inc. (Gaithersburg, MD) commercialized a high throughput version that enables 96 samples to be assayed on a single glass slide. Although this approach simplifies electrophoresis and imaging, it still requires a logistically challeng-

36

ing preparation procedure, because all samples must be counted and exposed prior to plating. The development of a multichamber plate (MCP) by Stang, et al. overcomes this requirement by enabling multiple cell samples or chemical concentrations to be treated in a 96-well format. Because the multichamber plate does not address issues associated with random distribution of cells in wells, four wells are required per sample (~25 cells per well), reducing the throughput from 96 to 24 samples per plate [153]. Furthermore, the approach applies only to adherent cells and requires an optimized seeding time for each cell type ranging from 2-4 hr with potential of over-adherence, which results in abnormal comet morphologies. This incubation requirement limits its utility for assessing primary cells. Another group focused on improving the reproducibility of the comet assay by incorporating BrdU labeled reference cells. Although this approach was important in identifying the contribution of subtle gel differences in slide-to-slide variation, it drastically reduced throughput by requiring the use of antibody detection and additional imaging of BrdU labeled control cells [154]. Many other groups have addressed specific issues such as imaging bias [155, 156], analysis algorithms [157, 158], statistical issues [159], interlab variability [160, 161], and protocol standardization [133, 162].

The major goal of this project was to overcome the limitations of throughput and reproducibility while maintaining the core strength of the comet assay, namely, a straight forward and inexpensive protocol with the ability to operate in a variety of modes for sensitive detection of a range of DNA lesions and their repair on a single cell basis. Shown in Figure 1-6, the comet assay protocol can be divided into seven steps according to the guidelines established by the International Workshop of Genotoxicty Test Procedures (IWGTP) [140]: slide preparation, lysis, alkaline unwinding, electrophoresis, neutralization, staining and imaging, and comet scoring. By exploring each step of the comet assay protocol, the sources of these limitations are revealed and an engineering approach is defined that not only improves throughput and reproducibility, but extends the utility of the comet assay for novel applications in new research settings.

Slide Preparation: Slide preparation is a time consuming and laborious proce-

dure. Slides must be pre-coated in agarose and cell samples must be counted in order to optimize the seeding concentration. Cell samples are then mixed in agarose, added to the pre-coated slides, cover-slipped to form a consistent layer, and allowed to settle to a uniform focal plane. Each sample requires a single slide, making it difficult to process more than 20-30 conditions at a time. This large slide requirement makes evaluating multiple chemical conditions a logistical challenge, so many researchers first expose cells in microtiter plates, which leads to savings in time and chemicals [163]. However, the subsequent trypsinization and slide preparation allows for DNA repair, which may contribute to issues in reproducibility. Trypsinization and centrifugation may also be damaging to the cells [164]. **Lysis:** Lysis is a straightforward step in which slides are placed in a cold, high salt, alkaline pH (>13) detergent solution to osmotically rupture cells and disrupt their nuclear membrane, leaving a tightly wound nucleoid of DNA. One issue with lysis is that agarose gels can be lost from the glass slides. **Alkaline unwinding:** The alkaline unwinding step denatures DNA, exposing SSBs and alkali labile sites. This step is excluded in the neutral version of the assay for detection of DSBs. **Electrophoresis:** Electrophoresis draws the negatively charged loops and fragments of DNA toward the anode, producing a "tail" that is used as a measure of DNA damage. The main limitation of this step is the volume of the electrophoresis box, which limits the number of slides that can be run simultaneously and therefore under identical DNA migration conditions. **Neutralization:** Tris buffer (pH 7.5) is used to neutralize slides from their alkaline state in preparation for DNA staining. **Staining and imaging:** A fluorescent DNA stain of choice (e.g. SYBR Gold) is used for visualization of comets. Imaging contributes the most to limitations in throughput. Slides are imaged individually under fluorescent microscope at a rate of approximately 10-15 per hour [111]. The optimal number of comets per visual field is "no more than a few," according to the IWGTP [140]. This restriction minimizes the number of unanalyzable comets resulting from overlap, but requires the imaging of numerous visual fields to obtain the minimum 50 comets that are sufficient for statistical analysis [165]. Imaging is generally a manual process and slides have to be switched by hand. Automated imaging systems with slide feeders are

becoming more prevalent, but are expensive and often limited in imaging efficiency due to difficulty of autofocusing on cells that are randomly distributed at multiple focal planes within the agarose. **Comet scoring:** A number of comet parameters can be derived from dimensional analysis of the comet "head" and "tail." In the alkaline version of the assay, both the proportion of DNA that migrates from the head (% tail DNA) and the distance it travels (tail length) correlate linearly with DNA damage. The use of % tail DNA, as a normalized parameter, is an unambiguous measure, minimizes inter-laboratory differences due to discrepancies in protocol (e.g. electrophoresis time), and is linearly related to DNA break frequency over a wide range of damage levels [140, 152]. In the neutral version of the assay, tail length is the preferred measure, because it best captures the presence of DNA fragments resulting from DSBs [111]. Scoring can be conducted manually using visual analysis or through the use of commercially available software. Although visual scoring has been shown to give reliable, quantitative results [158], the method is laborious and prone to bias even when conducted by a skilled operator [156]. Semi-automated computer algorithms, such as the Komet Software (Andor Technology, Belfast, Northern Ireland), automatically calculate parameters, providing a more rigorously quantitative analysis; however, such programs still require user selection of comets, which is tedious and potentially subjective. For high throughput applications, fully automated analysis is the logical approach, because it is fast and minimizes user involvement. Currently available software packages (e.g. Metafer, Metasystems, Germany) are prohibitively expensive and imperfect in that they can introduce error by not registering highly damaged comets, miscalculating head-to-tail thresholds, and by analyzing improper objects, overlapping comets, etc. [158].

In summary, the main limitations of the comet assay, low throughput and reproducibility, are factors of two key limitations: the use of one slide per condition, and the random distribution of cells in the agarose gel. The slide requirement directly limits throughput by demanding significant handling with inefficient use of chemicals and reagents. The slide requirement also makes for a logistically challenging protocol with many opportunities for human error, as well as error that is inherent to using multiple

gels, and running multiple electrophoresis chambers. The slide number also translates to a laborious imaging requirement. As others have demonstrated, this limitation can be overcome by housing all conditions on a single slide (Trevigen) [153]. However, this does not overcome the random distribution of cells within the agarose, which leads to inefficient use of slide surface area, and complications for automated imaging (i.e. focusing, comet identification) and automated analysis (i.e. overlapping comets). This limitation can be overcome by patterning cells in a two-dimensional array, which would maximize the number of comets per unit area, enabling simultaneous analysis of all conditions on a single slide for improved throughput and reproducibility. A cell array would also benefit the imaging process by maximizing the number of comets per visual field, eliminating overlapping comets, and reducing the focal range. Lastly, this approach would simplify automated analysis, because each cell would have a specific address and objects not found within the cell matrix could be disregarded as contamination. Our goal was to use microtechnology to reinvent the comet assay as a single cell microarray platform for high throughput DNA damage and repair analysis.

1.6 Patterning techniques

Microfabrication describes a collection of processes developed by the semi-conductor industry to produce miniature structures. In the past twenty years, these techniques have fueled innovation in biological engineering by enabling single-cell analysis. Cells are increasingly appreciated as heterogeneous entities, each with the potential to initiate disease. Understanding how cells respond one by one is important in diagnosing and understanding disease progression, as well as drug targeting. "Lab-on-a-chip" applications also minimize the amount of reagents that are required, increase throughput, enable faster analysis and integration with sequential processes, and reduce waste. Microfabrication is used to create well-, trap-, pattern-, and droplet-based devices for a wide range of single-cell technologies, including fluorescence-activated cell sorting, cytotoxicity evaluation, polymerase chain reaction, proteomic and genomic analysis, and the study of cellular interactions, dynamics, mechanics, division,

differentiation, morphology, etc. [166].

Photolithography, illustrated in Figure 1-7, is a powerful technique for the miniaturization of biological tools, because it provides the micrometer precision necessary to capture single cells. The founding principle is that ultraviolet (UV) radiation permanently crosslinks photoresist (i.e. SU-8) onto a silicon substrate for design of fluidic channels, wells, or other features. Polydimethylsiloxane (PDMS) is a silicone-based polymer that can be poured over a silicon-SU-8 device and allowed to harden into a durable microfeature device for direct use or as a reusable stamp for patterning of biomolecules in a process termed soft lithography. These technologies can be implemented to pattern cells through a variety of approaches, including bimolecular micropatterning, mechanical trapping, and microwell separation [166].

Soft lithography can be used to pattern surfaces with biomolecules (e.g. fibronectin or collagen) for directed cell adhesion. This technique enables high resolution patterning that is ideal for surface interaction studies, but is limited to adherent cell types [167]. Continuous flow microfluidic devices enable the analysis of cells with precise control over their microenvironment. For this application, a PDMS device is permanently bonded to glass using RF plasma techniques in order to form hydrophobic microchannels. Pumps and valves can be used to introduce specific reagents and mechanical traps can be utilized to separate cells for individual analysis. Although in principle, microfluidic devices offer a powerful, self-contained solution to cell patterning, they are inherently difficult to operate, because flow rates are dependent on the properties of the entire system and are thereby drastically affected by liquid properties (e.g. viscosity) and other factors (e.g. bubble formation) [166]. The use of microwells to capture single cells is the least challenging approach, and has been achieved in a variety of materials (e.g. PDMS, poly(ethylene glycol), polystyrene) [168, 169, 170]. Well size can be varied to accommodate one or more cells, which are captured by gravitational settling. Passive seeding leads to potential issues in cell loading efficiency. Another drawback is an inability to measure instant cellular responses to reagents due to limitations in practical liquid dispensing techniques [170].

1.7 Specific Aims

DNA damage is a critical risk factor for cancer, aging, and heritable diseases [21, 171, 1], and it is the underlying basis for most frontline cancer therapies [5]. Increased knowledge about DNA damage and repair would facilitate disease prevention, identification of individuals at increased risk of cancer, discovery of novel therapeutics, and better drug safety testing. Despite their obvious translational impact, most DNA damage assays have not changed significantly in more than two decades, and thus are not compatible with modern high throughput screening (HTS) technologies. To better assess the biological impact of damage, we need data that reflect the integrated effect of multiple DNA repair pathways and subpathways, in response to a range of DNA lesions, measured in an accurate and high throughput fashion.

This thesis describes our work aimed at transforming the well-established comet assay into a high throughput, reproducible assay for experimental, clinical, and epidemiological applications. The governing hypothesis was that by patterning cells using microfabrication technologies, we could both increase the number of samples assayed on a single device through miniaturization, and improve the quality and efficiency of analysis by utilizing automated imaging systems and developing software that takes advantage of spatial optimization of cells. We envisioned other advantages to an arrayed based comet assay, including the ability to precisely measure DNA repair kinetics on a single device, integrate the platform with standard HTS technologies, and multiplex endpoints such as cell viability to extend the utility of the assay.

Chapter II describes the development of a strategy to microarray single cells in agarose gel. We explored several distinct methods of cellular patterning, including the use of microfluidic trapping and collagen island adhesion. The requirement of molten agarose proved to be a barrier to a microfluidic approach. Collagen adhesion was successfully used to pattern primary rat hepatocytes for increased throughput radiation studies, but was ultimately abandoned due to limitations in throughput and cell type accommodation [172]. The use of microwells enabled an inexpensive,

straightforward and reproducible method for patterning numerous cell types. As anticipated, the use of patterning enabled multiple conditions to be assayed on a single gel and allowed us to develop software that automatically locates and analyzes comets based on their distinct locations in the array. Taken together, these advantages resulted in both increased throughput and reproducibility.

Ultimately, we want to provide an assay that is useful both in epidemiological applications, such as identifying susceptible populations, and in clinical practice, such as determining tumor sensitivities and guiding treatment strategies. It was therefore important to determine the assay's detection thresholds for various DNA damaging agents and confirm its ability to detect known deficiencies in repair. In the work described in Chapter III, we further increased throughput by improving our microfabrication process and adapting the technology to a 96-well version known as the CometChip, which integrates with standard HTS technologies. This enabled simultaneous evaluation of multiple cell types, chemical conditions, and repair time points on a single device. We demonstrated the usefulness of the CometChip for detection of a variety of DNA damaging agents, revealing the ability of the assay to detect subtle differences in lesion specific repair, which may be useful in characterizing the genotoxic effects of chemical agents. We also identified deficiencies in three excision repair pathways, providing support for existing mechanistic models of DNA repair, and supporting the use of the platform in applications such as the development of biomarkers of disease susceptibility.

In Chapter IV, we applied our single cell patterning approach to the neutral version of the comet assay for detection of DSB repair, which is known to be an important mechanism in tumor resistance and therefore a potential target for adjuvant chemotherapy. Currently available assays for DSB detection are limited in throughput and specificity and offer minimal information concerning kinetics of repair. In contrast, the CometChip measures physical DSBs for direct detection of repair. We demonstrated an ability to identify multiple genetic deficiencies in NHEJ and sensitively evaluate a set of clinically relevant inhibitors of DSB repair. In total, this work represents a signficant advance in DNA damage and repair assessment technology.

The CometChip enables high throughput, objective analysis of a variety of DNA lesions for potential use in applications such as the development of predictive assays for untested compounds, and enables direct measurement of DNA repair, which may be useful for the development of clinical assays.

References

[1] J. H. J. Hoeijmakers, "Dna damage, aging, and cancer," *N Engl J Med*, vol. 361, pp. 1475–85, Oct 2009.

[2] J. H. Hoeijmakers, "Genome maintenance mechanisms for preventing cancer," *Nature*, vol. 411, pp. 366–74, May 2001.

[3] D. Hanahan and R. A. Weinberg, "The hallmarks of cancer," *Cell*, vol. 100, pp. 57–70, Jan 2000. d break.

[4] J. Bernier, E. J. Hall, and A. Giaccia, "Radiation oncology: a century of achievements," *Nat Rev Cancer*, vol. 4, pp. 737–47, Sep 2004.

[5] T. Helleday, E. Petermann, C. Lundin, B. Hodgson, and R. A. Sharma, "Dna repair pathways as targets for cancer therapy," *Nat Rev Cancer*, vol. 8, pp. 193–204, Mar 2008.

[6] F. J, S. HR, B. F, F. D, M. C, and P. DM., "Cancer incidence and mortality worldwide," 2010.

[7] L. A. Loeb, "A mutator phenotype in cancer," *Cancer Research*, vol. 61, pp. 3230–9, Apr 2001.

[8] D. Hanahan and R. A. Weinberg, "Hallmarks of cancer: the next generation," *Cell*, vol. 144, pp. 646–74, Mar 2011.

[9] P. Anand, A. B. Kunnumakkara, A. B. Kunnumakara, C. Sundaram, K. B. Harikumar, S. T. Tharakan, O. S. Lai, B. Sung, and B. B. Aggarwal, "Cancer is

a preventable disease that requires major lifestyle changes," *Pharm Res*, vol. 25, pp. 2097–116, Sep 2008.

[10] A. C. Society, "Cancer facts and figures 2011," Atlanta: American Cancer Society, 2011.

[11] S. P. Faux, T. Tai, D. Thorne, Y. Xu, D. Breheny, and M. Gaca, "The role of oxidative stress in the biological responses of lung epithelial cells to cigarette smoke," *Biomarkers*, vol. 14 Suppl 1, pp. 90–6, Jul 2009.

[12] P. Fortini, G. Raspaglio, M. Falchi, and E. Dogliotti, "Analysis of dna alkylation damage and repair in mammalian cells by the comet assay," *Mutagenesis*, vol. 11, pp. 169–75, Mar 1996.

[13] L. M. Posnick and L. D. Samson, "Imbalanced base excision repair increases spontaneous mutation and alkylation sensitivity in escherichia coli," *J Bacteriol*, vol. 181, pp. 6763–71, Nov 1999.

[14] R. W. Sobol, D. E. Watson, J. Nakamura, F. M. Yakes, E. Hou, J. K. Horton, J. Ladapo, B. V. Houten, J. A. Swenberg, K. R. Tindall, L. D. Samson, and S. H. Wilson, "Mutations associated with base excision repair deficiency and methylation-induced genotoxic stress," *Proc Natl Acad Sci USA*, vol. 99, pp. 6860–5, May 2002.

[15] R. W. Sobol, M. Kartalou, K. H. Almeida, D. F. Joyce, B. P. Engelward, J. K. Horton, R. Prasad, L. D. Samson, and S. H. Wilson, "Base excision repair intermediates induce p53-independent cytotoxic and genotoxic responses," *The Journal of biological chemistry*, vol. 278, pp. 39951–9, Oct 2003.

[16] V. Simonelli, L. Narciso, E. Dogliotti, and P. Fortini, "Base excision repair intermediates are mutagenic in mammalian cells," *Nucleic Acids Research*, vol. 33, pp. 4404–11, Jan 2005.

[17] E. L. Goode, C. M. Ulrich, and J. D. Potter, "Polymorphisms in dna repair genes and associations with cancer risk," *Cancer Epidemiol Biomarkers Prev*, vol. 11, pp. 1513–30, Dec 2002.

[18] T. Paz-Elizur, Z. Sevilya, Y. Leitner-Dagan, D. Elinger, L. C. Roisman, and Z. Livneh, "Dna repair of oxidative dna damage in human carcinogenesis: potential application for cancer risk assessment and prevention," *Cancer Letters*, vol. 266, pp. 60–72, Jul 2008.

[19] D. Starcevic, S. Dalal, and J. B. Sweasy, "Is there a link between dna polymerase beta and cancer?," *Cell Cycle*, vol. 3, pp. 998–1001, Aug 2004.

[20] R. Brem and J. Hall, "Xrcc1 is required for dna single-strand break repair in human cells," *Nucleic Acids Research*, vol. 33, pp. 2512–20, Jan 2005.

[21] E. C. Friedberg, G. C. Walker, W. Siede, R. D. Wood, R. A. Schultz, and T. Ellenberger, *DNA Repair and Mutagenesis*. ASM Press, Washington, DC, USA, 2005.

[22] M. L. Hegde, T. K. Hazra, and S. Mitra, "Early steps in the dna base excision/single-strand interruption repair pathway in mammalian cells," *Cell Res*, vol. 18, pp. 27–47, Jan 2008.

[23] J. C. Shen, W. M. Rideout, and P. A. Jones, "The rate of hydrolytic deamination of 5-methylcytosine in double-stranded dna," *Nucleic Acids Research*, vol. 22, pp. 972–6, Mar 1994.

[24] T. Lindahl and D. E. Barnes, "Repair of endogenous dna damage," *Cold Spring Harb Symp Quant Biol*, vol. 65, pp. 127–33, Jan 2000.

[25] B. Demple, T. Herman, and D. S. Chen, "Cloning and expression of ape, the cdna encoding the major human apurinic endonuclease: definition of a family of dna repair enzymes," *Proc Natl Acad Sci USA*, vol. 88, pp. 11450–4, Dec 1991.

[26] D. M. Wilson and D. Barsky, "The major human abasic endonuclease: formation, consequences and repair of abasic lesions in dna," *Mutat Res*, vol. 485, pp. 283–307, May 2001.

[27] Y. Liu, W. A. Beard, D. D. Shock, R. Prasad, E. W. Hou, and S. H. Wilson, "Dna polymerase beta and flap endonuclease 1 enzymatic specificities sustain dna synthesis for long patch base excision repair," *The Journal of biological chemistry*, vol. 280, pp. 3665–74, Feb 2005.

[28] D. K. Srivastava, B. J. Berg, R. Prasad, J. T. Molina, W. A. Beard, A. E. Tomkinson, and S. H. Wilson, "Mammalian abasic site base excision repair. identification of the reaction sequence and rate-determining steps," *The Journal of biological chemistry*, vol. 273, pp. 21203–9, Aug 1998.

[29] D. M. Wilson, "Processing of nonconventional dna strand break ends," *Environ. Mol. Mutagen.*, vol. 48, pp. 772–82, Dec 2007.

[30] R. Prasad, R. K. Singhal, D. K. Srivastava, J. T. Molina, A. E. Tomkinson, and S. H. Wilson, "Specific interaction of dna polymerase beta and dna ligase i in a multiprotein base excision repair complex from bovine testis," *The Journal of biological chemistry*, vol. 271, pp. 16000–7, Jul 1996.

[31] R. B. PAINTER and R. E. RASMUSSEN, "Organization of the deoxyribonucleic acid replicating system in mammalian cells as revealed by the use of x-radiation and bromuracil deoxyriboside," *Nature*, vol. 201, pp. 162–5, Jan 1964.

[32] J. E. Cleaver, "Defective repair replication of dna in xeroderma pigmentosum," *Nature*, vol. 218, pp. 652–6, May 1968.

[33] V. Moreno, F. Gemignani, S. Landi, L. Gioia-Patricola, A. Chabrier, I. Blanco, S. González, E. Guino, G. Capellà, and F. Canzian, "Polymorphisms in genes of nucleotide and base excision repair: risk and prognosis of colorectal cancer," *Clin Cancer Res*, vol. 12, pp. 2101–8, Apr 2006.

[34] J. E. Cleaver, E. T. Lam, and I. Revet, "Disorders of nucleotide excision repair: the genetic and molecular basis of heterogeneity," *Nat Rev Genet*, vol. 10, pp. 756–68, Nov 2009.

[35] J. P. M. Melis, M. Luijten, L. H. F. Mullenders, and H. van Steeg, "The role of xpc: Implications in cancer and oxidative dna damage," *Mutat Res*, Jul 2011.

[36] R. Rosell, M. Taron, A. Barnadas, G. Scagliotti, C. Sarries, and B. Roig, "Nucleotide excision repair pathways involved in cisplatin resistance in non-small-cell lung cancer," *Cancer Control*, vol. 10, pp. 297–305, Jan 2003.

[37] M. A. Sabatino, M. Marabese, M. Ganzinelli, E. Caiola, C. Geroni, and M. Broggini, "Down-regulation of the nucleotide excision repair gene xpg as a new mechanism of drug resistance in human and murine cancer cells," *Molecular Cancer*, pp. 1–12, Oct 2010.

[38] N. L. May, J.-M. Egly, and F. Coin, "True lies: the double life of the nucleotide excision repair factors in transcription and dna repair," *J Nucleic Acids*, vol. 2010, Jan 2010.

[39] L. Staresincic, A. F. Fagbemi, J. H. Enzlin, A. M. Gourdin, N. Wijgers, I. Dunand-Sauthier, G. Giglia-Mari, S. G. Clarkson, W. Vermeulen, and O. D. Schärer, "Coordination of dual incision and repair synthesis in human nucleotide excision repair," *EMBO J*, vol. 28, pp. 1111–20, Apr 2009.

[40] R. B. Scott, "Cancer chemotherapy–the first twenty-five years," *Br Med J*, vol. 4, pp. 259–65, Oct 1970.

[41] B. Stordal and M. Davey, "Understanding cisplatin resistance using cellular models," *IUBMB Life*, vol. 59, pp. 696–9, Nov 2007.

[42] P. Wynne, C. Newton, J. A. Ledermann, A. Olaitan, T. A. Mould, and J. A. Hartley, "Enhanced repair of dna interstrand crosslinking in ovarian cancer cells from patients following treatment with platinum-based chemotherapy," *Br J Cancer*, p. 7, Sep 2007.

[43] L. J. Niedernhofer, J. S. Daniels, C. A. Rouzer, R. E. Greene, and L. J. Marnett, "Malondialdehyde, a product of lipid peroxidation, is mutagenic in human cells," *The Journal of biological chemistry*, vol. 278, pp. 31426–33, Aug 2003.

[44] V. Jonnalagadda, T. Matsuguchi, and B. Engelward, "Interstrand crosslink-induced homologous recombination carries an increased risk of deletions and insertions," *DNA Repair*, vol. 4, pp. 594–605, May 2005.

[45] O. D. Schärer, "Dna interstrand crosslinks: natural and drug-induced dna adducts that induce unique cellular responses," *Chembiochem*, vol. 6, pp. 27–32, Jan 2005.

[46] I. U. D. Silva, P. J. McHugh, P. H. Clingen, and J. A. Hartley, "Defining the roles of nucleotide excision repair and recombination in the repair of dna interstrand cross-links in mammalian cells," *Molecular and Cellular Biology*, vol. 20, pp. 7980–90, Nov 2000.

[47] L. J. Niedernhofer, H. Odijk, M. Budzowska, E. van Drunen, A. Maas, A. F. Theil, J. de Wit, N. G. J. Jaspers, H. B. Beverloo, J. H. J. Hoeijmakers, and R. Kanaar, "The structure-specific endonuclease ercc1-xpf is required to resolve dna interstrand cross-link-induced double-strand breaks," *Molecular and Cellular Biology*, vol. 24, pp. 5776–87, Jul 2004.

[48] P. J. McHugh, V. J. Spanswick, and J. A. Hartley, "Repair of dna interstrand crosslinks: molecular mechanisms and clinical relevance," *Lancet Oncol*, vol. 2, pp. 483–90, Aug 2001.

[49] P. H. Clingen, C. F. Arlett, J. A. Hartley, and C. N. Parris, "Chemosensitivity of primary human fibroblasts with defective unhooking of dna interstrand cross-links," *Exp Cell Res*, vol. 313, pp. 753–60, Feb 2007.

[50] A. Rothfuss and M. Grompe, "Repair kinetics of genomic interstrand dna cross-links: evidence for dna double-strand break-dependent activation of the fanconi

anemia/brca pathway," *Molecular and Cellular Biology*, vol. 24, no. 1, p. 123, 2004.

[51] C. A. Rabik and M. E. Dolan, "Molecular mechanisms of resistance and toxicity associated with platinating agents," *Cancer Treat Rev*, vol. 33, pp. 9–23, Feb 2007.

[52] H. Wang, A. R. Perrault, Y. Takeda, W. Qin, H. Wang, and G. Iliakis, "Biochemical evidence for ku-independent backup pathways of nhej," *Nucleic Acids Research*, vol. 31, pp. 5377–88, Sep 2003.

[53] G. Iliakis, H. Wang, A. R. Perrault, W. Boecker, B. Rosidi, F. Windhofer, W. Wu, J. Guan, G. Terzoudi, and G. Pantelias, "Mechanisms of dna double strand break repair and chromosome aberration formation," *Cytogenet Genome Res*, vol. 104, pp. 14–20, Jan 2004.

[54] M. McVey and S. E. Lee, "Mmej repair of double-strand breaks (director's cut): deleted sequences and alternative endings," *Trends Genet*, vol. 24, pp. 529–38, Nov 2008.

[55] S. Kuhfittig-Kulle, E. Feldmann, A. Odersky, A. Kuliczkowska, W. Goedecke, A. Eggert, and P. Pfeiffer, "The mutagenic potential of non-homologous end joining in the absence of the nhej core factors ku70/80, dna-pkcs and xrcc4-ligiv," *Mutagenesis*, vol. 22, pp. 217–33, May 2007.

[56] J. Guirouilh-Barbat, E. Rass, I. Plo, P. Bertrand, and B. S. Lopez, "Defects in xrcc4 and ku80 differentially affect the joining of distal nonhomologous ends," *Proc Natl Acad Sci USA*, vol. 104, pp. 20902–7, Dec 2007.

[57] R. Perrault, H. Wang, M. Wang, B. Rosidi, and G. Iliakis, "Backup pathways of nhej are suppressed by dna-pk," *J Cell Biochem*, vol. 92, pp. 781–94, Jul 2004.

51

[58] J. R. Walker, R. A. Corpina, and J. Goldberg, "Structure of the ku heterodimer bound to dna and its implications for double-strand break repair," *Nature*, vol. 412, pp. 607–14, Aug 2001.

[59] L. Spagnolo, A. Rivera-Calzada, L. H. Pearl, and O. Llorca, "Three-dimensional structure of the human dna-pkcs/ku70/ku80 complex assembled on dna and its implications for dna dsb repair," *Mol Cell*, vol. 22, pp. 511–9, May 2006.

[60] E. Feldmann, V. Schmiemann, W. Goedecke, S. Reichenberger, and P. Pfeiffer, "Dna double-strand break repair in cell-free extracts from ku80-deficient cells: implications for ku serving as an alignment factor in non-homologous dna end joining," *Nucleic Acids Research*, vol. 28, pp. 2585–96, Jul 2000.

[61] E. Weterings, N. S. Verkaik, H. T. Brüggenwirth, J. H. J. Hoeijmakers, and D. C. van Gent, "The role of dna dependent protein kinase in synapsis of dna ends," *Nucleic Acids Research*, vol. 31, pp. 7238–46, Dec 2003.

[62] M. Hammel, Y. Yu, B. L. Mahaney, B. Cai, R. Ye, B. M. Phipps, R. P. Rambo, G. L. Hura, M. Pelikan, S. So, R. M. Abolfath, D. J. Chen, S. P. Lees-Miller, and J. A. Tainer, "Ku and dna-dependent protein kinase dynamic conformations and assembly regulate dna binding and the initial non-homologous end joining complex," *The Journal of biological chemistry*, vol. 285, pp. 1414–23, Jan 2010.

[63] L. Chen, K. Trujillo, P. Sung, and A. E. Tomkinson, "Interactions of the dna ligase iv-xrcc4 complex with dna ends and the dna-dependent protein kinase," *The Journal of biological chemistry*, vol. 275, pp. 26196–205, Aug 2000.

[64] N. Uematsu, E. Weterings, K. ichi Yano, K. Morotomi-Yano, B. Jakob, G. Taucher-Scholz, P.-O. Mari, D. C. van Gent, B. P. C. Chen, and D. J. Chen, "Autophosphorylation of dna-pkcs regulates its dynamics at dna double-strand breaks," *The Journal of Cell Biology*, vol. 177, pp. 219–29, Apr 2007.

[65] Y. Nimura, T. Kawata, K. Uzawa, J. Okamura, C. Liu, M. Saito, H. Shimada, N. Seki, A. Nakagawara, H. Ito, T. Ochiai, and H. Tanzawa, "Silencing ku80

using small interfering rna enhanced radiation sensitivity in vitro and in vivo," *Int J Oncol*, vol. 30, pp. 1477–84, Jun 2007.

[66] I. M. I. Division, "Sroa benchmarking survey," tech. rep., IMV, 2004.

[67] M. D. Wyatt and D. L. Pittman, "Methylating agents and dna repair responses: Methylated bases and sources of strand breaks," *Chem. Res. Toxicol.*, vol. 19, pp. 1580–94, Dec 2006.

[68] V. S. Goldmacher, R. A. Cuzick, and W. G. Thilly, "Isolation and partial characterization of human cell mutants differing in sensitivity to killing and mutation by methylnitrosourea and n-methyl-n'-nitro-n-nitrosoguanidine," *The Journal of biological chemistry*, vol. 261, pp. 12462–71, Sep 1986.

[69] M. E. Hegi, L. Liu, J. G. Herman, R. Stupp, W. Wick, M. Weller, M. P. Mehta, and M. R. Gilbert, "Correlation of o6-methylguanine methyltransferase (mgmt) promoter methylation with clinical outcomes in glioblastoma and clinical strategies to modulate mgmt activity," *J Clin Oncol*, vol. 26, pp. 4189–99, Sep 2008.

[70] R. Trivedi, K. Almeida, J. Fornsaglio, S. Schamus, and R. Sobol, "The role of base excision repair in the sensitivity and resistance to temozolomide-mediated cell death," *Cancer Research*, vol. 65, no. 14, p. 6394, 2005.

[71] B. Engelward, G. Weeda, M. Wyatt, J. Broekhof, J. de Wit, I. Donker, J. Allan, B. Gold, J. Hoeijmakers, and L. Samson, "Base excision repair deficient mice lacking the aag alkyladenine dna glycosylase," *Proc Natl Acad Sci USA*, vol. 94, no. 24, p. 13087, 1997.

[72] H.-Y. Hu, J. K. Horton, M. R. Gryk, R. Prasad, J. M. Naron, D.-A. Sun, S. M. Hecht, S. H. Wilson, and G. P. Mullen, "Identification of small molecule synthetic inhibitors of dna polymerase beta by nmr chemical shift mapping," *The Journal of biological chemistry*, vol. 279, pp. 39736–44, Sep 2004.

[73] A. S. Jaiswal, S. Banerjee, H. Panda, C. D. Bulkin, T. Izumi, F. H. Sarkar, D. A. Ostrov, and S. Narayan, "A novel inhibitor of dna polymerase beta enhances

the ability of temozolomide to impair the growth of colon cancer cells," *Mol Cancer Res*, vol. 7, pp. 1973–83, Dec 2009.

[74] S. H. Wilson, W. A. Beard, D. D. Shock, V. K. Batra, N. A. Cavanaugh, R. Prasad, E. W. Hou, Y. Liu, K. Asagoshi, J. K. Horton, D. F. Stefanick, P. S. Kedar, M. J. Carrozza, A. Masaoka, and M. L. Heacock, "Base excision repair and design of small molecule inhibitors of human dna polymerase ," *Cell Mol Life Sci*, vol. 67, pp. 3633–47, Nov 2010.

[75] A. R. Evans, M. Limp-Foster, and M. R. Kelley, "Going ape over ref-1," *Mutat Res*, vol. 461, pp. 83–108, Oct 2000.

[76] S. Madhusudan, F. Smart, P. Shrimpton, J. L. Parsons, L. Gardiner, S. Houlbrook, D. C. Talbot, T. Hammonds, P. A. Freemont, M. J. E. Sternberg, G. L. Dianov, and I. D. Hickson, "Isolation of a small molecule inhibitor of dna base excision repair," *Nucleic Acids Research*, vol. 33, pp. 4711–24, Jan 2005.

[77] M. L. Fishel, Y. He, M. L. Smith, and M. R. Kelley, "Manipulation of base excision repair to sensitize ovarian cancer cells to alkylating agent temozolomide," *Clinical Cancer Research*, vol. 13, pp. 260–267, Jan 2007.

[78] A. Simeonov, A. Kulkarni, D. Dorjsuren, A. Jadhav, M. Shen, D. R. McNeill, C. P. Austin, and D. M. Wilson, "Identification and characterization of inhibitors of human apurinic/apyrimidinic endonuclease ape1," *PLoS ONE*, vol. 4, p. e5740, Jan 2009.

[79] S. Madhusudan and I. Hickson, "Dna repair inhibition: a selective tumour targeting strategy," *Trends in Molecular Medicine*, vol. 11, pp. 503–511, Nov 2005.

[80] M. J. O'Connor, N. M. B. Martin, and G. C. M. Smith, "Targeted cancer therapies based on the inhibition of dna strand break repair," *Oncogene*, vol. 26, pp. 7816–24, Dec 2007.

54

[81] N. Curtin, "Therapeutic potential of drugs to modulate dna repair in cancer," *Expert Opin Ther Targets*, vol. 11, pp. 783–99, Jun 2007.

[82] G. M. Ross, J. J. Eady, N. P. Mithal, C. Bush, G. G. Steel, P. A. Jeggo, and T. J. McMillan, "Dna strand break rejoining defect in xrs-6 is complemented by transfection with the human ku80 gene," *Cancer Research*, vol. 55, pp. 1235–8, Mar 1995.

[83] M. A. Stackhouse and J. S. Bedford, "An ionizing radiation-sensitive mutant of cho cells: irs-20. i. isolation and initial characterization," *Radiat Res*, vol. 136, pp. 241–9, Nov 1993.

[84] Y. Gao, J. Chaudhuri, C. Zhu, L. Davidson, D. T. Weaver, and F. W. Alt, "A targeted dna-pkcs-null mutation reveals dna-pk-independent functions for ku in v(d)j recombination," *Immunity*, vol. 9, pp. 367–76, Sep 1998.

[85] I. S. Committee, "Genotoxicity testing and data interpretation for pharmaceuticals intended for human use," tech. rep., FDA, 2008.

[86] C. M. Kelly and J. J. Latimer, "Unscheduled dna synthesis: a functional assay for global genomic nucleotide excision repair," *Methods Mol Biol*, vol. 291, pp. 303–20, Jan 2005.

[87] N. Joshi and S. G. Grant, "Dna double-strand break damage and repair assessed by pulsed-field gel electrophoresis," *Methods Mol Biol*, vol. 291, pp. 121–9, Jan 2005.

[88] L. J. Kuo and L.-X. Yang, "Gamma-h2ax - a novel biomarker for dna double-strand breaks," *In Vivo*, vol. 22, pp. 305–9, Jan 2008.

[89] A. Kinner, W. Wu, C. Staudt, and G. Iliakis, "Gamma-h2ax in recognition and signaling of dna double-strand breaks in the context of chromatin," *Nucleic Acids Research*, vol. 36, pp. 5678–94, Oct 2008.

[90] J. Fillingham, M.-C. Keogh, and N. J. Krogan, "γh2ax and its role in dna double-strand break repair," *Biochem. Cell Biol.*, vol. 84, pp. 568–577, Jan 2006.

[91] K. Rothkamm and S. Horn, "gamma-h2ax as protein biomarker for radiation exposure," *Ann Ist Super Sanita*, vol. 45, pp. 265–71, Jan 2009.

[92] K. Rothkamm and M. Löbrich, "Evidence for a lack of dna double-strand break repair in human cells exposed to very low x-ray doses," *Proc Natl Acad Sci USA*, vol. 100, pp. 5057–62, Apr 2003.

[93] Y.-N. Hou, A. Lavaf, D. Huang, S. Peters, R. Huq, V. Friedrich, B. S. Rosenstein, and J. Kao, "Development of an automated gamma-h2ax immunocytochemistry assay," *Radiat Res*, vol. 171, pp. 360–7, Mar 2009.

[94] D. Avondoglio, T. Scott, W. J. Kil, M. Sproull, P. J. Tofilon, and K. Camphausen, "High throughput evaluation of gamma-h2ax," *Radiat Oncol*, vol. 4, p. 31, Jan 2009.

[95] S. Kim, D. H. Jun, H. J. Kim, K.-C. Jeong, and C.-H. Lee, "Development of a high-content screening method for chemicals modulating dna damage response," *J Biomol Screen*, vol. 16, pp. 259–65, Feb 2011.

[96] G. Garty, Y. Chen, H. C. Turner, J. Zhang, O. V. Lyulko, A. Bertucci, Y. Xu, H. Wang, N. Simaan, G. Randers-Pehrson, Y. L. Yao, and D. J. Brenner, "The rabit: A rapid automated biodosimetry tool for radiological triage. ii. technological developments," *International Journal of Radiation Biology*, pp. 1–15, May 2011.

[97] J. An, Y.-C. Huang, Q.-Z. Xu, L.-J. Zhou, Z.-F. Shang, B. Huang, Y. Wang, X.-D. Liu, D.-C. Wu, and P.-K. Zhou, "Dna-pkcs plays a dominant role in the regulation of h2ax phosphorylation in response to dna damage and cell cycle progression," *BMC Mol Biol*, vol. 11, p. 18, Jan 2010.

[98] I. B. Nazarov, A. N. Smirnova, R. I. Krutilina, M. P. Svetlova, L. V. Solovjeva, A. A. Nikiforov, S.-L. Oei, I. A. Zalenskaya, P. M. Yau, E. M. Bradbury, and N. V. Tomilin, "Dephosphorylation of histone gamma-h2ax during repair of dna double-strand breaks in mammalian cells and its inhibition by calyculin a," *Radiat Res*, vol. 160, pp. 309–17, Sep 2003.

[99] M. Löbrich, A. Shibata, A. Beucher, A. Fisher, M. Ensminger, A. A. Goodarzi, O. Barton, and P. A. Jeggo, "gammah2ax foci analysis for monitoring dna double-strand break repair: strengths, limitations and optimization," *Cell Cycle*, vol. 9, pp. 662–9, Feb 2010.

[100] F. Bouquet, C. Muller, and B. Salles, "The loss of gammah2ax signal is a marker of dna double strand breaks repair only at low levels of dna damage," *Cell Cycle*, vol. 5, pp. 1116–22, May 2006.

[101] D. Chowdhury, M.-C. Keogh, H. Ishii, C. L. Peterson, S. Buratowski, and J. Lieberman, "gamma-h2ax dephosphorylation by protein phosphatase 2a facilitates dna double-strand break repair," *Mol Cell*, vol. 20, pp. 801–9, Dec 2005.

[102] M. Ishidate, K. F. Miura, and T. Sofuni, "Chromosome aberration assays in genetic toxicology testing in vitro," *Mutat Res*, vol. 404, pp. 167–72, Aug 1998.

[103] H. Norppa, S. Bonassi, I.-L. Hansteen, L. Hagmar, U. Strömberg, P. Rössner, P. Boffetta, C. Lindholm, S. Gundy, J. Lazutka, A. Cebulska-Wasilewska, E. Fabiánová, R. J. Srám, L. E. Knudsen, R. Barale, and A. Fucic, "Chromosomal aberrations and sces as biomarkers of cancer risk," *Mutat Res*, vol. 600, pp. 37–45, Aug 2006.

[104] S. Conrad, J. Künzel, and M. Löbrich, "Sister chromatid exchanges occur in g2-irradiated cells," *Cell Cycle*, vol. 10, pp. 222–8, Jan 2011.

[105] Y. Asakawa and E. Gotoh, "A method for detecting sister chromatid exchanges using prematurely condensed chromosomes and immunogold-silver staining," *Mutagenesis*, vol. 12, pp. 175–7, May 1997.

[106] A. Wojcik, E. Bruckmann, and G. Obe, "Insights into the mechanisms of sister chromatid exchange formation," *Cytogenet Genome Res*, vol. 104, pp. 304–9, Jan 2004.

[107] W. Schmid, "The micronucleus test," *Mutat Res*, vol. 31, pp. 9–15, Feb 1975.

[108] M. Kirsch-Volders, G. Plas, A. Elhajouji, M. Lukamowicz, L. Gonzalez, K. V. Loock, and I. Decordier, "The in vitro mn assay in 2011: origin and fate, biological significance, protocols, high throughput methodologies and toxicological relevance," *Arch Toxicol*, vol. 85, pp. 873–99, Aug 2011.

[109] S. M. Piperakis, "Comet assay: A brief history," *Cell Biol Toxicol*, vol. 25, pp. 1–3, Feb 2009.

[110] A. Dhawan, M. Bajpayee, and D. Parmar, "Comet assay: a reliable tool for the assessment of dna damage in different models," *Cell Biol Toxicol*, vol. 25, pp. 5–32, Feb 2009.

[111] P. Olive and J. Banáth, "The comet assay: a method to measure dna damage in individual cells," *Nat Meth*, vol. 1, no. 1, pp. 23–29, 2006.

[112] L. A. Loeb and B. D. Preston, "Mutagenesis by apurinic/apyrimidinic sites," *Annu Rev Genet*, vol. 20, pp. 201–30, Jan 1986.

[113] M. Wojewódzka, I. Buraczewska, and M. Kruszewski, "A modified neutral comet assay: elimination of lysis at high temperature and validation of the assay with anti-single-stranded dna antibody," *Mutat Res*, vol. 518, pp. 9–20, Jun 2002.

[114] V. Spanswick, J. Hartley, T. Ward, and J. Hartley, "Measurement of drug-induced dna interstrand crosslinking using the single cell gel electrophoresis (comet) assay," *Methods in molecular medicine*, vol. 28, pp. 143–154, 1999.

[115] A. R. Collins, V. L. Dobson, M. Dusinská, G. Kennedy, and R. Stětina, "The comet assay: what can it really tell us?," *Mutat Res*, vol. 375, pp. 183–93, Apr 1997.

[116] A. R. Trzeciak, J. Barnes, and M. K. Evans, "A modified alkaline comet assay for measuring dna repair capacity in human populations," *Radiat Res*, vol. 169, pp. 110–21, Jan 2008.

[117] F. Kassie, W. Parzefall, and S. Knasmüller, "Single cell gel electrophoresis assay: a new technique for human biomonitoring studies," *Mutat Res*, vol. 463, pp. 13–31, Jul 2000.

[118] G. Speit, "Investigations on the effect of cigarette smoking in the comet assay," *Mutation Research/Genetic Toxicology and Environmental Mutagenesis*, vol. 542, pp. 33–42, Dec 2003.

[119] H. Hoffmann, "The effect of smoking on dna effects in the comet assay: a meta-analysis," *Mutagenesis*, vol. 20, pp. 455–466, Aug 2005.

[120] M. Dusinska and A. R. Collins, "The comet assay in human biomonitoring: gene-environment interactions," *Mutagenesis*, vol. 23, pp. 191–205, May 2008.

[121] M. D. Vodenicharov, F. R. Sallmann, M. S. Satoh, and G. G. Poirier, "Base excision repair is efficient in cells lacking poly(adp-ribose) polymerase 1," *Nucleic Acids Research*, vol. 28, pp. 3887–96, Oct 2000.

[122] L. H. Thompson and M. G. West, "Xrcc1 keeps dna from getting stranded," *Mutat Res*, vol. 459, pp. 1–18, Feb 2000.

[123] C. Ryk, M. N. Routledge, J. M. Allan, C. P. Wild, R. Kumar, B. Lambert, and S. Hou, "Influence of dna repair gene polymorphisms on the initial repair of mms-induced dna damage in human lymphocytes as measured by the alkaline comet assay," *Environ. Mol. Mutagen.*, vol. 49, pp. 669–75, Dec 2008.

[124] E. Synowiec, J. Stefanska, Z. Morawiec, J. Blasiak, and K. Wozniak, "Association between dna damage, dna repair genes variability and clinical characteristics in breast cancer patients," *Mutat Res*, vol. 648, pp. 65–72, Dec 2008.

[125] Y. Zhu, H. Yang, Q. Chen, J. Lin, H. B. Grossman, C. P. Dinney, X. Wu, and J. Gu, "Modulation of dna damage/dna repair capacity by xpc polymorphisms," *DNA Repair*, vol. 7, pp. 141–8, Feb 2008.

[126] A. L. Miranda-Vilela, P. C. Alves, A. K. Akimoto, G. S. Lordelo, C. A. Gonçalves, C. K. Grisolia, and M. N. Klautau-Guimarães, "Gene polymorphisms against dna damage induced by hydrogen peroxide in leukocytes of healthy humans through comet assay: a quasi-experimental study," *Environ Health*, vol. 9, p. 21, Jan 2010.

[127] J. Slyskova, A. Naccarati, V. Polakova, B. Pardini, L. Vodickova, R. Stetina, J. Schmuczerova, Z. Smerhovsky, L. Lipska, and P. Vodicka, "Dna damage and nucleotide excision repair capacity in healthy individuals," *Environ. Mol. Mutagen.*, Apr 2011.

[128] M. Berwick and P. Vineis, "Markers of dna repair and susceptibility to cancer in humans: an epidemiologic review," *J Natl Cancer Inst*, vol. 92, pp. 874–97, Jun 2000.

[129] F. Marcon, "Assessment of individual sensitivity to ionizing radiation and dna repair efficiency in a healthy population," *Mutation Research/Genetic Toxicology and Environmental Mutagenesis*, vol. 541, pp. 1–8, Nov 2003.

[130] H.-K. Wong and D. M. Wilson, "Xrcc1 and dna polymerase beta interaction contributes to cellular alkylating-agent resistance and single-strand break repair," *J Cell Biochem*, vol. 95, pp. 794–804, Jul 2005.

[131] G. R. Wasson, V. J. McKelvey-Martin, and C. S. Downes, "The use of the comet assay in the study of human nutrition and cancer," *Mutagenesis*, vol. 23, pp. 153–62, May 2008.

[132] C. M. Gedik, S. P. Boyle, S. G. Wood, N. J. Vaughan, and A. R. Collins, "Oxidative stress in humans: validation of biomarkers of dna damage," *Carcinogenesis*, vol. 23, pp. 1441–6, Sep 2002.

[133] A. R. Collins, A. A. Oscoz, G. Brunborg, I. Gaivao, L. Giovannelli, M. Kruszewski, C. C. Smith, and R. Stetina, "The comet assay: topical issues," *Mutagenesis*, vol. 23, pp. 143–151, Feb 2008.

[134] S. Loft, P. H. Danielsen, L. Mikkelsen, L. Risom, L. Forchhammer, and P. Møller, "Biomarkers of oxidative damage to dna and repair," *Biochem. Soc. Trans*, vol. 36, pp. 1071–6, Oct 2008.

[135] A. Azqueta, Y. Lorenzo, and A. R. Collins, "In vitro comet assay for dna repair: a warning concerning application to cultured cells," *Mutagenesis*, vol. 24, pp. 379–81, Jul 2009.

[136] A. L. Dunne, M. E. Price, C. Mothersill, S. R. Mckeown, T. Robson, and D. G. Hirst, "Relationship between clonogenic radiosensitivity, radiation-induced apoptosis and dna damage/repair in human colon cancer cells," *Br J Cancer*, vol. 89, pp. 2277–2283, Dec 2003.

[137] D. J. McKenna, S. R. McKeown, and V. J. McKelvey-Martin, "Potential use of the comet assay in the clinical management of cancer," *Mutagenesis*, vol. 23, pp. 183–90, May 2008.

[138] A. Hartmann, M. Schumacher, U. Plappert-Helbig, P. Lowe, W. Suter, and L. Mueller, "Use of the alkaline in vivo comet assay for mechanistic genotoxicity investigations," *Mutagenesis*, vol. 19, pp. 51–9, Jan 2004.

[139] L. Henderson, A. Wolfreys, J. Fedyk, C. Bourner, and S. Windebank, "The ability of the comet assay to discriminate between genotoxins and cytotoxins," *Mutagenesis*, vol. 13, pp. 89–94, Jan 1998.

[140] R. R. Tice, E. Agurell, D. Anderson, B. Burlinson, A. Hartmann, H. Kobayashi, Y. Miyamae, E. Rojas, J. C. Ryu, and Y. F. Sasaki, "Single cell gel/comet

assay: guidelines for in vitro and in vivo genetic toxicology testing," *Environ. Mol. Mutagen.*, vol. 35, pp. 206–21, Jan 2000.

[141] A. Hartmann, E. Agurell, C. Beevers, S. Brendler-Schwaab, B. Burlinson, P. Clay, A. Collins, A. Smith, G. Speit, V. Thybaud, R. R. Tice, and 4th International Comet Assay Workshop, "Recommendations for conducting the in vivo alkaline comet assay. 4th international comet assay workshop," *Mutagenesis*, vol. 18, pp. 45–51, Jan 2003.

[142] G. Speit and A. Hartmann, "The comet assay: a sensitive genotoxicity test for the detection of dna damage," *Methods Mol Biol*, vol. 291, pp. 85–95, Jan 2005.

[143] S. Brendler-Schwaab, "The in vivo comet assay: use and status in genotoxicity testing," *Mutagenesis*, vol. 20, pp. 245–254, May 2005.

[144] Y. Sasaki, T. Nakamura, and S. Kawaguchi, "What is better experimental design for in vitro comet assay to detect chemical genotoxicity?," *Japanese Society for Alternatives to Animal Experiments*, 2008.

[145] S. Pfuhler, M. Fellows, J. van Benthem, R. Corvi, R. Curren, K. Dearfield, P. Fowler, R. Frötschl, A. Elhajouji, L. L. Hégarat, T. Kasamatsu, H. Kojima, G. Ouédraogo, A. Scott, and G. Speit, "In vitro genotoxicity test approaches with better predictivity: Summary of an iwgt workshop," *Mutat Res*, vol. 723, pp. 101–7, Aug 2011.

[146] A. Hartmann, A. Elhajouji, E. Kiskinis, F. Poetter, H. Martus, A. Fjällman, W. Frieauff, and W. Suter, "Use of the alkaline comet assay for industrial genotoxicity screening: comparative investigation with the micronucleus test," *Food Chem Toxicol*, vol. 39, pp. 843–58, Aug 2001.

[147] E. Giannotti, L. Vandin, P. Repeto, and R. Comelli, "A comparison of the in vitro comet assay with the in vitro chromosome aberration assay using whole human blood or chinese hamster lung cells: validation study using a range of novel pharmaceuticals," *Mutagenesis*, vol. 17, pp. 163–70, Mar 2002.

[148] S. Kawaguchi, T. Nakamura, A. Yamamoto, G. Honda, and Y. F. Sasaki, "Is the comet assay a sensitive procedure for detecting genotoxicity?," *J Nucleic Acids*, vol. 2010, p. 541050, Jan 2010.

[149] D. J. Kirkland and L. Müller, "Interpretation of the biological relevance of genotoxicity test results: the importance of thresholds," *Mutat Res*, vol. 464, pp. 137–47, Jan 2000.

[150] M. Z. Vasquez, "Combining the in vivo comet and micronucleus assays: a practical approach to genotoxicity testing and data interpretation," *Mutagenesis*, vol. 25, pp. 187–99, Mar 2010.

[151] A. R. Collins, "The comet assay for dna damage and repair: principles, applications, and limitations," *Mol Biotechnol*, vol. 26, pp. 249–61, Mar 2004.

[152] P. Moller, "Assessment of reference values for dna damage detected by the comet assay in human blood cell dna," *Mutation Research/Reviews in Mutation Research*, vol. 612, pp. 84–104, Mar 2006.

[153] A. Stang and I. Witte, "Performance of the comet assay in a high-throughput version," *Mutat Res*, vol. 675, pp. 5–10, Apr 2009.

[154] M. Zainol, J. Stoute, G. M. Almeida, A. Rapp, K. J. Bowman, G. D. D. Jones, and ECVAG, "Introducing a true internal standard for the comet assay to minimize intra- and inter-experiment variability in measures of dna damage and repair," *Nucleic Acids Research*, vol. 37, p. e150, Dec 2009.

[155] G. Dehon, L. Catoire, P. Duez, P. Bogaerts, and J. Dubois, "Validation of an automatic comet assay analysis system integrating the curve fitting of combined comet intensity profiles," *Mutat Res*, vol. 650, pp. 87–95, Feb 2008.

[156] D. G. McArt, G. R. Wasson, G. Mckerr, K. Saetzler, M. Reed, and C. V. Howard, "Systematic random sampling of the comet assay," *Mutagenesis*, vol. 24, pp. 373–8, Jul 2009.

[157] T. S. Kumaravel, B. Vilhar, S. P. Faux, and A. N. Jha, "Comet assay measurements: a perspective," *Cell Biol Toxicol*, vol. 25, pp. 53–64, Feb 2009.

[158] A. Azqueta, S. Meier, C. Priestley, K. B. Gutzkow, G. Brunborg, J. Sallette, F. Soussaline, and A. Collins, "The influence of scoring method on variability in results obtained with the comet assay," *Mutagenesis*, vol. 26, pp. 393–9, May 2011.

[159] D. P. Lovell and T. Omori, "Statistical issues in the use of the comet assay," *Mutagenesis*, vol. 23, pp. 171–182, Feb 2008.

[160] L. Forchhammer, C. Johansson, S. Loft, L. Möller, R. W. L. Godschalk, S. A. S. Langie, G. D. D. Jones, R. W. L. Kwok, A. R. Collins, A. Azqueta, D. H. Phillips, O. Sozeri, M. Stepnik, J. Palus, U. Vogel, H. Wallin, M. N. Routledge, C. Handforth, A. Allione, G. Matullo, J. P. Teixeira, S. Costa, P. Riso, M. Porrini, and P. Møller, "Variation in the measurement of dna damage by comet assay measured by the ecvagdagger inter-laboratory validation trial," *Mutagenesis*, vol. 25, pp. 113–23, Mar 2010.

[161] P. Møller, L. Möller, R. W. L. Godschalk, and G. D. D. Jones, "Assessment and reduction of comet assay variation in relation to dna damage: studies from the european comet assay validation group," *Mutagenesis*, vol. 25, pp. 109–11, Mar 2010.

[162] C. Johansson, P. Møller, L. Forchhammer, S. Loft, R. W. L. Godschalk, S. A. S. Langie, S. Lumeij, G. D. D. Jones, R. W. L. Kwok, A. Azqueta, D. H. Phillips, O. Sozeri, M. N. Routledge, A. J. Charlton, P. Riso, M. Porrini, A. Allione, G. Matullo, J. Palus, M. Stepnik, A. R. Collins, and L. Möller, "An ecvag trial on assessment of oxidative damage to dna measured by the comet assay," *Mutagenesis*, vol. 25, pp. 125–32, Mar 2010.

[163] E. Kiskinis, W. Suter, and A. Hartmann, "High throughput comet assay using 96-well plates," *Mutagenesis*, vol. 17, pp. 37–43, Jan 2002.

[164] N. P. Singh, R. R. Tice, R. E. Stephens, and E. L. Schneider, "A microgel electrophoresis technique for the direct quantitation of dna damage and repair in individual fibroblasts cultured on microscope slides," *Mutat Res*, vol. 252, pp. 289–96, Jun 1991.

[165] S. J. Wiklund and E. Agurell, "Aspects of design and statistical analysis in the comet assay," *Mutagenesis*, vol. 18, pp. 167–75, Mar 2003.

[166] S. Lindström and H. Andersson-Svahn, "Overview of single-cell analyses: microdevices and applications," *Lab Chip*, vol. 10, pp. 3363–72, Dec 2010.

[167] S. N. Bhatia, M. Toner, R. G. Tompkins, and M. L. Yarmush, "Selective adhesion of hepatocytes on patterned surfaces," *Annals of the New York Academy of Sciences*, vol. 745, pp. 187–209, Nov 1994.

[168] K. Leong, A. K. Boardman, H. Ma, and A. K.-Y. Jen, "Single-cell patterning and adhesion on chemically engineered poly(dimethylsiloxane) surface," *Langmuir*, vol. 25, pp. 4615–4620, Apr 2009.

[169] H.-C. Moeller, M. K. Mian, S. Shrivastava, B. G. Chung, and A. Khademhosseini, "A microwell array system for stem cell culture," *Biomaterials*, vol. 29, pp. 752–63, Feb 2008.

[170] S. Lindström and H. Andersson-Svahn, "Miniaturization of biological assays – overview on microwell devices for single-cell analyses," *Biochim Biophys Acta*, vol. 1810, pp. 308–16, Mar 2011.

[171] T. Helleday, J. Lo, D. Vangent, and B. Engelward, "Dna double-strand break repair: From mechanistic understanding to cancer treatment," *DNA Repair*, vol. 6, pp. 923–935, Jul 2007.

[172] J. T. Mutamba, *XRCC1 and DNA MTases: Direct and Indirect Modulation of Inflammation-Induced DNA Damage*. PhD thesis, Massachusetts Institute of Technology, 77 Massachusetts Avenue, Cambridge, MA 02139, May 2011.

[173] O. D. Schärer, "Chemistry and biology of dna repair," *Angew Chem Int Ed Engl*, vol. 42, pp. 2946–74, Jul 2003.

[174] A. Guainazzi, A. J. Campbell, T. Angelov, C. Simmerling, and O. D. Schärer, "Synthesis and molecular modeling of a nitrogen mustard dna interstrand crosslink," *Chemistry*, vol. 16, pp. 12100–3, Oct 2010.

[175] M. Raschle, P. Knipscheer, M. Enoiu, T. Angelov, J. Sun, J. Griffith, T. Ellenberger, O. Scharer, and J. Walter, "Mechanism of replication-coupled dna interstrand crosslink repair," *Cell*, vol. 134, pp. 969–980, Sep 2008.
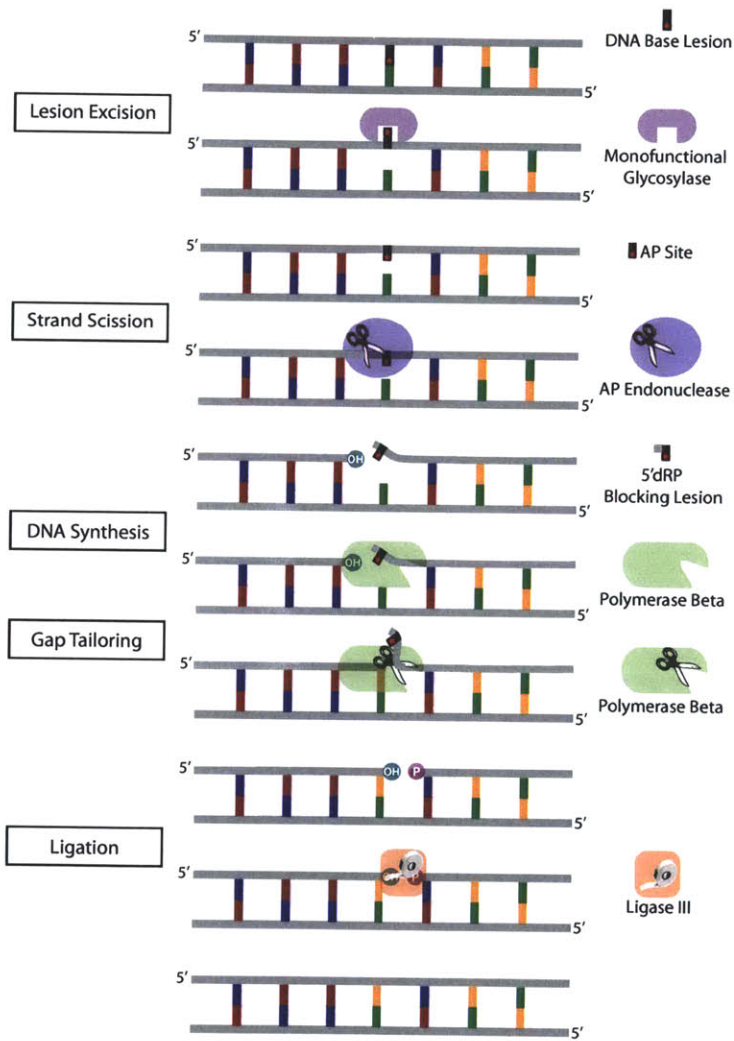
Figure 1-1: **Model of Short-patch Monofunctional Glycosylase Mediated Base Excision Repair (BER).** Adapted from [173].

1) Damage recognition

2) TFIIH binding
Partial helix opening

3) Full helix opening
Damage verification

4) 5' cleavage
by ERCC1-XPF

5) Recruitment of
RFC, PCNA and
polymerase δ/ε
3' cleavage by XPG

6) Completion of
repair synthesis

7) Ligation by
Ligase I or III
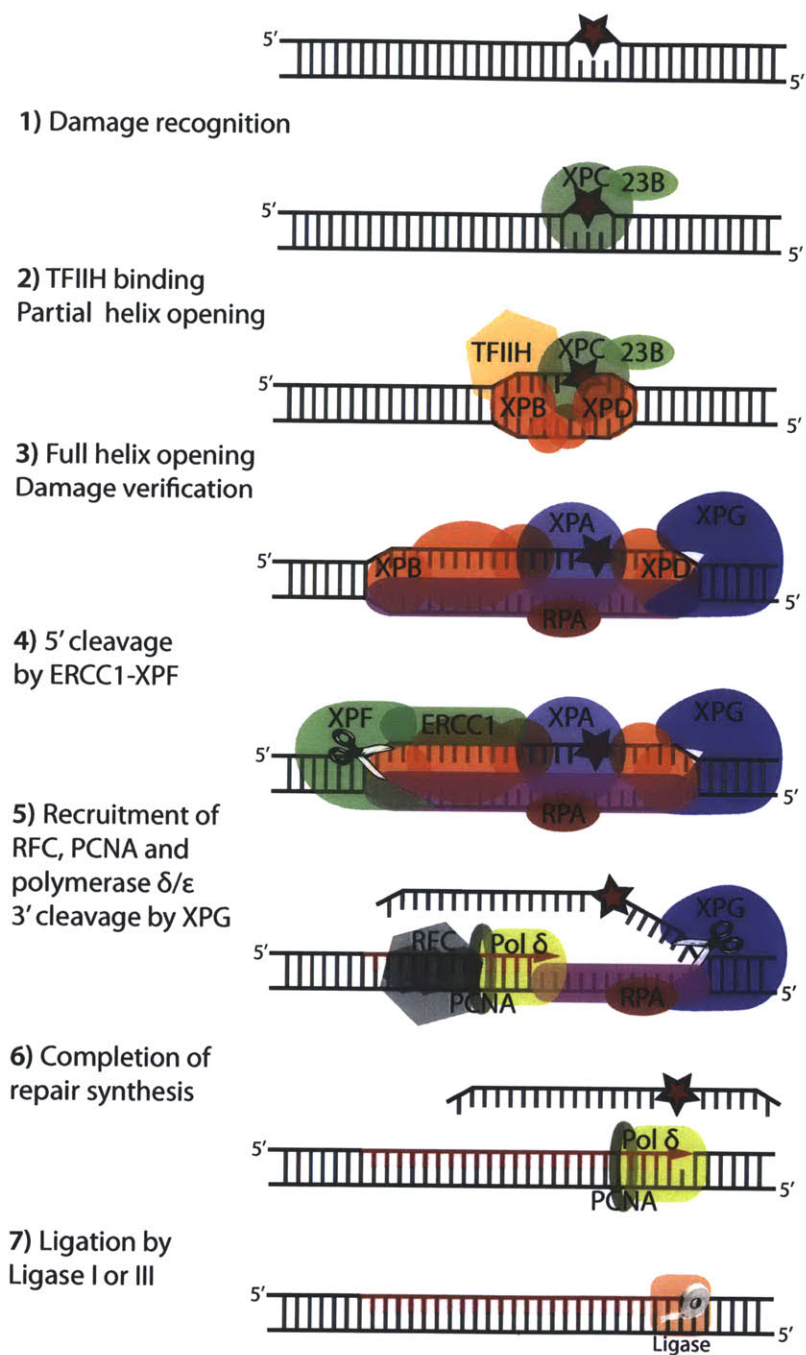
Figure 1-2: **Model of Global Genome Nucleotide Excision Repair (NER).** Adapted from [45, 173].

Double Strand
Break Recognition

Ku70/Ku80

DNA-PK Formation
Strand Alignment
Autophosphorylation

DNA-PKcs

Recruitment of
Additional
NHEJ Proteins

XRCC4/Ligase IV
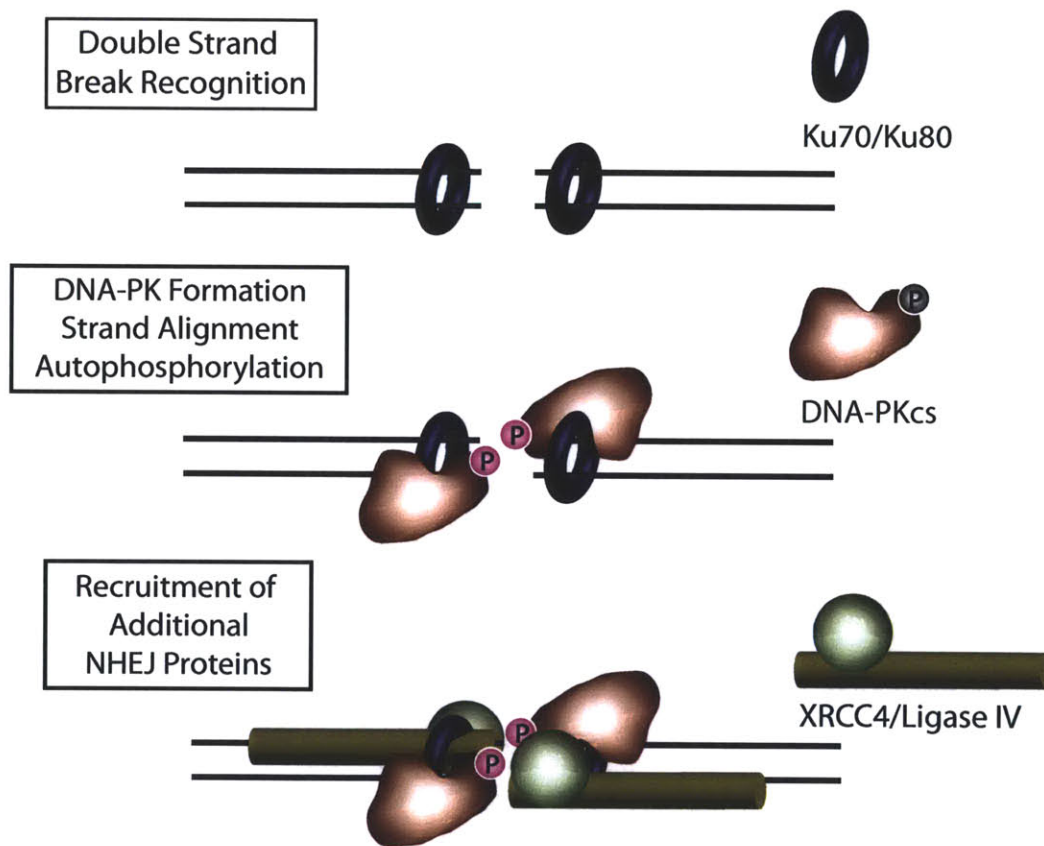
Figure 1-3: **Model of Non-homologous End Joining (NHEJ).**

(a)

DNA

ICL

DNA

(b)

Rightward Fork

Leftward Fork

Leading Strand

Lagging Strand

ICL
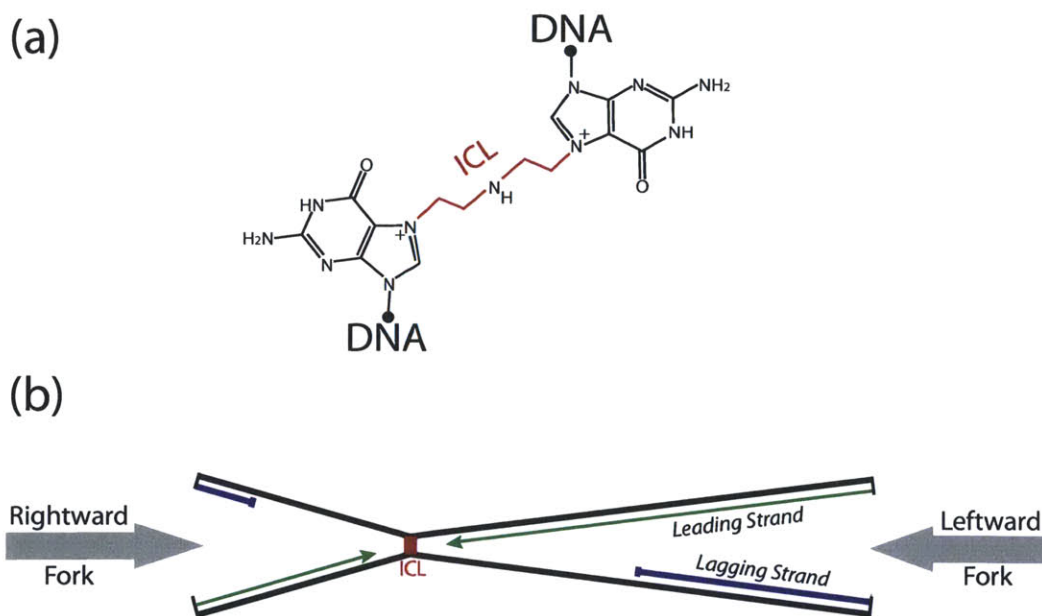
Figure 1-4: **Interstrand Crosslink (ICL) Structure and Recognition.** (a) ICL formed by nitrogen mustard between two guanine residues (N7 positions). Adapted from [174]. (b) Structure of ICL impeding DNA replication. Adapted from [175].
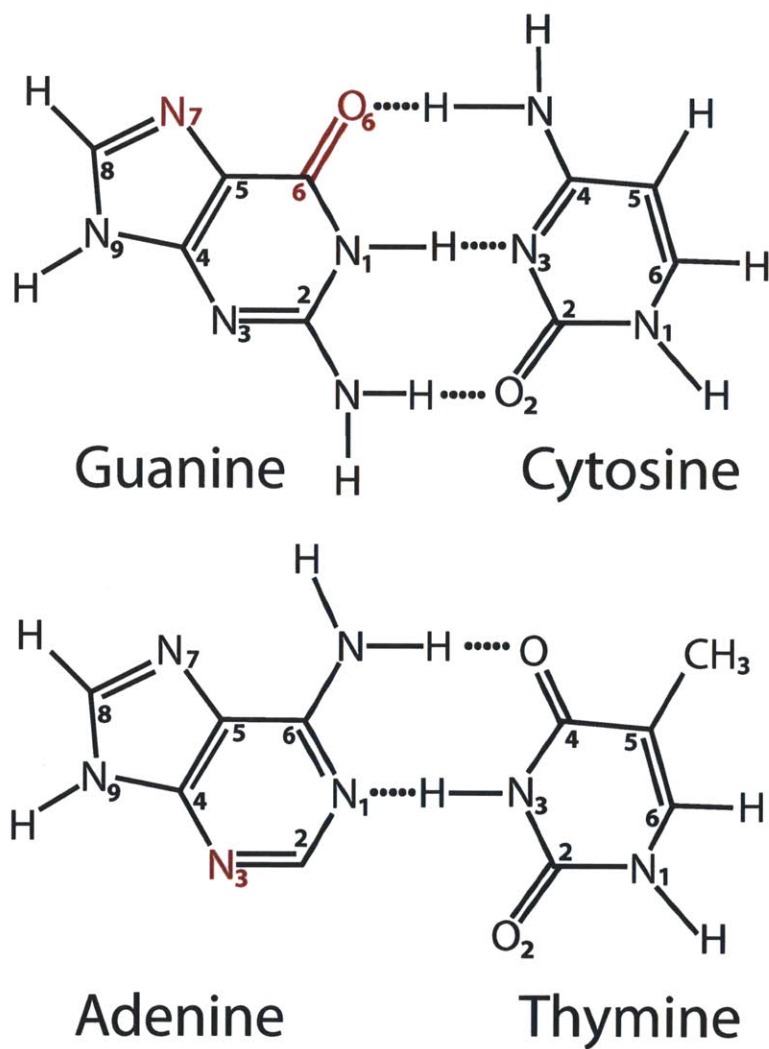
Figure 1-5: **Structure of DNA Bases.** N^7-guanine and N^3-adenine and O^6-guanine indicated in red as major targets of alkylation.
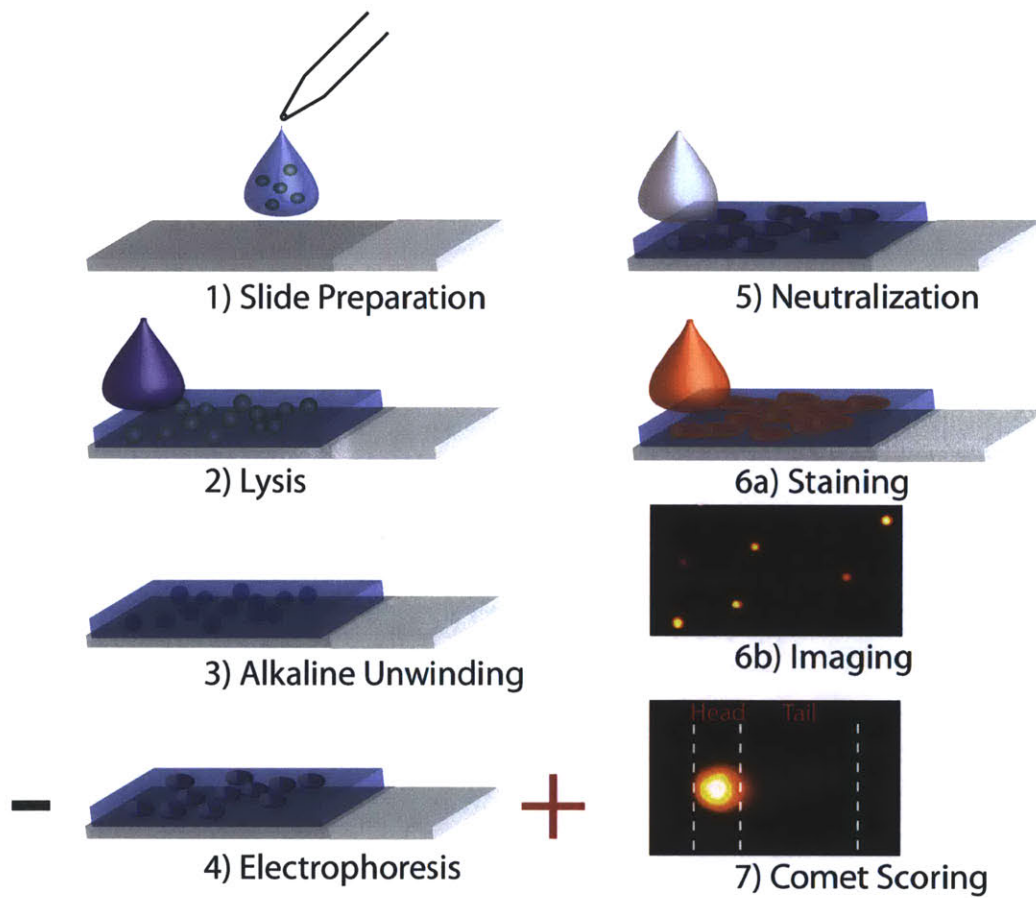
Figure 1-6: **Standard Comet Assay Protocol.** As described by [140].

1) Pour SU-8 on Wafer

SU-8 Photoresist

Silicon Wafer

2) Spin SU-8 Photoresist

Spinner

3) Shield with Mask

Transparency with
Micro-features

4) Crosslink SU-8 with UV

Broadband UV

5) Develop with Solvent

6) Cast PDMS from
Silicon/SU-8 Mold

7) PDMS Device

PDMS with Micro-Features
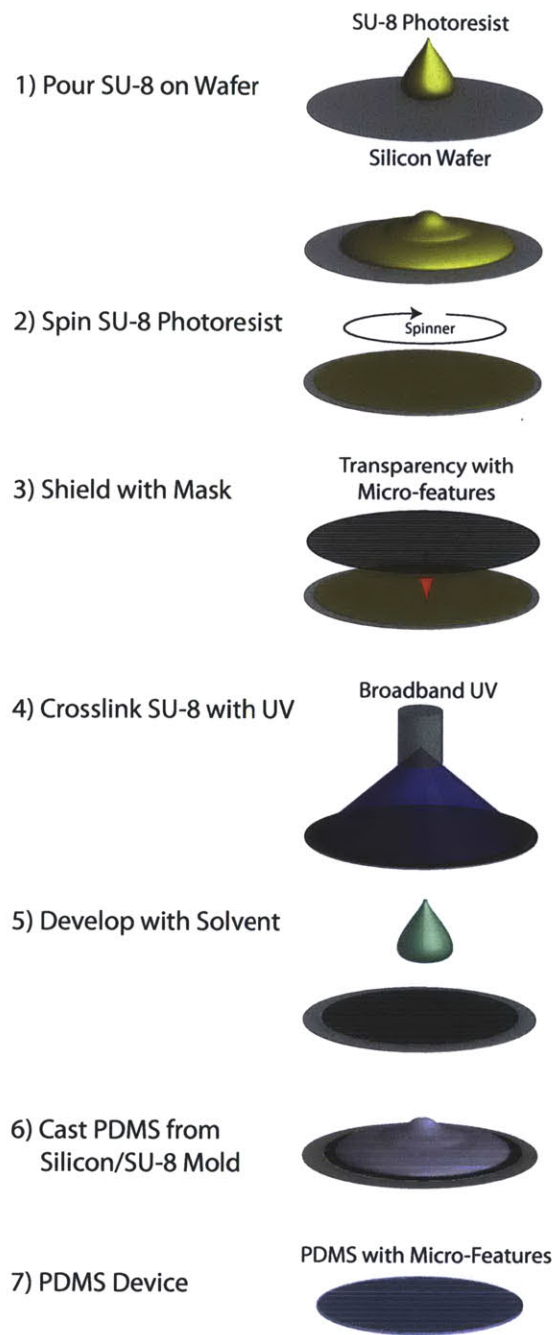
Figure 1-7: **Microfabrication of PDMS Mold using SU-8 Photolithography.**

Chapter 2

Single cell trapping and DNA damage analysis using microwell arrays

2.1 Abstract

With a direct link to cancer, aging, and heritable diseases as well as a critical role in cancer treatment, the importance of DNA damage is well established. The intense interest in DNA damage in applications ranging from epidemiology to drug development drives an urgent need for robust, high throughput, and inexpensive tools for objective, quantitative DNA damage analysis. We have developed a simple method for high throughput DNA damage measurements that provides information on multiple lesions and pathways. Our method utilizes single cells captured by gravity into a microwell array with DNA damage revealed morphologically by gel electrophoresis. Spatial encoding enables simultaneous assays of multiple experimental conditions performed in parallel with fully automated analysis. This method also enables novel functionalities, including multiplexed labeling for parallel single cell assays, as well as DNA damage measurement in cell aggregates. We have also developed 24- and 96-well versions, which are applicable to high throughput screening. Using this plat-

form, we have quantified DNA repair capacities of individuals with different genetic backgrounds, and compared the efficacy of potential cancer chemotherapeutics as inhibitors of a critical DNA repair enzyme, human AP endonuclease (APE-1). This platform enables high throughput assessment of multiple DNA repair pathways and subpathways in parallel, thus enabling new strategies for drug discovery, genotoxicity testing, and environmental health.

2.2 Introduction

DNA damage is a critical risk factor for cancer, aging, and heritable diseases [1, 2, 3], and it is the underlying basis for most frontline cancer therapies [4]. Increased knowledge about DNA damage and repair would facilitate disease prevention, identification of individuals at increased risk of cancer, discovery of novel therapeutics, and better drug safety testing. Despite their obvious translational impact, most DNA damage assays have not changed significantly in more than two decades, and thus are not compatible with modern high throughput screening technologies. In order to better assess the biological impact of damage, we need data that reflect the integrated effect of multiple DNA repair pathways and subpathways, in response to a range of DNA lesions, measured in an accurate and high throughput fashion.

The single cell gel electrophoresis or "comet" assay is based on the principle that relaxed loops (induced by single strand breaks (SSBs)) and DNA fragments migrate farther in an agarose gel than undamaged DNA [5, 6, 7, 8]. The alkali comet assay sensitively detects a range of DNA lesions, including strand breaks (single and double), as well as alkali sensitive sites. Although most base lesions are not directly detected, base adducts can be detected when converted to abasic sites or SSBs with the addition of purified DNA repair enzymes [7, 8, 9, 10, 11]. The comet assay has been used in a variety of applications, including genotoxicity testing, human biomonitoring and epidemiology, environmental health, and basic research on DNA damage and repair [7, 8, 12, 13, 14, 15, 16, 17, 18, 19]. Compared with other DNA damage assays [20, 21, 22], the comet assay is relatively inexpensive, is very sensitive, and can

assess the integrated cellular response to many kinds of DNA lesions simultaneously [7, 8, 19].

Wider acceptance of the comet assay has been limited, however, by low throughput; poor reproducibility between slides, users, and laboratories; and image processing and analysis methods that are laborious, time-consuming, and potentially biased. The need for improvement is widely recognized, and previous approaches include reducing space requirements for electrophoresis (CometAssay 96, Trevigen), using a multiwell format for treating samples [23], incorporating internal controls [24, 25], or improving imaging [26]. These methods address individual issues, but do not provide a comprehensive solution for DNA damage analysis.

Here we present a high throughput platform for DNA damage analysis with the sensitivity and versatility of the comet assay. We spatially register cells by capturing them into a microwell array patterned directly into agarose (Figure 2-1). This passive patterning method requires only gravity to capture cells and introduces minimal external stress. Array registration allows multiple experimental conditions to be spatially encoded on a single slide. Additionally, the microwells provide a new method for assessing DNA damage in collections of cells or cell aggregates. The arrays also facilitate fully automated imaging and analysis, requiring no user input or special equipment.

In order to facilitate the high throughput analysis of drugs, patient samples or other experimental conditions, we have also developed 24- and 96-well implementations of the microwell array, which can be integrated with standard high throughput screening (HTS) techniques. We have validated this platform in two key applications. By incorporating multiple cell types and multiple DNA repair time points on a single plate, we directly compare DNA repair kinetics between human lymphocytes from individuals with different genetic backgrounds. We also demonstrate how this assay could be used in the context of drug screening by comparing the performance of potential inhibitors of base excision repair (BER).

77

2.3 Materials and Methods

2.3.1 Cell Culture

TK6 human lymphoblasts were cultured in suspension in RPMI 1640 with L-glutamine and supplemented with 10% horse serum. OVCAR-8 human ovarian cancer cells were cultured in RPMI 1640 with L-glutamine and supplemented with 10% fetal bovine serum (FBS). Human B-lymphocyte lines from the NIGMS Human Genetic Cell Repository were obtained from the Coriell Institute. The lines GM15268, GM15242 and GM15224 were cultured in suspension in RMPI 1640 with L-glutamine and supplemented with 15% FBS. Primary hepatocytes were isolated from 2- to 3-month-old adult female Lewis rats (Charles River Laboratories, Wilmington, MA) weighing 180-200 g. Detailed procedures for hepatocyte isolation and purification have been described [27, 28]. Hepatocyte culture medium consisted of DMEM with high glucose, 10% (vol/vol) FBS, 0.5 units/ml insulin, 7 ng/ml glucagon, and 7.5 mg/ml hydrocortisone. All cell culture media were supplemented with 100 units/ml penicillin-streptomycin. Cytoplasmic staining of live cells in Figure 2-1c was done with Cell-Tracker (Green CMFDA and Orange CMRA, Invitrogen, Carlsbad, CA) according to the manufacturer's instructions.

2.3.2 Microwell Fabrication

The microwell molds were fabricated by lithographically patterning SU-8 photoresist (SU-8 2000 series, MicroChem Corp, Newton, MA) according to the manufacturer's instructions. Briefly, SU-8 was spun to the desired thickness onto silicon wafers. Soft-baking the resist was followed by broadband UV exposure through a transparency mask, which included transparent circular features of the desired microwell diameter on a dark background. Post-exposure bake and development in propylene glycol monomethyl ether acetate revealed the patterned SU-8 microposts. Micropost depth and width were varied from 20 - 50 mm to optimize well filling for various cell types. Microwells were cast from the molds as shown in Figure 2-1a. Molten 1% normal

melting point (NMP) agarose (Omnipur Agarose, Invitrogen Corp, Carlsbad, CA) was applied to a sheet of GelBond film (Lonza, Basel, Switzerland) and the mold was allowed to float on top until the agarose set. PBS was added to assist in carefully removing the mold without tearing the microwells. Hydrated gels could be stored at 4°C for several weeks until ready for use.

2.3.3   Comet Slide Preparation

As shown in Figure 2-1a, cells were allowed to settle gravitationally into the microwells by incubating for 15 min in complete growth media. Afterwards, the gel was gently rinsed twice with PBS while holding the gel surface at a 15° angle. Most unwanted cells are washed away because they do not adhere readily to agarose, while cells trapped inside the wells are protected from the fluid shear [29, 30]. Finally, 1% low melting point (LMP) agarose (Ultrapure, Invitrogen, Carsbad, CA) in PBS was applied to the surface and allowed to gel at 4°C for 10 min to seal the cells within the microwells. To prepare traditional comet slides, as described by Olive and Bánath [31], a suspension of cells was prepared and mixed 1:1 with 2% LMP agarose in PBS at 37°C to make a final concentration of 50,000 cells/ml in 1% LMP agarose. A total volume of 0.25 ml of cell-agarose suspension was applied to 3 cm x 4 cm GelBond slides on a 37°C slide warmer. Coverslips were applied to level the gels, while the cells were allowed to settle for 10 min. Finally, the slides were placed at 4°C for 10 min to allow the agarose to set, and the coverslips were removed.

2.3.4   Multiwell Comet Arrays

The multiwell version of the comet platform was prepared by sealing a microwell gel between a glass plate and a bottomless 24-well plate (Greiner Bio-One, Monroe, NC) (Figure 2-5a). Cells were then loaded into each well as described above and sealed with 1% LMP agarose.

2.3.5 Exposure to Ionizing Radiation

Cells were exposed to IR after encapsulation in agarose for both traditional comet and microwell comet array assays. Cells were irradiated using 250 kVp X-rays at 1 Gy/m (Philips RT-250). After exposure cells were placed in lysis buffer (10 mM Tris-HCl, 100 mM Na$_2$EDTA, 2.5 M NaCl, 1% Triton X-100) at pH 10 and 4°C. In order to evaluate repair kinetics on a single multiwell "CometChip", wells were synchronized during lysis after repairing in media for varying time intervals. This protocol required a 37°C lysis for 0 min and 30 min repair time points. For this we used a special lysis buffer formulation (50 mM Tris-HCl, 1 mM Na$_2$EDTA, 20 mM NaCl, 0.1% sodium dodecyl sulfate (SDS) at pH 8.0). After the final repair time, all samples were placed into standard lysis solution with 1% Triton X-100 at 4°C.

2.3.6 Comet Assay

The comet assay was performed using a modified version of the alkaline comet protocol as described by Singh et al. [6]. After a minimum of 1 hr in lysis, comet slides were placed into an electrophoresis chamber and covered with alkaline unwinding buffer (0.3 M NaOH and 1 mM Na$_2$EDTA) for 40 min, followed by 30 min electrophoresis at 1 V/cm and a total current of 300 mA. The slides were then neutralized twice for 10 min in fresh buffer (0.4 M Tris-HCl at pH 7.5) and stored at 4°C until ready to be stained and analyzed.

2.3.7 Fluorescence Imaging and Comet Analysis

Slides were stained with SYBR Gold (Invitrogen Corp, Carlsbad, CA) according to the manufacturer's instructions and imaged on a Nikon 80i upright microscope fitted with a scanning stage. For microwell comets, NIS-Elements software (Nikon Instruments, Melville, NY) was used to automatically step the stage between frames and capture images. Images were then automatically analyzed using custom software designed in MATLAB (The Mathworks, Natick, MA). As shown in Figure 2-2, this software automatically filters images for comets located on a rectangular grid. The software

sums each comet image in the vertical direction to map the 2D image to a 1D profile. The upper 10% of the comet image is empty and is used to calculate the background level, which is subtracted from the comet line profile. The beginning and end of the comet are determined using user-definable thresholds. The head/tail division is readily identified as an inflection point in the line profile, immediately following the head. Once the beginning, end, and head/tail division are known, typical comet parameters are calculated using standard methods [32, 31]. Traditional comet slides were scored using a commercial comet analysis software package (Komet 5.5, Andor Technology, Belfast, UK). All DNA damage is reported as % Tail DNA, which is the ratio of fluorescence in the comet tail to the total comet fluorescence.

2.4 Results

2.4.1 Micropatterned Cell Arrays

The traditional comet assay uses cells randomly dispersed in agarose. Random cell placement leads to several problems, including difficulty in locating cells automatically and large numbers of unanalyzable cells due to overlap. Spatial registration of cells in a defined array obviates these problems and allows spatial encoding of multiple experimental conditions on the same slide, and cell spacing can be tuned in order to maximize the number of conditions per slide.

Several methods currently exist for patterning cells, including dielectrophoresis [33], hydrostatic trapping [34], and microwell cell traps [35, 36, 37]. Of these methods, only microwells capture cells passively, eliminating the need for external energy sources and introducing minimal external stress on cells. Current microwell material systems, however, including polydimethyl siloxane (PDMS) and polyethylene glycol (PEG) are not compatible with DNA electrophoresis. We have developed a method that uses a microfabricated stamp to pattern microscopic wells, directly into hydrated agarose (Figure 2-1a). The stamp consists of microposts (Figure 2-1b), which are photolithographically defined and can be varied in width and depth to optimally

accommodate specific cell types (see *Methods*). Molten agarose sets around the posts, and the stamp is removed to form arrayed microwells in the agarose gel. Cells are then trapped in the wells using gravity. Captured cells are protected from rinsing shear so that excess cells are easily rinsed away, leaving the captured cells patterned into a defined array. Figure 2-1c shows patterned cells that have been labelled with a fluorescent cytoplasmic stain. The resulting arrays typically show > 90% filling.

By directly patterning the agarose gel, we have created a system that is fully compatible with the comet assay (Figure 2-1d). Figure 2-1e shows that the morphology of the resulting comets is comparable to that seen in the traditional comet assay [8]. There is a well-defined head consisting of tightly wound and high molecular weight DNA. The head is followed by a comet tail, which consists of relaxed loops and fragments. This is further demonstrated in Figure 2-1f, which shows microwell comets from varying doses of ionizing radiation (IR). Typical comet morphology is also seen in the dose response, with heads growing dimmer and tails growing longer and brighter with increasing dose.

One potential application of the microwell array is multiplexing cell types or conditions using colors or other labels. Cell multiplexing is demonstrated in Figure 2-1c, where two groups of cells, one stained red and the other green, have been loaded simultaneously into the microwell arrays. Fluorescent images of the cells are taken before lysis, and the color information can be recorded for each cell position and correlated with the final comet output.

2.4.2 Automated Imaging and Analysis

Imaging traditional comets is both laborious and tedious. Complications include sparse comet distribution, unanalyzable cell clumps, as well as random debris, which require users to distinguish analyzable objects. Automated imaging systems do exist, but they are expensive and either require manual comet selection or machine learning algorithms, which can be biased in their training. Comet analysis requires accurately discerning the transition from comet head to comet tail, which demands complex image analysis that can produce erroneous results. The microwell arrays obviate these

problems and provide a simple route to automated imaging and analysis. We use a standard fluorescence microscope with automated stage (see *Methods*) combined with a suite of custom analysis software (Figure 2-2), which utilizes simple algorithms to identify and analyze comets. Our software selects comets based on array registration, which eliminates problems with overlapping comets and debris. Further, because of the microwell fabrication method, all cells are located in a single focal plane, which eliminates the need for users to adjust the focus for each individual comet. Finally, the fixed head size provided by the microwell geometry simplifies the problem of identifying the head/tail transition, ensuring accurate determination of comet parameters (Figure 2-2). The result is the capability to fully automate imaging and analysis with no user intervention and with no special equipment or complex software.

2.4.3   Spatially-Encoded Microwell Comet Assay

A major advantage of the micropatterned array is the ability to increase throughput by spatially encoding multiple dosing conditions on the same slide. As shown in Figure 2-3a, using a moving shield to dynamically protect areas of the sample, different regions of the same comet slide can be treated with unique doses of IR, a key cancer therapeutic that has been well-characterized with the comet assay. To test the robustness of this platform for measuring DNA damage, we performed an IR dose response for human lymphoblast cells using either the traditional comet assay scored using commercial software or our spatially-encoded microwell assay scored using our automated analysis tools. The results, shown in Figure 2-3b, show consistent linear dose responses to IR in both implementations of the assay, demonstrating the efficacy of our platform for DNA damage analysis. Additionally, all IR doses for the microwell comets were incorporated on the same microscope slide. Due to differences in experimental protocols (see *Methods*), we did not compare absolute levels of damage between the two assays. Additionally, the microwell size can be tuned to accommodate virtually any cell type. For example, using different microwell sizes and spatial encoding of 10 IR doses, human lymphoblasts, ovarian cancer cells and primary hepatocytes were analyzed (Figure 2-3c). These data demonstrate efficacy

for generating dose-response curves for multiple cell types.

2.4.4 Self-Calibrating Microwell Comets

In the traditional comet assay, single cell suspensions are required. Remarkably, the simple innovation of microwells overcomes this limitation by physically restraining the DNA within the walls of the microwell following lysis, giving rise to a uniform and analyzable comet head. The uniform head size combined with an analysis that is normalized to the total amount of DNA makes the microwells self-calibrating. This feature means that any number of cells can be combined in a microwell and analyzed as a single comet, providing a new method for assessing DNA damage in small clusters of cells. Figure 2-4a shows human lymphoblast cells captured in wells with a range of diameters. The smallest wells (19 μm diameter) typically capture single cells, while the largest wells (54 μm diameter) can capture more than 10 cells. Figure 2-4b demonstrates that comets remain morphologically consistent over a range of IR damage and microwell diameters. The consistency with single cell comets is also reflected in the quantitative analysis (Figure 2-4c). Further, all IR doses and well sizes were combined on the same microscope slide, demonstrating a 20-fold higher throughput than the traditional comet assay. Absolute levels of DNA damage appear to decrease with increasing microwell size, which could be the result of incomplete DNA migration from the larger wells. Longer electrophoresis times or a stronger field could increase DNA migration.

2.4.5 Multiwell Comet Array

In order to measure DNA damage induced by different chemicals, or among different samples of cells, we created a multiwell version of our micropatterned comet array (Figure 2-5a). Figure 2-5a illustrates the 24-well version of the assay, where the floor of each well is a patterned array of agarose microwells. Cells are loaded into the microwells and, once embedded in agarose, can be treated with chemical damaging agents, lysis solution, or repair media. After treatment, the multiwell structure can

be removed, leaving only the cells embedded in agarose. The "CometChip" can then be carried through the standard comet assay protocol, enabling 24 or 96 samples to be run simultaneously. Importantly, this platform is fully compatible with our automated imaging and analysis tools.

There is significant interest in determining the extent of variation in DNA damage sensitivity and repair capacity between populations and individuals [38, 24]. Although it is extremely sensitive, the traditional comet assay is impractical for most large-scale studies. Our multiwell CometChip, however, allows all samples and repair times to be analyzed simultaneously. Further, by including all replicates and conditions in the same agarose slab, this platform reduces the noise introduced by slide-to-slide variation. When comparing between wells of a 96-well plate, we observe an 8.8% coefficient of variation (CV) in the population medians (Figure 2-6), which is less than the observed CV between slides in the traditional assay [25]. As a proof of concept, we used the 96-well platform to evaluate the repair capacity in response to IR of three B-lymphocyte lines (Coriell Research Institute) from individuals with different genetic backgrounds. The experiment is shown schematically in Figure 2-5b. All three cell lines, non-treated controls, and three repair time points (0 min, 30 min, 60 min) were performed on a single plate by lysing cells in wells adjacent to cells that were allowed to repair at 37°C. As shown in Figure 2-5c, nearly all of the damage is repaired within 30 min of treatment with IR for all cell types. Additionally, it appears that no significant difference exists between the repair capacities of these cell lines for IR-induced damage. In contrast, these same cells were previously shown to have significantly different sensitivities to a methylating agent (N-methyl-N'-nitro-N-nitrosoguanidine (MNNG)) [39]. While the majority of IR-induced DNA damage is repaired by the BER pathway [4] (Figure 2-7a), the cytotoxicity of MNNG is largely due to O^6-methylguanine, which is primarily repaired by direct reversal. Thus, these cells show different repair capacities for different repair pathways.

2.4.6 Small Molecule Inhibitors of Human AP Endonuclease

DNA damaging agents are the frontline treatment for most cancers, but cells have numerous DNA repair mechanisms, which can limit therapeutic efficacy or contribute to resistance [4]. Inhibiting DNA repair has therefore the potential to sensitize cancer cells to treatment and is now a common theme in cancer therapy research [4]. The BER pathway (Figure 2-7a) has received particular interest because of its relevance to numerous types of cancer therapies, including IR and monofunctional alkylators [4]. Following removal of a damaged base by a monofunctional DNA glycosylase, the major human apurinic/apyramidinic (AP) endonuclease, APE-1, is responsible for cleavage of AP sites prior to processing by downstream BER machinery (Figure 2-7a) [40]. Inhibition of APE-1 activity blocks the BER pathway and leads to accumulation of AP sites, which can be highly cytotoxic [41, 42]. From a clinical perspective, APE-1 overexpression has been observed in numerous cancer types [43]. Additionally, reduced expression of APE-1 using RNA interference has been shown to sensitize cells to treatment by numerous therapeutic agents [44, 45, 46, 47]. Small molecules that inhibit the AP endonuclease activity of APE-1 could thus be extremely valuable in combination therapies for treating cancer.

Several small molecules have previously been identified as potential inhibitors of APE-1's AP endonuclease activity [48, 49, 50]. Cytotoxicity of these molecules was evaluated by clonogenic surviva lwhich does not illuminate the mechanism by which the molecules are cytotoxic. The comet assay can directly reveal abasic sites that accumulate due to APE-1 inhibition. As a proof of concept screen, we utilized the 96-well CometChip to test three potential small molecule inhibitors of APE-1: 7-nitro-1H-indole-2-carboxylic acid (NCA) [51], myricetin (MYR) [49] and 6-hydroxy-DL-DOPA (DOPA) [49]. Cells treated with either DOPA (Figure 2-7b) or MYR (Figure 2-7c) show a dose-dependent increase in DNA damage levels, presumably as a result of the accumulation of BER intermediates that is expected from the high levels of spontaneous BER (estimated to be > 10,000 BER events per day [10]). All concentrations of these two molecules tested show a significant increase in damage over

the controls. At 50 μM the damage induced by myricetin was so severe as to saturate the assay. Although there may be some direct damage resulting from these small molecules, the findings agree well with the observation of abasic site accumulation by Simeonov et al. [49]. In contrast, cells treated with the candidate molecule NCA (Figure 2-7d) do not show greatly increased damage, as compared to control. Only the highest concentration (50 μM) shows a statistically significant (21%) increase in damage over the control, whereas DOPA and MYR induce a 48% and 50% increase in damage, respectively, at 10-fold lower concentrations. Interestingly, two studies have reported no effect on cell survival when using NCA with DNA damaging agents [49, 52]. Our results suggest that NCA may have some effect on cells, but both DOPA and MYR are far more potent. As potent inhibitors of APE-1, these molecules could potentially be used in combination therapies to treat tumors more aggressively.

2.5 Discussion

We present a new technique for measuring DNA damage that combines sensitivity, versatility, high throughput, and ease of use. This platform has potential to impact a broad range of applications in the laboratory and clinic. Having the capacity to handle dozens of conditions in parallel will shed light on how cells respond to multiple classes of DNA damaging agents, acted upon by a variety of DNA repair pathways and subpathways. With increased granularity in the human DNA repair landscape, it should become possible to reveal novel predictive biomarkers and prognostic indicators.

A major strength of the comet assay is its versatility. It has been used to study a variety of cell types and species from all three biological kingdoms [17]. The microwell arrays further increase the versatility of this assay by enabling new capabilities, including cell multiplexing and analysis of cell aggregates. Cell multiplexing could be used to analyze multiple readouts from the same cell. This could be useful in several contexts, including antibody labeling of mixed populations or determining viability of cryo-preserved primary samples on a single cell basis. The microwells also facili-

tate DNA damage analysis in small cell aggregates (Figure 2-4). Cell aggregates are common in research and the clinic, in the form of tissue samples, tumor spheroids or embryos, and embryonic stem cells. Maintaining cell-cell contact is often necessary to preserve important features of the sample, such as autocrine signaling and tight junctions that might influence cellular response to DNA damage. The microwell technique allows for DNA damage quantification in such samples, potentially without sacrificing important biological information.

We present here the first demonstration of a platform in which multiple cell types, repair time points, DNA damaging agents, DNA repair enzymes or inhibitors, and other conditions can be assayed simultaneously and in combination. Unlike other high throughput comet assay implementations ([23] and Trevigen), the multiwell platform is compatible with any cell type, whether cultured adherently or in suspension, and also incorporates significant improvements in imaging and analysis. Further, we provide the ability to assay repair kinetics on multiple cell types without introducing slide-to-slide variation, which could be critical for revealing subtle biological effects. The 8.8% CV observed between individual wells of a 96-well plate is less than the reported variation between individual comet slides using the traditional assay [25], and this could potentially be reduced further by including internal controls [25].

This platform has potential for both epidemiology and drug screening applications. Our findings on the repair kinetics of B-lymphocyte lines highlight the importance of measuring repair capacities through multiple pathways and by different agents, and they demonstrate the utility of a high throughput approach. For drug screening, the platform offers an integrated readout of multiple biological pathways. Specific subsets of DNA lesions can be detected by the application of DNA repair enzymes that convert otherwise undetectable damaged bases into detectable SSBs or AP sites. Modifications in the basic comet protocol provide increased specificity, thus enabling testing of therapeutics that damage DNA or that target DNA repair pathways. Additionally, the 96-well platform integrates with standard HTS techniques making it well-suited for drug development.

2.6 Conclusions

With the ability to measure acute DNA damage levels as well as repair kinetics, the comet assay is uniquely relevant to a variety of biological and clinical applications. The significant improvements afforded by this platform make the measurement of DNA damage easier and more readily applicable. Further, the approach is simple and scalable, offering a route to mass produce gels and distribute them in a manner similar to DNA and protein electrophoresis. This would bring critical information about DNA damage and repair to researchers and clinicians in a range of fields, and the use of this knowledge to facilitate disease prevention and treatment could be fully realized. Through the integration of traditional methods in biology and engineering, the platform described here represents a significant technological advance, providing high throughput, objective, and quantitative measurements that have the potential to become a new standard in DNA damage analysis.

References

[1] E. C. Friedberg, G. C. Walker, W. Siede, R. D. Wood, R. A. Schultz, and T. Ellenberger, *DNA Repair and Mutagenesis*. ASM Press, Washington, DC, USA, 2005.

[2] T. Helleday, J. Lo, D. C. van Gent, and B. P. Engelward, "Dna double-strand break repair: from mechanistic understanding to cancer treatment," *DNA Repair*, vol. 6, pp. 923–935, 2007.

[3] J. H. J. Hoeijmakers, "Dna damage, aging, and cancer," *New Engl. J. Med.*, vol. 361, pp. 1475–1485, 2009.

[4] T. Helleday, E. Petermann, C. Lundin, B. Hodgson, and R. A. Sharma, "Dna repair pathways as targets for cancer therapy," *Nat. Rev. Cancer*, vol. 8, pp. 193–204, Mar. 2008.

[5] O. Ostling and K. J. Johanson, "Microelectrophoretic study of radiation-induced dna damages in individual mammalian cells," *Biochem. Biophys. Res. Commun.*, vol. 123, pp. 291–298, 1984.

[6] N. P. Singh, M. T. McCoy, R. R. Tice, and E. L. Scheider, "A simple technique for quantitation of low levels of dna damage in individual cells," *Exp. Cell Res.*, vol. 175, pp. 184–191, 1988.

[7] A. R. Collins, "The comet assay for dna damage and repair: principles, applications, and limitations.," *Mol. Biotechnol.*, vol. 26, no. 3, pp. 249–261, 2004.

[8] P. L. Olive and J. P. Banath, "The comet assay: a method to measure dna damage in individual cells," *Nat. Protoc.*, vol. 1, no. 1, pp. 23–29, 2006.

[9] M. Dusinska and A. Collins, "Detection of oxidised purines and uv-induced photoproducts in dna of single cells, by inclusion of lesion-specific enzymes in the comet assay," *ATLA*, vol. 24, pp. 405–411, 1996.

[10] P. Fortini, G. Raspaglio, M. Falchi, and E. Dogliotti, "Analysis of dna alkylation damage and repair in mammalian cells by the comet assay.," *Mutagenesis*, vol. 11, pp. 169–175, Mar 1996.

[11] A. R. Collins, M. Dusinska, and A. Horska, "Detection of alkylation damage in human lymphocyte dna with the comet assay," *Acta Biochim. Pol.*, vol. 48, pp. 611–614, 2001.

[12] S. Brendler-Schwaab, A. Hartmann, S. Pfuhler, and G. Speit, "The in vivo comet assay: use and status in genotoxicity testing," *Mutagenesis*, vol. 20, pp. 245–254, 2005.

[13] I. Witte, U. Plappert, H. de Wall, and A. Hartmann, "Genetic toxicity assessment: employing the best science for human safety evaluation part iii: the comet assay as an alternative to in vitro clastogenicity tests for early drug candidate selection," *Toxicol. Sci.*, vol. 97, pp. 21–26, 2007.

[14] M. Valverde and E. Rojas, "Environmental and occupational biomonitoring using the comet assay," *Mutat. Res.*, vol. 681, pp. 93–109, 2009.

[15] P. Moller, "Genotoxicity of environmental agents assessed by the alkaline comet assay," *Basic Clin. Pharmacol.*, vol. 96, pp. 1–42, 2005.

[16] M. Dusinska and A. R. Collins, "The comet assay in human biomonitoring: gene-environment interactions," *Mutagenesis*, vol. 23, pp. 191–205, 2008.

[17] A. Dhawan, M. Bajpayee, and D. Parmar, "Comet assay: a reliable tool for the assessment of dna damage in different models," *Cell Biol. Toxicol.*, vol. 25, pp. 5–32, 2009.

[18] D. J. McKenna, S. R. McKeown, and V. J. McKelvey-Martin, "Potential use of the comet assay in the clinical management of cancer," *Mutagenesis*, vol. 23, pp. 183–190, 2008.

[19] J. Cadet, T. Douki, and J.-L. Ravanat, "Oxidatively generated damage to the guanine moiety of dna: mechanistic aspects and formation in cells," *Acc Chem Res*, vol. 41, pp. 1075–83, Aug 2008.

[20] H. C. Birnboim and J. J. Jevcak, "Fluorometric method for rapid detection of dna strand breaks in human white blood cells produced by low doses of radiation," *Cancer Res.*, vol. 41, pp. 1889–1892, 1981.

[21] G. Ahnstrom, "Techniques to measure dna single-strand breaks in cells: a review," *Int. J. Radiat. Biol.*, vol. 54, pp. 695–707, 1988.

[22] L. J. Kuo and L. X. Yang, "Gamma-h2ax - a novel biomarker for dna double-strand breaks," *In Vivo*, vol. 22, pp. 305–309, 2008.

[23] A. Stang and I. Witte, "Performance of the comet assay in a high-throughput version," *Mutat. Res.*, vol. 675, pp. 5–10, 2009.

[24] A. R. Trzeciak, J. Barnes, and M. K. Evans, "A modified alkaline comet assay for measuring dna repair capacity in human populations," *Radiat. Res.*, vol. 169, pp. 110–121, 2008.

[25] M. Zainol, J. Stoute, G. M. Almeida, A. Rapp, K. J. Bowman, G. D. D. Jones, and ECVAG, "Introducing a true internal standard for the comet assay to minimize intra- and inter-experiment variability in measures of dna damage and repair," *Nucleic Acids Res.*, pp. 1–9, 2009.

[26] D. G. McArt, G. R. Wasson, G. McKerr, K. Saetzler, M. Reed, and C. V. Howard, "Systematic random sampling of the comet assay," *Mutagenesis*, vol. 24, no. 4, pp. 373–378, 2009.

[27] P. O. Seglen, "Preparation of isolated rat liver cells," *Method. Cell Biol.*, vol. 13, pp. 29–83, 1976.

[28] J. C. Dunn, R. G. Tompkins, and M. L. Yarmush, "Long-term in vitro function of adult hepatocytes in a collagen sandwich configuration," *Biotechnol. Progr.*, vol. 7, pp. 237–245, 1991.

[29] J. R. Rettig and A. Folch, "Large-scale single-cell trapping and imaging using microwell arrays," *Anal Chem*, vol. 77, pp. 5628–34, Sep 2005.

[30] A. Rosenthal, A. Macdonald, and J. Voldman, "Cell patterning chip for controlling the stem cell microenvironment," *Biomaterials*, vol. 28, pp. 3208–16, Jul 2007.

[31] P. Olive and J. Banáth, "The comet assay: a method to measure dna damage in individual cells," *Nat Meth*, vol. 1, no. 1, pp. 23–29, 2006.

[32] A. R. Collins, "The comet assay for dna damage and repair: principles, applications, and limitations," *Mol Biotechnol*, vol. 26, pp. 249–61, Mar 2004.

[33] D. S. Gray, J. L. Tan, J. Voldman, and C. S. Chen, "Dielectrophoretic registration of living cells to a microelectrode array," *Biosens. Bioelectron.*, vol. 15, pp. 1765–1774, July 2004.

[34] D. DiCarlo and L. P. Lee, "Dynamic single-cell analysis for quantitative biology," *Anal. Chem.*, vol. 78, pp. 7918–7925, 2006.

[35] J. Rettig and A. Folch, "Large-scale single-cell trapping and imaging using microwell arrays," *Anal. Chem.*, vol. 77, no. 17, pp. 5628–5634, 2005.

[36] V. I. Chin, P. Taupin, S. Sanga, J. Scheel, F. H. Gage, and S. N. Bhatia, "Microfabricated platform for studying stem cell fates.," *Biotechnol. Bioeng.*, vol. 88, pp. 399–415, Nov 2004.

[37] A. Rosenthal, A. Macdonald, and J. Voldman, "Cell patterning chip for controlling the stem cell microenvironment.," *Biomaterials*, vol. 28, no. 21, pp. 3208–3216, 2007.

[38] F. Marcon, C. Andreoli, S. Rossi, A. Verdina, R. Galati, and R. Crebelli, "Assessment of individual sensitivity to ionizing radiation and dna repair efficiency in a healthy population," *Mutat. Res.*, vol. 541, pp. 1–8, 2003.

[39] C. F. Fry, J. P. Svensson, C. Valiathan, E. Wang, B. J. Hogan, S. Bhattacharya, J. M. Bugni, C. A. Whittaker, and L. D. Samson, "Genomic predictors of interindividual differences in response to dna damaging agents," *Genes Dev.*, vol. 22, pp. 2621–2626, 2008.

[40] M. L. Hegde, T. K. Hazra, and S. Mitra, "Early steps in the dna base excision/single-strand interruption repair pathway in mammalian cells," *Cell Res.*, vol. 18, no. 1, pp. 27–47, 2008.

[41] L. A. Loeb and B. D. Preston, "Mutagenesis by apurinic apyrimidinic sites," *Annu. Rev. Genet.*, vol. 20, pp. 201–230, 1986.

[42] E. J. Spek, L. N. Vuong, T. Matsuguchi, M. G. Marinus, and B. P. Engelward, "Nitric oxide induced homologous recombination in escherichia coli is promoted by dna glycosylases," *J. Bacteriol.*, vol. 184, pp. 3501–3507, 2002.

[43] A. R. Evans, M. Limp-Foster, and M. R. Kelley, "Going ape over ref-1," *Mutat. Res.-DNA Repair.*, vol. 461, no. 2, pp. 83–108, 2000.

[44] J. P. Lau, K. L. Weatherdon, V. Skalski, and D. W. Hedley, "Effects of gemcitabine on ape/ref-1 endonuclease activity in pancreatic cancer cells, and the therapeutic potential of antisense oligonucleotides," *Brit. J. Cancer*, vol. 91, pp. 1166–1173, Sept. 2004.

[45] D. Wang, M. Luo, and M. R. Kelley, "Human apurinic endonuclease 1 (ape1) expression and prognostic significance in osteosarcoma: Enhanced sensitivity

of osteosarcoma to dna damaging agents using silencing rna apel expression inhibition," *Mol. Cancer Ther.*, vol. 3, no. 6, pp. 679–686, 2004.

[46] M. S. Bobola, L. S. Finn, R. G. Ellenbogen, J. R. Geyer, M. S. Berger, J. M. Braga, E. H. Meade, M. E. Gross, and J. R. Silber, "Apurinic/apyrimidinic endonuclease activity is associated with response to radiation and chemotherapy in medulloblastoma and primitive neuroectodermal tumors," *Clin. Cancer Res.*, vol. 11, pp. 7405–7414, Oct. 2005.

[47] M. L. Fishel and M. R. Kelley, "The dna base excision repair protein apel/ref-1 as a therapeutic and chemopreventive target," *Mol. Aspects Med.*, vol. 28, no. 3-4, pp. 375–395, 2007.

[48] S. Madhusudan, F. Smart, P. Shrimpton, J. L. Parsons, L. Gardiner, S. Houl-brook, D. C. Talbot, T. Hammonds, P. A. Freemont, M. J. E. Sternberg, G. L. Dianov, and I. D. Hickson, "Isolation of a small molecule inhibitor of dna base excision repair," *Nucleic Acids Research*, vol. 33, pp. 4711–24, Jan 2005.

[49] A. Simeonov, A. Kulkarni, D. Dorjsuren, A. Jadhav, M. Shen, D. R. McNeill, C. P. Austin, and D. M. Wilson, "Identification and characterization of inhibitors of human apurinic/apyrimidinic endonuclease apel," *PLoS ONE*, vol. 4, p. e5740, Jan 2009.

[50] L. A. Seiple, J. H. Cardellina, R. Akee, and J. T. Stivers, "Potent inhibition of human apurinic/apyrimidinic endonuclease 1 by arylstibonic acids.," *Mol. Pharmacol.*, vol. 73, pp. 669–677, Mar 2008.

[51] S. Madhusudan, F. Smart, P. Shrimpton, J. L. Parsons, L. Gardiner, S. Houl-brook, D. C. Talbot, T. Hammonds, P. A. Freemont, M. J. E. Sternberg, G. L. Dianov, and I. D. Hickson, "Isolation of a small molecule inhibitor of dna base excision repair.," *Nucleic Acids Res.*, vol. 33, no. 15, pp. 4711–4724, 2005.

[52] A. Bapat, M. Fishel, and M. R. Kelley, "Going ape as an approach to cancer therapeutics," *Antioxid. Redox Signal.*, vol. 11, pp. 571–574, 2009.
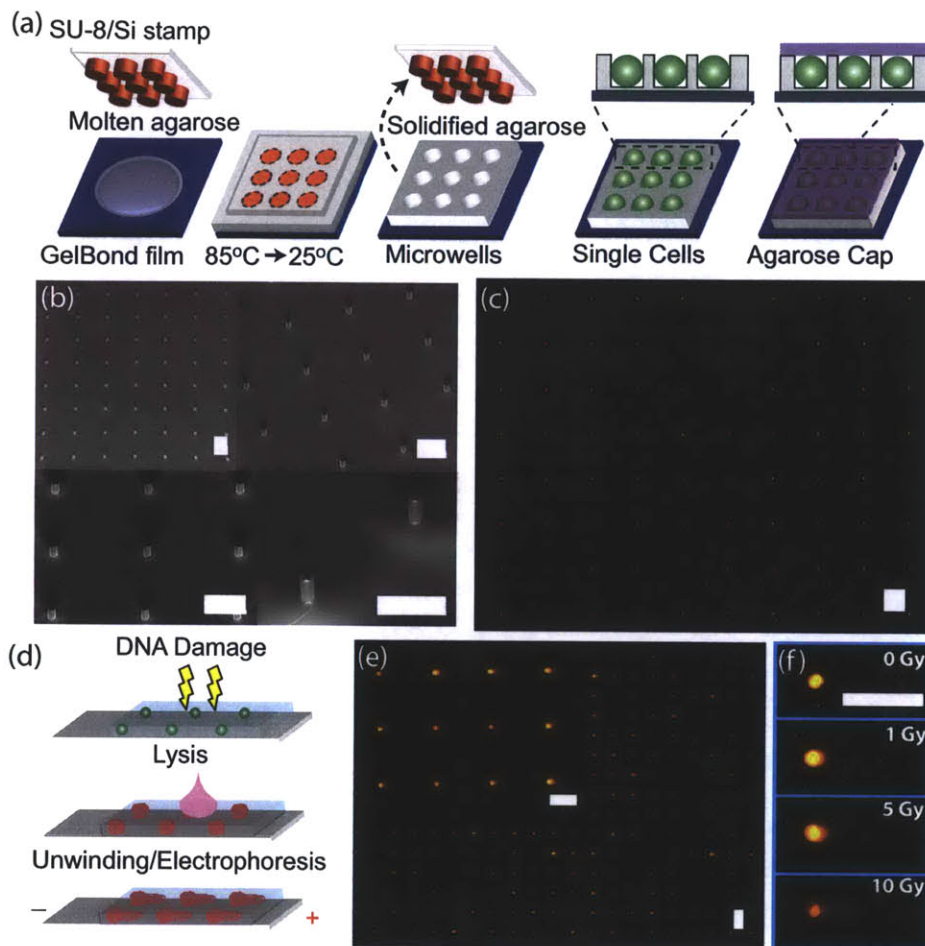
Figure 2-1: **Single Cell Gel Electrophoresis Array.** (a) Microwell fabrication. A microfabricated stamp is placed onto molten agarose. Agarose is cooled to set, and the stamp is removed. Cells are loaded into wells by gravitational settling, and an agarose overlay covers the cells. (b) Scanning electron micrograph of SU-8 posts patterned onto a silicon substrate. (c) Two populations stained red and green, loaded into wells concurrently, are shown by cytoplasmic staining. (d) Comet assay. Cells are treated with DNA damaging agent. Cells are lysed in the gel, exposing the DNA. The DNA is unwound and electrophoresed under alkaline conditions. Relaxed loops and low molecular weight fragments migrate out of the packed chromatin, forming a comet tail. (e) Arrayed microwell comets. (f) Microwell comets with varying doses of IR damage. Horizontal scale bars are 100 μm.
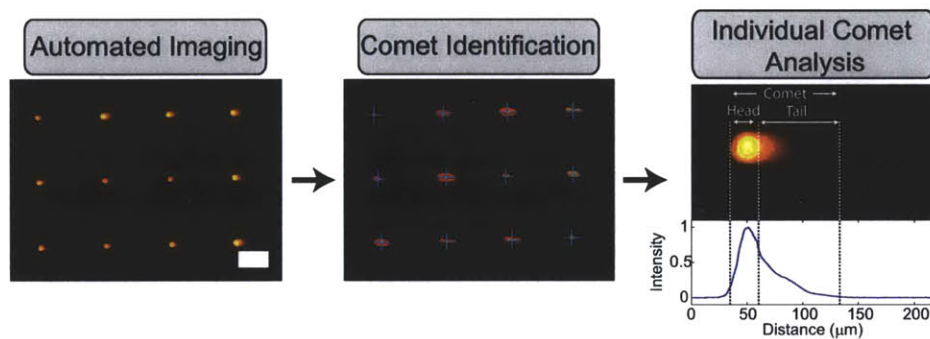
Figure 2-2: **Comet Analysis Pipeline.** Images of comets are acquired automatically. Identification software recognizes comets in a defined array. Image of arrayed comets before and after identification are shown. Identified comets are labelled with blue crosses. Scale bar is 100 μm. Finally comet analysis software identifies beginning and end of comet as well as head/tail division (dashed vertical lines) and calculates comet parameters. A comet is shown along with its corresponding line profile from which the comet parameters are calculated.
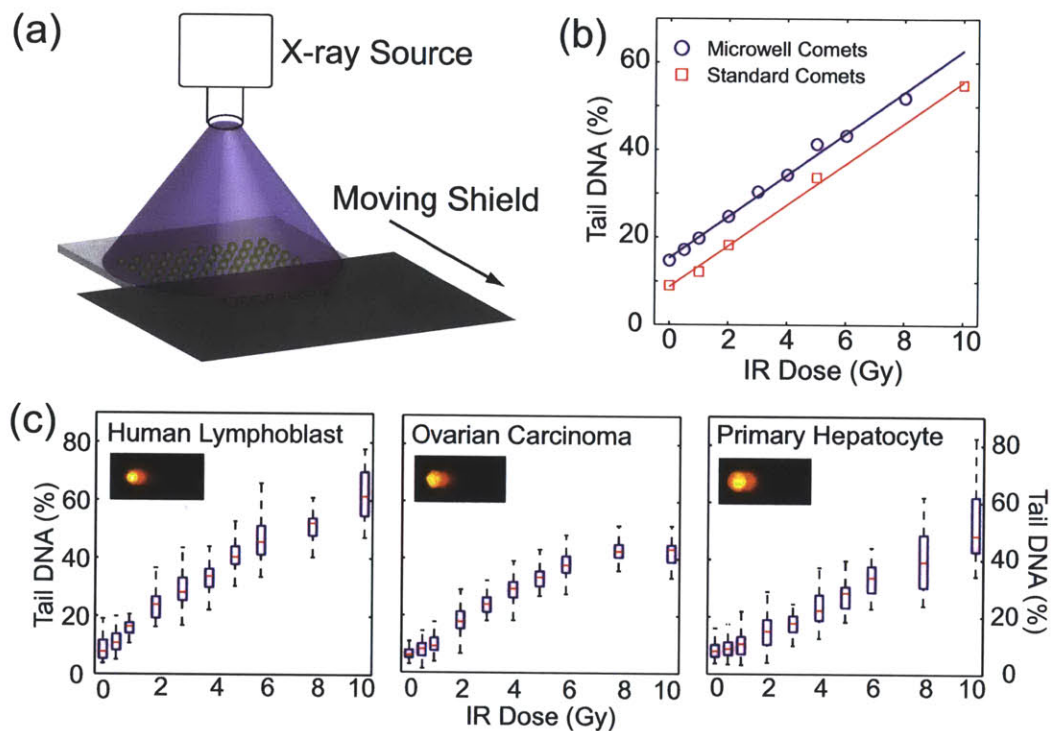
Figure 2-3: **Spatially-Encoded Comet Assay.** (a) Method for spatially encoding IR doses on the same microscope slide. A moving lead shield exposes different regions of the slide to IR for varying lengths of time. (b) Comparison of IR dose response between traditional comet slides scored using commercial software and microwell comets scored using automated software. Each data point is the median of 50 individual comets. (c) IR dose responses for TK6 human lymphoblasts, OVCAR-8 human ovarian carcinoma cells, and freshly isolated primary rat hepatocytes. Representative images are shown from 10 Gy dose for each cell type. Box plots show median of 50 comets as a red line and the lower and upper quartiles as a blue box. Whiskers show extent of furthest data points within 150% of interquartile range.
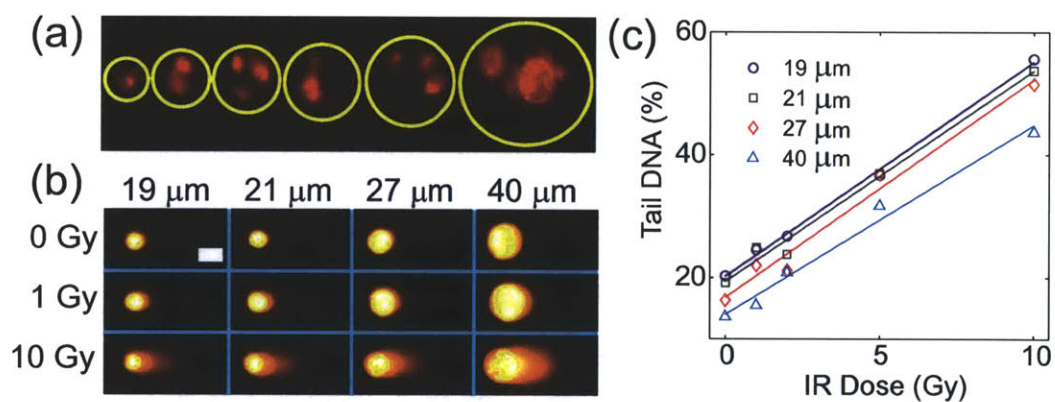
Figure 2-4: **Self-Calibrating Microwells.** (**A**) Fluorescence image of (from left to right) 19, 25, 29, 33, 40 and 54 μm diameter microwells filled with propidium iodide stained TK6 human lymphoblasts. (**b**) Morphological and (**c**) quantitative IR dose response of TK6 cells loaded into different sized microwells on the same slide. White scale bar in (**b**) is 25 μm. Each data point in (**c**) is the median of 50 comets.
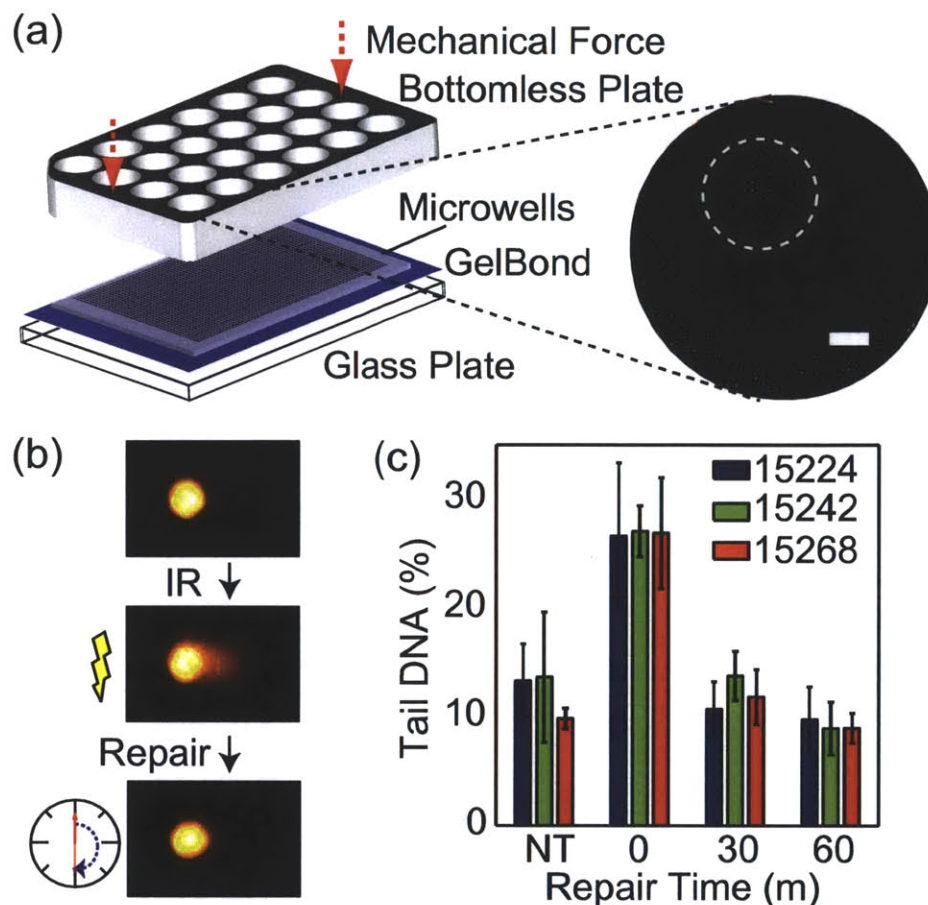
Figure 2-5: **Multiwell Comet Array.** (a) Assembly of multiwell comet array. Agarose gel with microwells is sandwiched between a glass substrate and a bottomless multiwell plate and sealed with mechanical force. Arrayed microwells comprise the bottom of the multiwell. A large field scan of one well of a 24-well plate is shown with a fish-eye magnification (2X) of a small region. White scale bar is 2 mm. (b) Schematic of repair study with representative comets. Cells are treated with IR and allowed to repair in media at 37°C before lysis. (c) Repair kinetics of human B-lymphocyte lines GM15224, GM15242 and GM15268 after treatment with 7.5 Gy IR. Non-treated (NT) cells were not exposed to IR. Bars and error bars represent averages and standard deviations, respectively, of three independent experiments with at least 50 comets scored for each condition in each experiment.
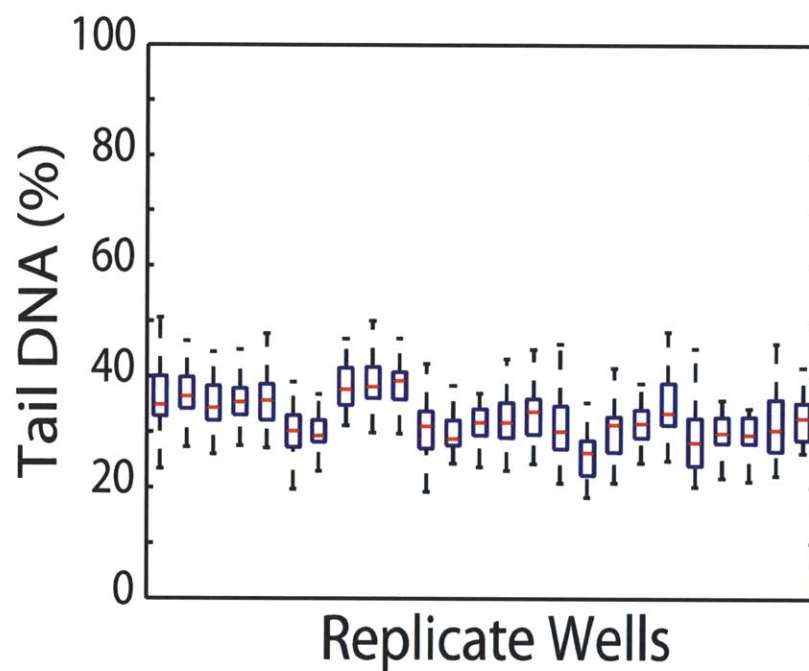
Figure 2-6: **Well-to-Well Variation.** Distribution of comets from individual wells of a 96-well plate. TK6 human lymphoblast cells were loaded into the microwell array and treated with 5 Gy IR in the 96-well format. Data from 25 wells are shown. Each box represents 100 individual comets. Outliers not shown.
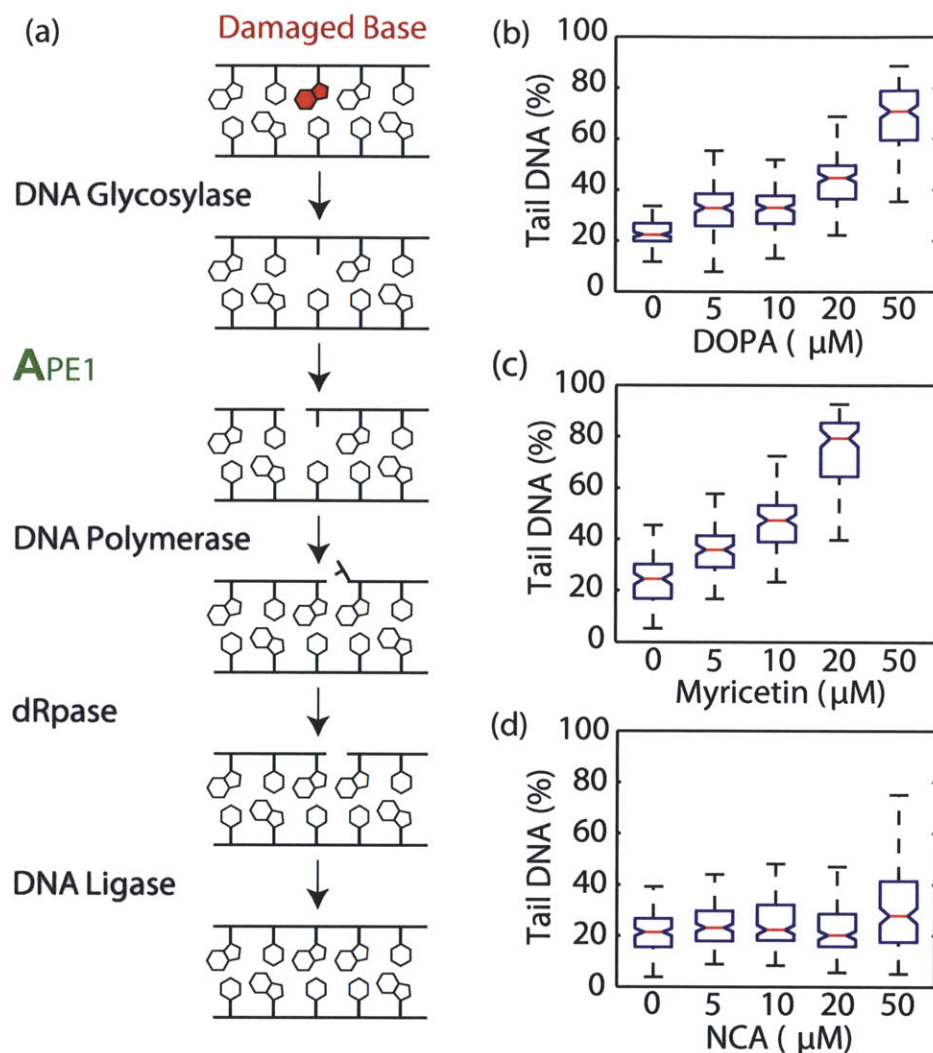
Figure 2-7: **Potency of APE-1 Inhibitors.** (a) Schematic of short patch BER for repairing methylated bases. The base is removed by a monofunctional glycosylase, and APE-1 cleaves the backbone 5′ to the resulting abasic site. The new base is inserted by DNA polymerase, the 5' flap is removed by a dRpase, and the nick is sealed by a DNA ligase. (b - d) Human lymphoblasts (TK6) treated with increasing doses of (b) 6-hydroxy-DL-DOPA (DOPA), (c) myricetin, or (d) 7-nitro-1H-indole-2-carboxylic acid (NCA). Each data set is a representative from three independent experiments. Box plots for NCA and DOPA include 150 individual comets per condition. 100 comets per condition are shown for MYR. Assay readout was saturated at 50 μM MYR. Notches represent 95% confidence interval of medians, determined using Kruskal-Wallis nonparametric analysis of variance. Boxes with non-overlapping notches represent different populations with at least 95% confidence.

Chapter 3

Evaluation of Multiple Chemical Conditions and Detection of DNA Repair Deficiencies using the CometChip

3.1 Abstract

DNA damage, whether environmentally or endogenously induced, can be both cytotoxic and mutagenic and is an important risk factor for many diseases, including cancer [1]. It is now well established that heritable DNA repair deficiencies can promote cancer, and the list of DNA repair genes that are critical in cancer prevention includes genes from every major DNA repair pathway [2]. Ironically, DNA damage is also important as the primary mechanism in most frontline cancer therapies. Thus, the ability to assess DNA damage and repair levels in populations or in individuals is important for predicting cancer susceptibility as well as response to therapies. However, available technologies for assaying DNA damage and repair suffer from being low throughput. Therefore, an assay that can accurately measure DNA damage levels in a robust and automated way would be highly valuable in applications such as

human biomonitoring, epidemiology, and drug development. We have recently developed the CometChip, which enables parallel analysis of DNA damage in multiple cell samples. Here, we set out to validate the use of the CometChip for high throughput measurement of DNA repair after exposure to a variety of DNA damaging agents. The CometChip enables the precise analysis of DNA repair kinetics, which may be useful in advancing models of DNA repair, and identifying new drug targets. Furthermore, we demonstrate an ability to detect deficiences in base excision repair (BER), nucleotide excision repair (NER), and interstrand crosslink repair (ICLR), supporting the use of the CometChip both for mechanistic studies of DNA repair as well as for use in health related applications.

3.2   Introduction

The integrity of our genome is maintained by a complex network of proteins that continuously monitor our DNA for strand breaks, base mispairing, and the presence of base damage that might disrupt replication or transcription, and consequently promote cell mutation or death. It is now well established that deficiencies in DNA repair proteins are critical to carcinogenesis, as they promote genomic instability. The so-called "mutator phenotype" is a hallmark of cancer that enables tumor cells to outcompete normal cells through the accumulation of traits providing advantages such as proliferation and resistance to cell death [3, 4]. Initiation of a mutator phenotype may result from inherited mutations in DNA repair genes [5, 2]. Ironically, DNA damage is also a frontline mechanism in cancer treatment, as rapidly dividing tumor cells are more sensitive to agents that interfere with replication and transcription [6]. Understanding DNA repair capacity and the coordination of proteins in the various pathways is therefore important not only in predicting cancer susceptibility, but also in evaluating tumor sensitivity and guiding cancer treatment.

To learn more about DNA repair capacity, we set out to develop better assays for specific DNA repair paths. There are two main pathways for excision of damaged DNA nucleotides: base excision repair (BER) for single base lesions and nucleotide

excision repair (NER) for helix-distorting bulky damage. The BER pathway is initiated by a variety of glycosylases that remove specific base lesions through hydrolysis of their N-glycosidic bond. For example, alkyladenine DNA glycosylase (AAG) protects the cell from numerous damaging agents through removal of a wide range of substrates [7, 8]. Glycosylases are further categorized based on whether they possess the bifunctional activity to cleave the phosphodiester DNA backbone. Bifunctional glycosylases can perform base excision and lyase in a concerted reaction, while monofunctional glycosylase initiated BER requires the 5'dRP lyase activity of Polβ, which is known to be rate limiting [9]. In either case, initiation of BER leads to BER intermediates (i.e. single strand breaks (SSBs), abasic sites) that may be more toxic and mutagenic to the cell than the initial DNA lesion if not repaired efficiently [8, 10]. So, for example, while AAG deficient cells are hypersensitive to alkylation damage [11], overexpresssion of AAG results in a build up of toxic 5'dRP blocking lesions due to the rate limiting kinetics of polymerase beta (Polβ) gap tailoring [12, 13, 14]. This accumulation effect can also result from or be enhanced by inhibiting or knocking down expression of Polβ, or other downstream repair proteins, such as AP Endonuclease (see Chapter 2) or a ligase (e.g. Ligase III) [15]. People with BER gene polymorphisms have increased susceptibility to cancer and numerous cancers are found to contain BER deficiencies [16, 17, 18, 2]. Thus, proper coordination of BER proteins is critical for genomic stability and disruption of this balance may lead to carcinogenesis.

Understanding the coordination and balance of BER proteins is also important to understanding tumor resistance and guiding chemotherapeutic intervention. For example, the use of radiation and temozolmoide, a potent alkylating agent, has significantly increased the life expectancy of glioblastoma patients in recent years, but the development of tumor resistance prevents their sustained success [19, 20]. Temozolomide efficacy is largely attributed to the formation of O^6-methylguanine lesions, which are efficiently removed in the direct reversal process by O^6-methylguanine methyl-transferase (MGMT). While MGMT serves as a common path to resistance in gliomas [20], strategies to both overcome resistance or provide alternate path-

ways to chemosensitivity are of great interest. One such strategy is to target BER, which is responsible for the efficient removal of the majority of alkylation damage (i.e. N^7-methyguanine, N^3-methyladenine) [21]. In addition to AP Endonuclease, which was explored in Chapter 2, Polβ is being studied as a potential target for adjuvant chemotherapy [22, 23]. Determining the roles of key BER proteins may allow for strategic disruption of this process in order to provide enhanced chemosensitivity to resistant tumors [24, 25]. Additionally, information about BER imbalances may advance biological models of DNA repair and generate insights into tumor sensitivity and treatment [26].

The study of NER is equally relevant to human health, as NER capacity has been shown to be an important factor in cancer susceptibility and mutations in many NER genes are associated with diseases, most notably, xeroderma pigmentosum (XP) and Cockayne's syndrome [27]. NER describes the process in which more than 30 proteins coordinate to remove bulky lesions through the incision of a 24-32 nucleotide long sequence surrounding the damage [28]. There are a number of XP conditions resulting from deficiencies in proteins named for the disease. For example, deficiencies in XPF, which makes the incision 5′ to the lesion, and XPG, which makes the 3′ incision, result in hypersensitivity to ultraviolet sun light (UV) and increased risk of skin cancer [29]. XPB is part of the helicase complex that unwinds DNA for XPF to make the 5′ incision. Although not directly responsible for incision, deficiencies in other NER proteins, such as XPB, result in XP symptoms and other genetic diseases such as trichothiodystrophy [29]. Therefore, determining the relative contributions of NER proteins to DNA damage clearance is important for understanding mechanisms of disease progression.

DNA interstrand crosslinks (ICLs), are extremely cytotoxic, because they covalently link the two strands of DNA, preventing strand separation and blocking DNA replication and transcription [30]. ICLR is therefore a critical process, as further evidenced by its association with numerous diseases and cancers [31, 32, 33]. Components of various DNA repair pathways, including NER and homologous recombination, have been shown to participate in ICLR, but details of the mechanism remain largely un-

known [34]. This may be due, in part, to a lack of available tools for ICL detection. A high throughput ICLR assay may therefore help advance biological models and could assist in disease diagnosis and also in designing treatment strategies, as ICL agents are highly efficacious against many cancers. As an example, metastatic testicular germ cell cancer, which was once a fatal disease, is now curable in 80% of patients due to increased ICL sensitivity of tumors with low levels of XPF expression [35, 36]. Other tumors are resistant to ICL agents, reinforcing the potential clinical value of a robust ICLR assay [37].

Quantitative assessment of DNA damage and repair is important in both epidemiological and clinical applications [38, 39, 40, 41, 42], but there is a lack of tools that are available to evaluate repair kinetics, as most DNA damage assays detect artifacts of damage, such as the incorporation of nucleotides, but reveal minimal information concerning damage induction and the kinetics of repair [43]. In contrast, the alkaline comet assay provides a relatively accurate analysis of multiple pathways of DNA repair, by directly measuring the formation and disappearance of single strand breaks (SSBs) and alkali labile sites, which arise both from direct damage and as repair intermediates [44]. Figure 3-1 illustrates the various lesions of detection as well as the concept of directly measuring the repair process through visualization of repair intermediates. The ability of the comet assay to detect subtle variations in repair capacity is central to its utility as an epidemiological tool [45, 46, 47], but the assay has not been widely adopted by epidemiologists and clinicians due to its low throughput and laborious analysis requirement.

In order to increase throughput and robustness of the comet assay, we developed the 96-well CometChip, which provides the capacity to simultaneously assess interindividual differences in DNA damage or DNA repair. Prior to performing larger scale human studies, it is important to characterize the range and conditions under which various DNA repair pathways are active. Here, we used cell lines with known genetic deficiencies in BER, NER, and ICLR to evaluate the potential of the CometChip for assessment of repair efficiency using model chemical agents. The results of the studies described demonstrate the versatility of the CometChip for detection of a

variety of DNA lesions and support its use for high throughput applications that require assessment of multiple cell types, chemical conditions, and repair time points. We used transgenic cell lines to provide meaningful insight into BER coordination and support existing mechanistic models of NER in the repair of bulky and ICL lesions. This work demonstrates the usefulnes of the CometChip for assessment of numerous DNA repair deficiencies, supporting its use in a applications such as the development of biomarkers of disease susceptibility, development of predictive assays for untested compounds, and development of clinical assays for optimizing treatment regimens.

3.3 Materials and Methods

3.3.1 Cell Culture

TK6 human lymphoblastoids were cultured in suspension in RPMI 1640 with L-glutamine and supplemented with 10% horse serum. The glioblastoma cell lines were kindly supplied by Dr. Robert Sobol (Department of Pharmacology Chemical Biology, Pittsburgh University). Wild type glioblastoma cells were cultured in alpha MEM (MediaTech Manassas, VA), 10% fetal bovine serum (FBS) (Atlanta Biologics, Lawrenceville, GA), antibiotic/antimycotic (Sigma), gentamycin, and L-glutamine (Sigma). The transgenic cell lines with polymerase beta knockdown (PolβKD), alkyladenine DNA glycosylase overexpressed (AAGOE), or Polβ KD with AAG OE (Pol-BKD/AAGOE) were cultured in the same media with 1 μg/mL puromycin (Sigma) added to select for shRNA expressing cells. XPGWT, XPG/E791A, and XP-G human fibroblasts were kindly gifted by Dr. Orlando D Schärer. The wild type Chinese hamster ovary (CHO) cell line (AA8) and CHO cell lines deficient in XPB (UV23) and XPF (UV41) were kindly gifted by Dr. Larry H. Thompson (Lawrence Livermore National Laboratory). Both CHO and human fibroblast cell lines were cultured in DMEM (Invitrogen) supplemented with 10% FBS (Atlanta Biologicals, Atlanta, GA). All cell culture media were supplemented with 100 units/ml penicillin-streptomycin.

3.3.2 Microwell Fabrication

Figure 3-2 illustrates 96-well CometChip fabrication using a PDMS mold. Briefly, 15 mL of molten normal point agarose was applied to gel bond (Lonza, Switzerland) in a 150 mm dish. The agarose was allowed to gel with the PDMS mold on top. PBS was added to aid in removal of the mold, which revealed patterned microwells across the surface of the gel. After the bottomless 96-well plate was applied, at least 10,000 cells were added to each multiwell and allowed to settle by gravity in complete growth media at 37°C, 5% CO_2. Excess cells were aspirated after 15 min and the bottomless plate was removed in order to enclose the arrayed cells in a layer of 1% low melting point agarose.

3.3.3 Analysis of BER Repair Kinetics

One CometChip loaded with exponentially growing TK6 lymphoblastoid cells was used per chemical treatment. All chemicals were prepared immediately prior to exposure. Hydrogen peroxide (H_2O_2) was diluted to 25 μM in 4°C phosphate buffered saline (PBS). Methyl methanesulfonate (MMS) was obtained from Sigma and diluted in PBS to concentrations of 10, 100, and 1000 μM. N-methyl-N'-nitro-N-nitrosoguanidine (MNNG) was dissolved in dimethylsulfoxide (DMSO) and diluted to concentrations of approximately 1, 10, 20 μM in PBS. For each chemical concentration, cells were treated in triplicate for 30 min at 4°C. The chemicals were then aspirated and the CometChip wells were rinsed twice with PBS before adding complete media and allowing cells to repair in the incubator at 37°C, 5% CO_2. To evaluate repair kinetics, 4°C lysis buffer was added at each time point for 15 min to stop repair activity and then removed to prevent the conversion of heat labile sites. At the completion of the final time point, the multiwell plate was removed and the entire gel was submerged in 4°C lysis buffer over night.

3.3.4 4NQO Exposure and Ultraviolet Irradiation

Human fibroblasts with either functional XPG (XPGWT), XPG deficiency (XP-
G), or a mutation abolishing catalytic activity (XPG/E791A) were loaded into a
single CometChip, which was cut into 3x3 well pieces and exposed to 500 nM 4-
Nitroquinoline 1-oxide (4NQO) (Sigma) in 4°C PBS. Each 3x3 gel contained all three
cell types in triplicate and was allowed to repair individually for 0, 1, 2, or 4 hr in
complete growth medium in the incubator. The same protocol was used to assess
ultraviolet radiation damage. 3x3 well gels were individually exposed to 0 to 10 J/m^2
using a 254 nm UVC Lamp (UVG-11, UVP, Upland, CA) calibrated with a UVX
Radiometer (UVP, Upland, CA) to 0.5 ± 0.1 J/m^2/s. Cells were allowed to repair
for three hours in order to assess NER using the comet assay.

3.3.5 Interstrand Crosslinking Assay

Exponentially growing AA8 (wild type), UV41 (XPF-/-), and UV23 (XPB-/-) CHO
cells were loaded into the 96-well version of the CometChip. Three plates were pre-
pared for measurement of interstrand crosslinking repair (ICLR) efficiency: a non-
treated plate and 0 and 24 h time points. The ICLR version of the comet assay
was then performed as described by Spanswick, et al. [48]. Briefly, wells of the
CometChip were treated with 20 μM nitrogen mustard (NM) in FBS-free medium or
medium without NM for 1 hr at 37°C. The wells were then washed three times with
PBS and medium was replaced with fresh complete medium. The multiwell plates
were then removed and the CometChip gels were allowed to incubate for the required
post-incubation repair time. At the time of analysis, each gel was put in cold PBS on
ice and irradiated with 12 Gy of gamma-radiation from a cesium-137 source. The gels
were then immediately submerged in cold lysis solution overnight before performing
the standard comet assay protocol. The degree of DNA interstrand crosslinking re-
pair was calculated as the relative increase in % DNA in tail compared to both the
untreated (0%) and NM treated (100%) control samples at 0 hr.

112

3.3.6 Fluorescence Imaging and Comet Analysis

After electrophoresis, gels were neutralized in 0.4 M Tris, pH 7.5 (3x5 min). Slides were then stained with SYBR Gold (Invitrogen). Images were captured automatically using an epifluorescent microscope and analyzed automatically using custom software written in MATLAB (The Mathworks). Traditional comet slides were scored manually using Komet 5.5 (Andor Technology).

3.4 Results

3.4.1 96-well CometChip

Currently available assays to measure DNA damage and repair are limited in throughput, which acts as a barrier to their use in epidemiological studies. We recently developed the CometChip to enable DNA damage assessment of multiple conditions and cell types on a single platform and increase processing speed through integration with automated analysis platforms [49]. To further increase throughput, we developed the CometChip technology into a 96-well version by replacing the use of silicon/SU-8 microwell stamps with PDMS. This represented a significant advance, because numerous molds can be made from a single master, and PDMS molds are more durable than silicon/SU-8, because they are made from a single material rather than two. In addition, PDMS is pliable and hydrophobic, which simplifies its removal from agarose and allows for the creation of a microwell patterned surface large enough to cover the area of an entire microtiter plate.

The 96-well version integrates with high throughput screening (HTS) technologies, such as robotic liquid handling systems and automated imaging platforms. To demonstrate this ability, we loaded a CometChip with TK6 lymphoblastoids and used an automated liquid handler (Digilab, Holliston, MA) to deliver a range of H_2O_2 concentrations (Figure 3-3). These data support the ability of the CometChip to be integrated with HTS equipment, where larger sets of chemicals could be administered to cells in an automated fashion. The data also show the range of H_2O_2 damage de-

tection, revealing a dose of 25 μM as an appropriate exposure for assessment of base excision repair kinetics because it produces a large signal without saturation. This is consistent with doses used by other groups in clinical assessments of BER capacity [50, 51].

3.4.2   Evaluation of Base Excision Repair Kinetics

The alkaline comet assay detects the presence of SSBs and also alkali labile sites (e.g. abasic sites), making it especially well suited for the measure of BER kinetics [44]. Using the CometChip, multiple cell types and conditions can be assayed on a single device, increasing throughput, reducing volume of chemicals required, and significantly decreasing labor and experimental noise [49]. Furthermore, multiple repair time points can be precisely assessed by lysing cells in wells adjacent to cells undergoing further repair incubation. To test the multiwell platform for measuring BER kinetics, we exposed TK6 lymphoblastoid cells to 25 μM H_2O_2 and allowed repair for up to two hours with time increments as short as five min. The entire experiment was conducted on a single chip at 0°C, in order to minimize the initiation of repair during exposure. We similiarly exposed TK6 cells on a separate CometChip to three concentrations of both MMS and MMNG. Figure 3-4a shows that H_2O_2 induced damage is completely repaired in less than 30 min with kinetics similar to the repair of radiation induced damage [52, 49]. In contrast, alkylation damage induced by MMS and MNNG persists signficantly longer, as seen in Figure 3-4b and Figure 3-4c, respectively. With regard to measuring BER with the comet assay, we must consider the contribution of repair intermediates, even at the initial time point, due to the rapid glycosylase activity during treatment [3]. The decrease in signal can then be interpreted as a measure of the net excision of base lesions and the repair of intermediates [53]. Interestingly, the rate of BER, seen as the slope of each repair curve, appears to be consistent among concentrations of the same chemical, suggesting a tightly controlled coordination of BER protein activities.

To directly compare the repair kinetics between H_2O_2, MMS, and MNNG, the data for the highest concentration of each chemical were normalized relative to its

initial damage level (Figure 3-5). The first interesting result is a significantly faster repair of H_2O_2 induced damage compared to both MMS and MNNG, ($t_{1/2} \approx 15$, 60, and 120 min, respectively). This variation can be attributed to differences in the major glycosylase used to initiate BER. H_2O_2, like irradiation, induces a large proportion of oxidized base lesions, which are excised by a bifunctional glycosylase (i.e. OGG1), eliminating the requirement of gap tailoring by Polβ. In contrast, alkyation induced damage is primarily excised by a monofunctional glycosylase (i.e. AAG) with strand scission by AP Endonuclease, and therefore requires the rate limiting dRP lyase activity of Polβ [9, 52, 54]. Interestingly, we observe variation in repair rate between MMS and MNNG, which have simliar alkylation lesion spectra. The main difference between the two chemicals is that MNNG induces 7% O^6-methylguanine lesions through SN1 attack, while MMS is known to act through an SN2 mechanism and form less than 1% O^6 adducts [55]. O^6-methylguanine is repaired through direct reversal by methylguanine methyltransferase (MGMT), but the lesion has been shown to induce many cellular responses that may help to explain the reduced rate of repair [56, 57]. Interestingly, the relative toxicities of H_2O_2, MMS, MNNG are in agreement with the relative rates in which the damage they induce is repaired. Taken together, the CometChip enables precise assessment of repair kinetics that may be useful not only in characterizing chemical exposures, but also in interpreting mechanisms of toxicity.

3.4.3 Detection of BER deficiency

We used transgenic glioblastoma cell lines to more closely examine the role of key BER proteins in the repair of alkylation damage. The use of MMS, a model alkylating agent, enables a focused study of BER, as it induces a relatively low proportion of O^6-methylguanine adducts, and instead induces mainly N^7-methylguanine and N^3-methyladenine lesions [55]. We used the CometChip to assess the repair capacities of glioblastoma cell lines with deficiencies in both BER initiation (i.e. AAG) and/or progression/completion (i.e. Polβ). LN428 cells were generously gifted by the Laboratory of Dr. Robert Sobol (University of Pittsburg). The cell lines were engineered

through shRNA lentiviral integration to overexpress AAG (LN428 AAGOE), or to have knock-down expression of Polβ (LN428 PolβKD), or to both overexpress AAG and have knock-down expression of Polβ (LN428 PolβKD/AAGOE). This combination of genotypes enabled us to modulate the rate of BER initiation versus progression in order to investigate the processing tolerance of Polβ and the ability to detect a BER deficiency using the CometChip platform.

To determine if the CometChip can be used to detect BER deficiencies, we exposed all four LN428 genotypes to 1 mM MMS and measured their repair over 2 hr using a single device (Figure 3-6). The results suggest equivalent repair kinetics in WT, PolβKD, and AAOE cells, with only the combined AAGOE and PolβKD genotype resulting in a persistent damage signal. This implies that an increase in BER intermediates resulting from AAOE is tolerated by Polβ. There does appear to be a slight increase in comet signal in the AAGOE cells at 120 min, suggesting Polβ saturation, but this difference was not found to be statistically significant. The data also imply that PolβKD can tolerate BER intermediates, which conflicts with results from similar studies that showed a significant accumulation of BER intermediates by comet assay in PolβKD cells [58, 52]. This suggests either an alternative route of repair for AAG initiated intermediates or inherently low AAG expression. In fact, LN428 glioblastoma cell lines have been shown to possess undetectable AAG expression by Western blot [58, 59]. This additional information helps clarify the PolβKD result, emphasizing that it is the balance of many coordinated proteins in the BER pathway that must be considered when evaluating the impact of BER deficiencies [60].

An important limitation to consider is the inability to detect absolute levels of alkylation damage using the CometChip in this format. Instead, the comet signal represents the level of BER intermediates resulting from the net excision of base lesions and the repair of intermediates. As such, a repair deficiency, such as low expression of AAG, which is known to promote sensitivity to alkylating agents [61], can go undetected by the comet assay. It would therefore be interesting to probe the absolute levels of alkylation damage using post-lysis enzymatic treatment (e.g. AlkA)

[62]. The adoption of this procedure might enable a more sensitive detection of Polβ, AAG, and other BER protein deficiencies. However, even in its standard format, the CometChip provides a quick method to directly measure repair intermediates, which have been shown to contribute significantly to the toxicity of methylation damage [8, 10, 63].

3.4.4 Detection of NER deficiency

Imbalances in NER are associated with both increased cancer susceptibility and chemotherapeutic resistance [64]. Dual incision by key proteins, XPF and XPG, is especially critical, because their improper coordination can result in potentially toxic repair intermediates (Figure 3-8) [65]. Many traditional assays measure the incorporation of repaired nucleotides (i.e. unscheduled DNA synthesis (UDS)), which is highly laborious and cannot be used for detection of initial damage levels or dual incision repair intermediates. While the comet assay does not directly detect the presence of NER substrates (i.e. bulky lesions), their incision, both partial and complete, is revealed by an increase in comet signal [66]. In collaboration with the laboratory of Dr. Orlando Schärer, we set out to determine if the CometChip is capable of detecting NER deficiencies and also investigate the mechanism of dual incision.

To explore the role of XPG in the dual incision process, we used three human fibroblast cell lines: XPGWT has functional XPG activity, XPG/E791A is catalytically inactive, and XP-G is deficient [67]. We exposed all three cell types in a single CometChip to 4NQO, which is known to induce bulky adducts that are repaired by NER [68]. Wild type cells repaired the majority of the damage within four hours (Figure 3-7). In contrast, a significant amount of damage remained in both XPG deficient cell lines. According to the dual incision model, XP-G deficient cells are unable to make either the 3' incision by XPF or the 5' incision by XPG, while XPG/E791A cells are capable of making the 3' incision by XPF but not the 5' incision by XPG [65]. The theoretical intermediates that are detectable at later time points are shown in Figure 3-8. According to previous studies, we expected to see one-sided incision in the XPG/E791A cells and no significant accumulation of repair intermediates in

117

the XP-G cell line. The results show significant differences in the repair response of the three genotyptes, but offer little mechanistic insight. The results, however, agree with Staresincic et al. [65], who found residual XPG activity in the XPG/E791A cells and also described the ability of XP-G cells to initiate NER and conduct some UDS. It would be interesting to further compare CometChip results to previous results by evaluating cells with deficiencies in XPF, as XPF has been shown to be required for incision by XPG, and XP-F cells were shown to have even less UDS than XP-G [65]. We would therefore expect an XPF deficiency to have even less damage induction than XP-G cells.

In an attempt to further reveal the XPG deficiencies, we used 254 nm ultraviolet light (UVC), which is known to induce pyrimidine dimers, which are specifically repaired by NER. UVC also induces SSBs and other oxidative lesions [66]. To increase the specificity of our signal for NER, we evaluated damage levels after 3 hr, when we expected most BER mediated repair to be complete and the signal to therefore be more representative of the NER intermediates proposed in Figure 3-8. The results show a dose dependent increase in damage levels in XPGWT cells, which is consistent with a dose dependent increase in prymidine dimers (Figure 3-9). In XP-G cells, the comet signal was independent of UV dose, which supports the dual incision hypothesis that XPG is required for both 3' and 5' incisions. Lastly, the XPG/E791A cells were found to be extremely sensitive to UV radiation, as would be expected by accumulation of one-sided incision. Although this approach does not provide direct measurement of NER, it represents a novel approach to identify dual incision deficiencies.

3.4.5 Detection of ICL deficiency

ICL agents represent the oldest class of DNA damaging chemotherapies and are still used in treatment of numerous cancers, although they are largely limited by tumor resistance [69]. In order to test the efficacy of the CometChip to detect a deficiency in ICLR, we administered NM to three CHO cell lines: AA8 (wild type), UV41 (XPF-/-), and UV23 (XPB-/-). The extent of "unhooking" was determined according to

Spanswick, et al. as seen in Figure 3-10 and described in *Materials and Methods* [70]. Figure 3-11 demonstrates complete "unhooking" by wild type and XPB-/- cells after 24 hr repair. In contrast, there was significantly less ICLR in the XPF-/- cells. This is in agreement with findings by De Silva, et al. [71], and serves as a proof of principle for the use of the CometChip to screen for ICL resistance or potential ICL activity in drug discovery. In addition, the CometChip can be used to assess roles of various NER proteins in ICLR and thereby advance mechanistic models that are still largely incomplete in human cells [34].

3.5 Conclusion

We explored the versatility of the alkaline CometChip to measure repair from a variety of DNA damaging agents known to produce oxidized and alkylated base lesions, bulky adducts, strand breaks, and DNA crosslinks, etc. Our data demonstrate the potential use of the alkaline CometChip in applications such as preclinical drug screening or evaluating sensitivities to chemotherapeutical agents. A comparison between similarly acting alkylating agents (i.e. MMS and MNNG), revealed differential repair kinetics, raising the importance of relative glycosylase activities and perhaps even suggesting differences in the kinetics between BER sub-pathways. To explore this concept, we investigated the effect of multiple BER deficiencies in the repair of MMS induced damage. An imbalance in Polβ was detected only by enhancing BER initiation, revealing the importance of coordination between multiple BER proteins in maintaining pathway balance. Lastly, we demonstrated an ability to detect multiple genetic deficiencies in two other DNA repair pathways (NER and ICL), supporting the use of the CometChip in identifying susceptible populations and guiding treatment strategies.

Collectively, this work serves as proof of principle for the use of the CometChip in studies to advance mechanistic models of DNA repair and also as a high throughput tool for evaluating genotoxicity of multiple chemical conditions or assessing DNA repair through numerous pathways. The CometChip may be useful in public health,

as there is increasing evidence supporting a correlation between DNA repair capacity and cancer incidence [2, 72, 73]. In addition, effective individualized therapies require knowledge of the sensitivity of a particular tumor. The versatility of the CometChip, its straight forward and inexpensive protocol, and its ability to integrate with high throughput screening and analysis platforms give it value in a variety of research settings.

References

[1] J. H. J. Hoeijmakers, "Dna damage, aging, and cancer," *N Engl J Med*, vol. 361, pp. 1475–85, Oct 2009.

[2] R. Hakem, "Dna-damage repair; the good, the bad, and the ugly," *EMBO J*, vol. 27, pp. 589–605, Feb 2008.

[3] L. A. Loeb and B. D. Preston, "Mutagenesis by apurinic/apyrimidinic sites," *Annu Rev Genet*, vol. 20, pp. 201–30, Jan 1986.

[4] D. Hanahan and R. A. Weinberg, "Hallmarks of cancer: the next generation," *Cell*, vol. 144, pp. 646–74, Mar 2011.

[5] L. A. Loeb, "A mutator phenotype in cancer," *Cancer Research*, vol. 61, pp. 3230–9, Apr 2001.

[6] J. H. Hoeijmakers, "Genome maintenance mechanisms for preventing cancer," *Nature*, vol. 411, pp. 366–74, May 2001.

[7] K. Larson, J. Sahm, R. Shenkar, and B. Strauss, "Methylation-induced blocks to in vitro dna replication," *Mutat Res*, vol. 150, pp. 77–84, Jan 1985.

[8] L. M. Posnick and L. D. Samson, "Imbalanced base excision repair increases spontaneous mutation and alkylation sensitivity in escherichia coli," *J Bacteriol*, vol. 181, pp. 6763–71, Nov 1999.

[9] R. W. Sobol, R. Prasad, A. Evenski, A. Baker, X. P. Yang, J. K. Horton, and S. H. Wilson, "The lyase activity of the dna repair protein beta-polymerase

protects from dna-damage-induced cytotoxicity," *Nature*, vol. 405, pp. 807–10, Jun 2000.

[10] R. W. Sobol, M. Kartalou, K. H. Almeida, D. F. Joyce, B. P. Engelward, J. K. Horton, R. Prasad, L. D. Samson, and S. H. Wilson, "Base excision repair intermediates induce p53-independent cytotoxic and genotoxic responses," *The Journal of biological chemistry*, vol. 278, pp. 39951–9, Oct 2003.

[11] B. P. Engelward, A. Dreslin, J. Christensen, D. Huszar, C. Kurahara, and L. Samson, "Repair-deficient 3-methyladenine dna glycosylase homozygous mutant mouse cells have increased sensitivity to alkylation-induced chromosome damage and cell killing," *EMBO J*, vol. 15, pp. 945–52, Feb 1996.

[12] F. Calléja, J. G. Jansen, H. Vrieling, F. Laval, and A. A. van Zeeland, "Modulation of the toxic and mutagenic effects induced by methyl methanesulfonate in chinese hamster ovary cells by overexpression of the rat n-alkylpurine-dna glycosylase," *Mutat Res*, vol. 425, pp. 185–94, Apr 1999.

[13] M. Rinne, D. Caldwell, and M. R. Kelley, "Transient adenoviral n-methylpurine dna glycosylase overexpression imparts chemotherapeutic sensitivity to human breast cancer cells," *Molecular Cancer Therapeutics*, vol. 3, pp. 955–67, Aug 2004.

[14] R. Trivedi, K. Almeida, J. Fornsaglio, S. Schamus, and R. Sobol, "The role of base excision repair in the sensitivity and resistance to temozolomide-mediated cell death," *Cancer Research*, vol. 65, no. 14, p. 6394, 2005.

[15] D. K. Srivastava, B. J. Berg, R. Prasad, J. T. Molina, W. A. Beard, A. E. Tomkinson, and S. H. Wilson, "Mammalian abasic site base excision repair. identification of the reaction sequence and rate-determining steps," *The Journal of biological chemistry*, vol. 273, pp. 21203–9, Aug 1998.

122

[16] E. L. Goode, C. M. Ulrich, and J. D. Potter, "Polymorphisms in dna repair genes and associations with cancer risk," *Cancer Epidemiol Biomarkers Prev*, vol. 11, pp. 1513–30, Dec 2002.

[17] J. B. Sweasy, J. M. Lauper, and K. A. Eckert, "Dna polymerases and human diseases," *Radiat Res*, vol. 166, pp. 693–714, Nov 2006.

[18] T. Sliwinski, P. Ziemba, Z. Morawiec, M. Kowalski, M. Zadrozny, and J. Blasiak, "Polymorphisms of the dna polymerase beta gene in breast cancer," *Breast Cancer Res Treat*, vol. 103, pp. 161–6, Jun 2007.

[19] R. Stupp, W. P. Mason, M. J. van den Bent, M. Weller, B. Fisher, M. J. B. Taphoorn, K. Belanger, A. A. Brandes, C. Marosi, U. Bogdahn, J. Curschmann, R. C. Janzer, S. K. Ludwin, T. Gorlia, A. Allgeier, D. Lacombe, J. G. Cairncross, E. Eisenhauer, R. O. Mirimanoff, E. O. for Research, T. of Cancer Brain Tumor, R. Groups, and N. C. I. of Canada Clinical Trials Group, "Radiotherapy plus concomitant and adjuvant temozolomide for glioblastoma," *N Engl J Med*, vol. 352, pp. 987–96, Mar 2005.

[20] J. Zhang, M. F. G. Stevens, C. A. Laughton, S. Madhusudan, and T. D. Bradshaw, "Acquired resistance to temozolomide in glioma cell lines: molecular mechanisms and potential translational applications," *Oncology*, vol. 78, pp. 103–14, Jan 2010.

[21] N. J. Curtin, L.-Z. Wang, A. Yiakouvaki, S. Kyle, C. A. Arris, S. Canan-Koch, S. E. Webber, B. W. Durkacz, H. A. Calvert, Z. Hostomsky, and D. R. Newell, "Novel poly(adp-ribose) polymerase-1 inhibitor, ag14361, restores sensitivity to temozolomide in mismatch repair-deficient cells," *Clin Cancer Res*, vol. 10, pp. 881–9, Feb 2004.

[22] S. H. Wilson, W. A. Beard, D. D. Shock, V. K. Batra, N. A. Cavanaugh, R. Prasad, E. W. Hou, Y. Liu, K. Asagoshi, J. K. Horton, D. F. Stefanick, P. S. Kedar, M. J. Carrozza, A. Masaoka, and M. L. Heacock, "Base excision

repair and design of small molecule inhibitors of human dna polymerase ," *Cell Mol Life Sci*, vol. 67, pp. 3633–47, Nov 2010.

[23] A. S. Jaiswal, S. Banerjee, H. Panda, C. D. Bulkin, T. Izumi, F. H. Sarkar, D. A. Ostrov, and S. Narayan, "A novel inhibitor of dna polymerase beta enhances the ability of temozolomide to impair the growth of colon cancer cells," *Mol Cancer Res*, vol. 7, pp. 1973–83, Dec 2009.

[24] J. K. Horton and S. H. Wilson, "Hypersensitivity phenotypes associated with genetic and synthetic inhibitor-induced base excision repair deficiency," *DNA Repair*, vol. 6, pp. 530–43, Apr 2007.

[25] E. M. Goellner, B. Grimme, A. R. Brown, Y.-C. Lin, X. hong Wang, K. F. Sugrue, L. Mitchell, R. N. Trivedi, J. bo Tang, and R. W. Sobol, "Overcoming temozolomide resistance in glioblastoma via dual inhibition of nad+ biosynthesis and base excision repair," *Cancer Research*, vol. 71, pp. 2308–17, Mar 2011.

[26] J. N. Sarkaria, G. J. Kitange, C. D. James, R. Plummer, H. Calvert, M. Weller, and W. Wick, "Mechanisms of chemoresistance to alkylating agents in malignant glioma," *Clin Cancer Res*, vol. 14, pp. 2900–8, May 2008.

[27] J. Slyskova, A. Naccarati, V. Polakova, B. Pardini, L. Vodickova, R. Stetina, J. Schmuczerova, Z. Smerhovsky, L. Lipska, and P. Vodicka, "Dna damage and nucleotide excision repair capacity in healthy individuals," *Environ. Mol. Mutagen.*, Apr 2011.

[28] O. D. Schärer, "Dna interstrand crosslinks: natural and drug-induced dna adducts that induce unique cellular responses," *Chembiochem*, vol. 6, pp. 27–32, Jan 2005.

[29] K.-M. Thoms, C. Kuschal, and S. Emmert, "Lessons learned from dna repair defective syndromes," *Exp Dermatol*, vol. 16, pp. 532–44, Jun 2007.

[30] P. J. McHugh, V. J. Spanswick, and J. A. Hartley, "Repair of dna interstrand crosslinks: molecular mechanisms and clinical relevance," *Lancet Oncol*, vol. 2, pp. 483–90, Aug 2001.

[31] L. J. Niedernhofer, A. S. Lalai, and J. H. Hoeijmakers, "Fanconi anemia (cross)linked to dna repair," *Cell*, vol. 123, pp. 1191–1198, Dec 2005.

[32] P. H. Clingen, C. F. Arlett, J. A. Hartley, and C. N. Parris, "Chemosensitivity of primary human fibroblasts with defective unhooking of dna interstrand cross-links," *Exp Cell Res*, vol. 313, pp. 753–60, Feb 2007.

[33] P. R. Andreassen and K. Ren, "Fanconi anemia proteins, dna interstrand crosslink repair pathways, and cancer therapy," *Curr Cancer Drug Targets*, vol. 9, pp. 101–17, Feb 2009.

[34] P. A. Muniandy, J. Liu, A. Majumdar, S.-T. Liu, and M. M. Seidman, "Dna interstrand crosslink repair in mammalian cells: step by step," *Crit Rev Biochem Mol Biol*, vol. 45, pp. 23–49, Feb 2010.

[35] J. R. W. Masters and B. Köberle, "Curing metastatic cancer: lessons from testicular germ-cell tumours," *Nat Rev Cancer*, vol. 3, pp. 517–25, Jul 2003.

[36] S. Usanova, A. Piée-Staffa, U. Sied, J. Thomale, A. Schneider, B. Kaina, and B. Köberle, "Cisplatin sensitivity of testis tumour cells is due to deficiency in interstrand-crosslink repair and low ercc1-xpf expression," *Mol Cancer*, vol. 9, p. 248, Jan 2010.

[37] A. J. Deans and S. C. West, "Dna interstrand crosslink repair and cancer," *Nat Rev Cancer*, vol. 11, pp. 467–80, Jan 2011.

[38] A. Memisoglu and L. Samson, "Contribution of base excision repair, nucleotide excision repair, and dna recombination to alkylation resistance of the fission yeast schizosaccharomyces pombe," *J Bacteriol*, vol. 182, pp. 2104–12, Apr 2000.

[39] K. H. Chen, D. K. Srivastava, and S. H. Wilson, "Relationship between base excision repair capacity and dna alkylating agent sensitivity in mouse monocytes," *Mutat Res*, vol. 487, pp. 121–6, Dec 2001.

[40] V. J. Spanswick, C. Craddock, M. Sekhar, P. Mahendra, P. Shankaranarayana, R. G. Hughes, D. Hochhauser, and J. A. Hartley, "Repair of dna interstrand crosslinks as a mechanism of clinical resistance to melphalan in multiple myeloma," *Blood*, vol. 100, pp. 224–9, Jul 2002.

[41] P. Wynne, C. Newton, J. A. Ledermann, A. Olaitan, T. A. Mould, and J. A. Hartley, "Enhanced repair of dna interstrand crosslinking in ovarian cancer cells from patients following treatment with platinum-based chemotherapy," *Br J Cancer*, p. 7, Sep 2007.

[42] C. Li, L.-E. Wang, and Q. Wei, "Dna repair phenotype and cancer susceptibility—a mini review," *Int J Cancer*, vol. 124, pp. 999–1007, Mar 2009.

[43] V. Valdiglesias, E. Pásaro, J. Méndez, and B. Laffon, "Assays to determine dna repair ability," *Journal of Toxicology and Environmental Health, Part A*, vol. 74, pp. 1094–1109, Aug 2011.

[44] A. R. Collins, "The comet assay for dna damage and repair: principles, applications, and limitations," *Mol Biotechnol*, vol. 26, pp. 249–61, Mar 2004.

[45] V. Calini, C. Urani, and M. Camatini, "Comet assay evaluation of dna single- and double-strand breaks induction and repair in c3h10t1/2 cells," *Cell Biol Toxicol*, vol. 18, pp. 369–79, Jan 2002.

[46] F. Faust, "The use of the alkaline comet assay with lymphocytes in human biomonitoring studies," *Mutation Research/Reviews in Mutation Research*, vol. 566, pp. 209–229, May 2004.

[47] M. Shahidi, H. Mozdarani, and P. E. Bryant, "Radiation sensitivity of leukocytes from healthy individuals and breast cancer patients as measured by the alkaline and neutral comet assay," *Cancer Letters*, vol. 257, pp. 263–73, Nov 2007.

126

[48] V. Spanswick, J. Hartley, T. Ward, and J. Hartley, "Measurement of drug-induced dna interstrand crosslinking using the single cell gel electrophoresis (comet) assay," *Methods in molecular medicine*, vol. 28, pp. 143–154, 1999.

[49] D. K. Wood, D. M. Weingeist, S. N. Bhatia, and B. P. Engelward, "Single cell trapping and dna damage analysis using microwell arrays," *Proc Natl Acad Sci USA*, vol. 107, pp. 10008–13, Jun 2010.

[50] R. A. El-Zein, C. M. Monroy, A. Cortes, M. R. Spitz, A. Greisinger, and C. J. Etzel, "Rapid method for determination of dna repair capacity in human peripheral blood lymphocytes amongst smokers," *BMC Cancer*, vol. 10, p. 439, Jan 2010.

[51] F. Caple, E. A. Williams, A. Spiers, J. Tyson, B. Burtle, A. K. Daly, J. C. Mathers, and J. E. Hesketh, "Inter-individual variation in dna damage and base excision repair in young, healthy non-smokers: effects of dietary supplementation and genotype," *Br J Nutr*, vol. 103, pp. 1585–93, Jun 2010.

[52] J. K. Horton, M. Watson, D. F. Stefanick, D. T. Shaughnessy, J. A. Taylor, and S. H. Wilson, "Xrcc1 and dna polymerase beta in cellular protection against cytotoxic dna single-strand breaks," *Cell Res*, vol. 18, pp. 48–63, Jan 2008.

[53] B. A. Sokhansanj, G. R. Rodrigue, J. P. Fitch, and D. M. Wilson, "A quantitative model of human dna base excision repair. i. mechanistic insights," *Nucleic Acids Research*, vol. 30, pp. 1817–25, Apr 2002.

[54] D. Svilar, E. M. Goellner, K. H. Almeida, and R. W. Sobol, "Base excision repair and lesion-dependent subpathways for repair of oxidative dna damage," *Antioxid Redox Signal*, vol. 14, pp. 2491–507, Jun 2011.

[55] M. D. Wyatt and D. L. Pittman, "Methylating agents and dna repair responses: Methylated bases and sources of strand breaks," *Chem. Res. Toxicol.*, vol. 19, pp. 1580–94, Dec 2006.

[56] B. Kaina, "Mechanisms and consequences of methylating agent-induced sces and chromosomal aberrations: a long road traveled and still a far way to go," *Cytogenet Genome Res*, vol. 104, pp. 77–86, Jan 2004.

[57] D. I. Beardsley, "N-methyl-n'-nitro-n-nitrosoguanidine activates cell-cycle arrest through distinct mechanisms activated in a dose-dependent manner," *Molecular Pharmacology*, vol. 68, pp. 1049–1060, Jul 2005.

[58] R. W. Sobol, D. E. Watson, J. Nakamura, F. M. Yakes, E. Hou, J. K. Horton, J. Ladapo, B. V. Houten, J. A. Swenberg, K. R. Tindall, L. D. Samson, and S. H. Wilson, "Mutations associated with base excision repair deficiency and methylation-induced genotoxic stress," *Proc Natl Acad Sci USA*, vol. 99, pp. 6860–5, May 2002.

[59] J. bo Tang, D. Svilar, R. N. Trivedi, X. hong Wang, E. M. Goellner, B. Moore, R. L. Hamilton, L. A. Banze, A. R. Brown, and R. W. Sobol, "N-methylpurine dna glycosylase and dna polymerase beta modulate ber inhibitor potentiation of glioma cells to temozolomide," *Neuro-oncology*, Mar 2011.

[60] R. N. Trivedi, X. hong Wang, E. Jelezcova, E. M. Goellner, J. bo Tang, and R. W. Sobol, "Human methyl purine dna glycosylase and dna polymerase beta expression collectively predict sensitivity to temozolomide," *Molecular Pharmacology*, vol. 74, pp. 505–16, Aug 2008.

[61] B. Engelward, G. Weeda, M. Wyatt, J. Broekhof, J. de Wit, I. Donker, J. Allan, B. Gold, J. Hoeijmakers, and L. Samson, "Base excision repair deficient mice lacking the aag alkyladenine dna glycosylase," *Proc Natl Acad Sci USA*, vol. 94, no. 24, p. 13087, 1997.

[62] A. R. Collins, M. Dusinská, and A. Horská, "Detection of alkylation damage in human lymphocyte dna with the comet assay," *Acta Biochim Pol*, vol. 48, pp. 611–4, Jan 2001.

[63] M. L. Rinne, Y. He, B. F. Pachkowski, J. Nakamura, and M. R. Kelley, "N-methylpurine dna glycosylase overexpression increases alkylation sensitivity by rapidly removing non-toxic 7-methylguanine adducts," *Nucleic Acids Research*, vol. 33, pp. 2859–67, Jan 2005.

[64] D. Leibeling, P. Laspe, and S. Emmert, "Nucleotide excision repair and cancer," *J Mol Hist*, vol. 37, pp. 225–38, Sep 2006.

[65] L. Staresincic, A. F. Fagbemi, J. H. Enzlin, A. M. Gourdin, N. Wijgers, I. Dunand-Sauthier, G. Giglia-Mari, S. G. Clarkson, W. Vermeulen, and O. D. Schärer, "Coordination of dual incision and repair synthesis in human nucleotide excision repair," *EMBO J*, vol. 28, pp. 1111–20, Apr 2009.

[66] C. Alapetite, T. Wachter, E. Sage, and E. Moustacchi, "Use of the alkaline comet assay to detect dna repair deficiencies in human fibroblasts exposed to uvc, uvb, uva and gamma-rays," *International Journal of Radiation Biology*, vol. 69, pp. 359–69, Mar 1996.

[67] M. Wakasugi, J. T. Reardon, and A. Sancar, "The non-catalytic function of xpg protein during dual incision in human nucleotide excision repair," *The Journal of biological chemistry*, vol. 272, pp. 16030–4, Jun 1997.

[68] C. J. Jones, S. M. Edwards, and R. Waters, "The repair of identified large dna adducts induced by 4-nitroquinoline-1-oxide in normal or xeroderma pigmentosum group a human fibroblasts, and the role of dna polymerases alpha or delta," *Carcinogenesis*, vol. 10, pp. 1197–201, Jul 1989.

[69] R. B. Scott, "Cancer chemotherapy–the first twenty-five years," *Br Med J*, vol. 4, pp. 259–65, Oct 1970.

[70] V. J. Spanswick, J. M. Hartley, and J. A. Hartley, "Measurement of dna interstrand crosslinking in individual cells using the single cell gel electrophoresis (comet) assay," *Methods Mol Biol*, vol. 613, pp. 267–82, Jan 2010.

[71] I. U. D. Silva, P. J. McHugh, P. H. Clingen, and J. A. Hartley, "Defining the roles of nucleotide excision repair and recombination in the repair of dna interstrand cross-links in mammalian cells," *Molecular and Cellular Biology*, vol. 20, pp. 7980–90, Nov 2000.

[72] T. Paz-Elizur, Z. Sevilya, Y. Leitner-Dagan, D. Elinger, L. C. Roisman, and Z. Livneh, "Dna repair of oxidative dna damage in human carcinogenesis: potential application for cancer risk assessment and prevention," *Cancer Letters*, vol. 266, pp. 60–72, Jul 2008.

[73] F. Marcon, "Assessment of individual sensitivity to ionizing radiation and dna repair efficiency in a healthy population," *Mutation Research/Genetic Toxicology and Environmental Mutagenesis*, vol. 541, pp. 1–8, Nov 2003.
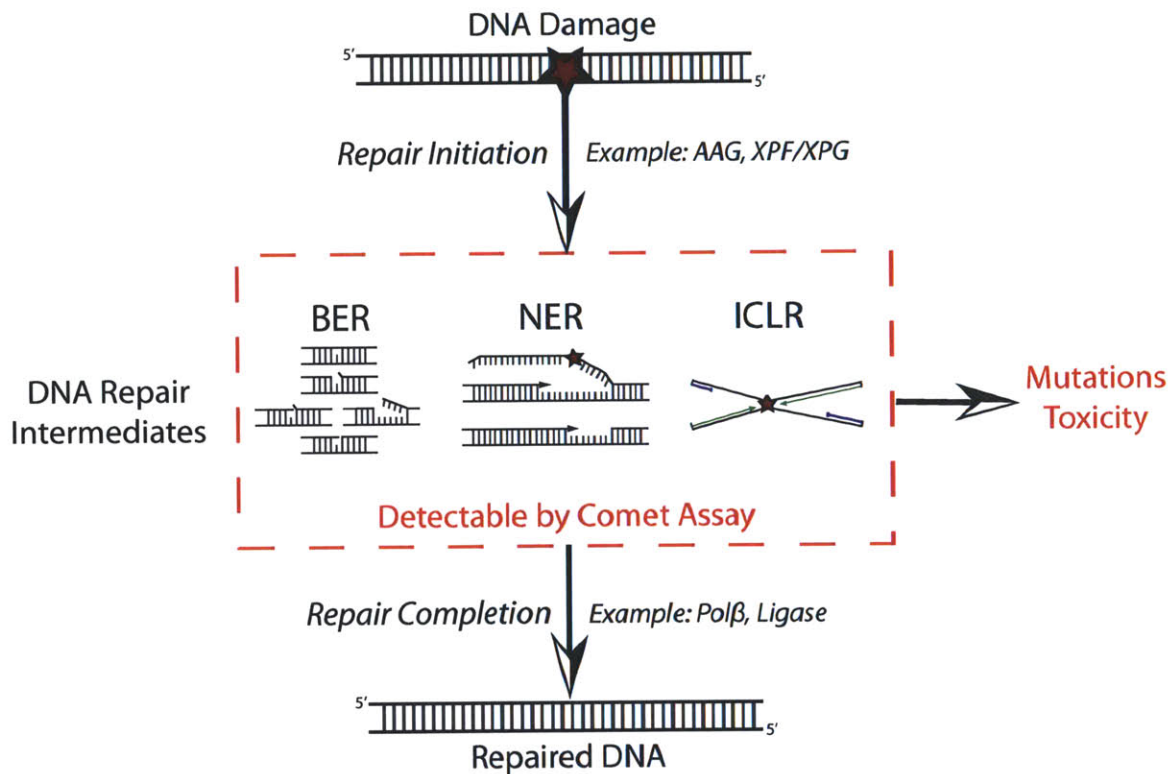
Figure 3-1: **Detection of DNA Repair Intermediates.** The alkaline comet assay detects single strand breaks and alkali labile sites. Its use for detection of base lesions is therefore dependent on their excision by DNA repair enzymes and their repair by downstream enzymes. Examples of detectable repair intermediates for BER, NER, and ICLR are provided.

1) Pour Molten Agarose

Molten Agarose

Gel Bond

2) Apply PDMS Mold
Allow Agarose to Gel

PDMS Mold

Molten Agarose on Gel Bond

Microposts
(20x50μm)

3) Peel Off PDMS Mold

PDMS

Agarose with Microwells

4) Align 96-well Plate

Bottomless 96-well Plate

Glass Plate

5) Clamp 96-well Plate

Bottomless 96-well Plate

Glass Plate
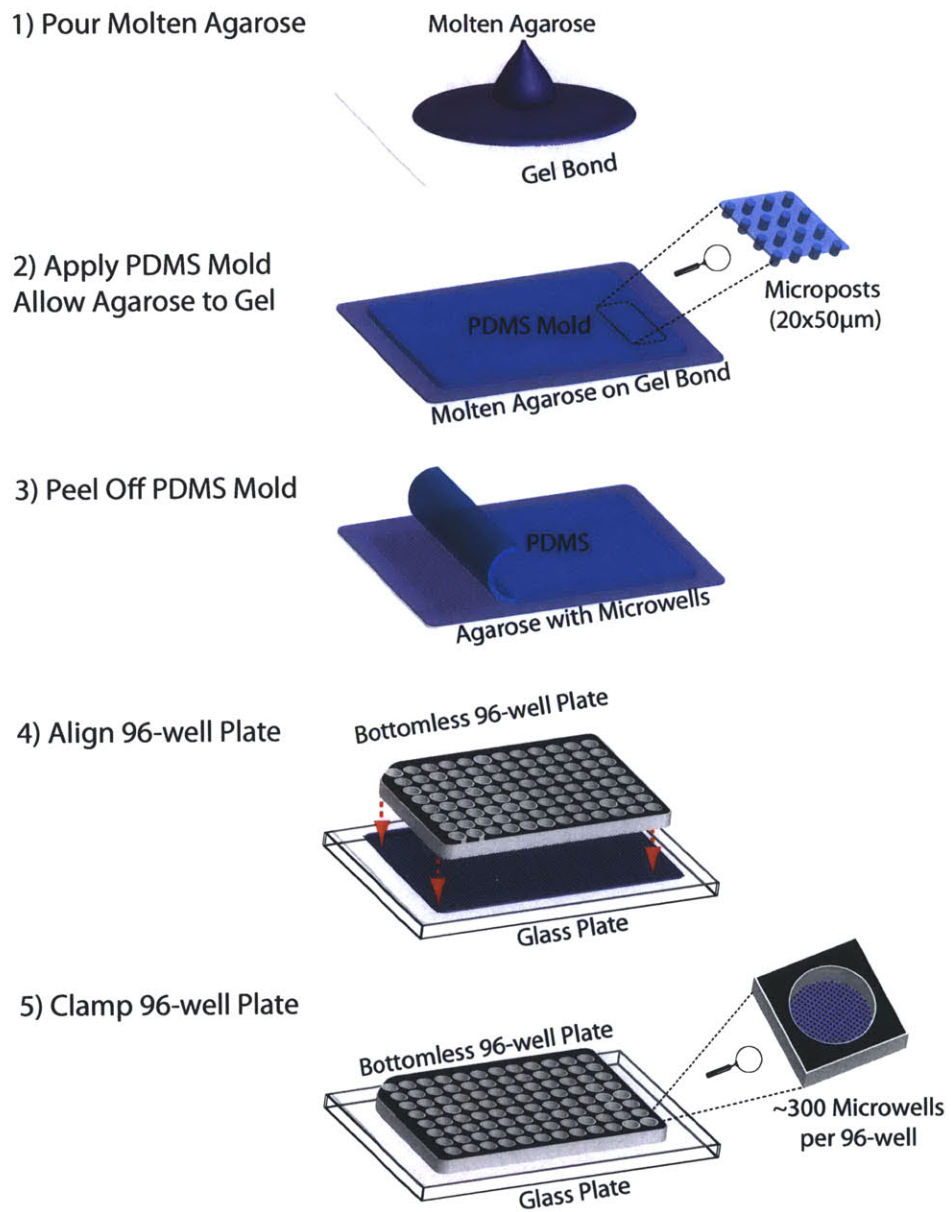
~300 Microwells
per 96-well

Figure 3-2: **96-well CometChip Fabrication using PDMS Mold.**
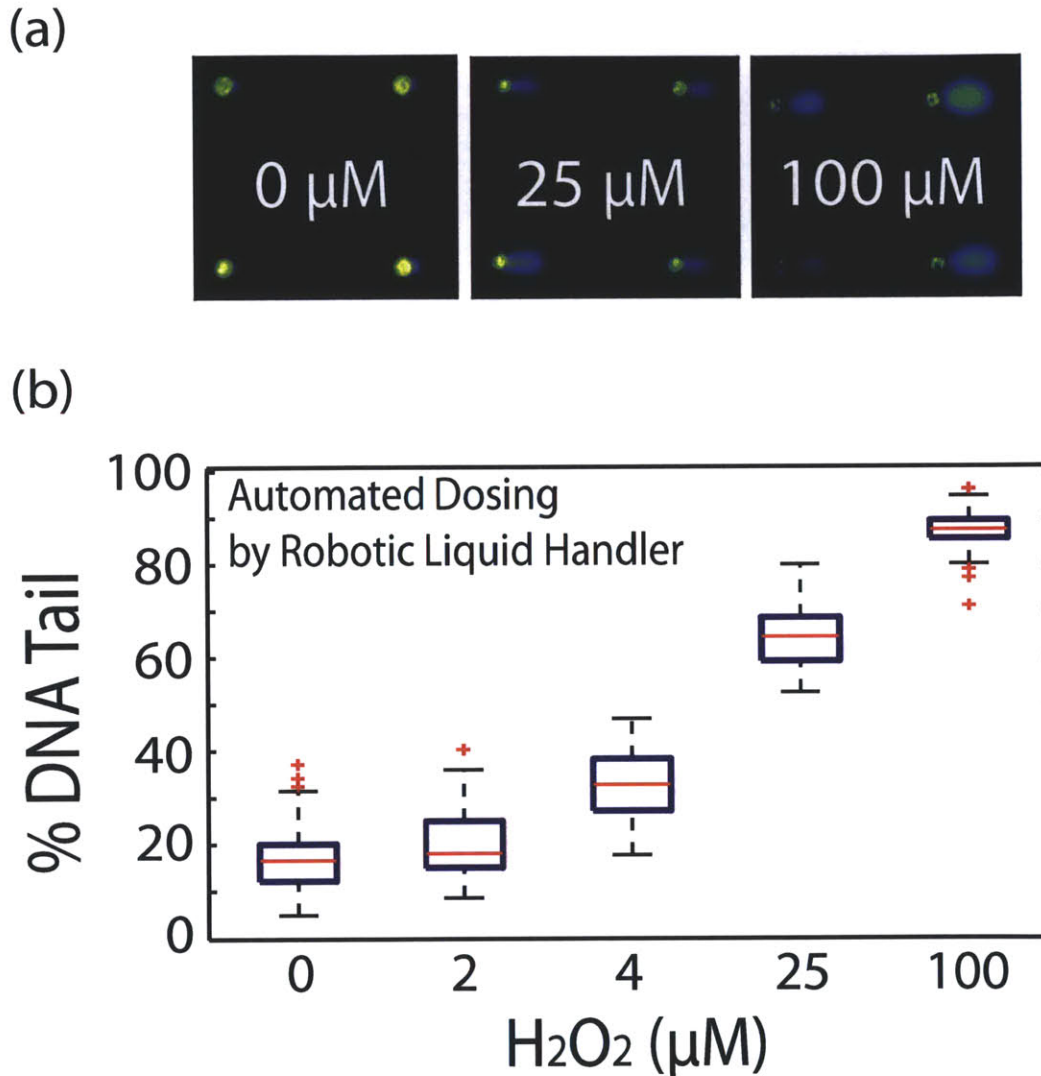
Figure 3-3: **Evaluation of Hydrogen Peroxide using Automated Dosing by Robotic Liquid Handler.** (a) Morphologies of patterned comets resulting from exposure to 0, 25, and 100 μM H_2O_2. (b) H_2O_2 dose response administered using robotic liquid handler. Box plots show median of 50 comets as a red line and the lower and upper quartiles as a blue box. Whiskers show extent of farthest data points within 150% of interquartile range. Red pluses indicate outliers.
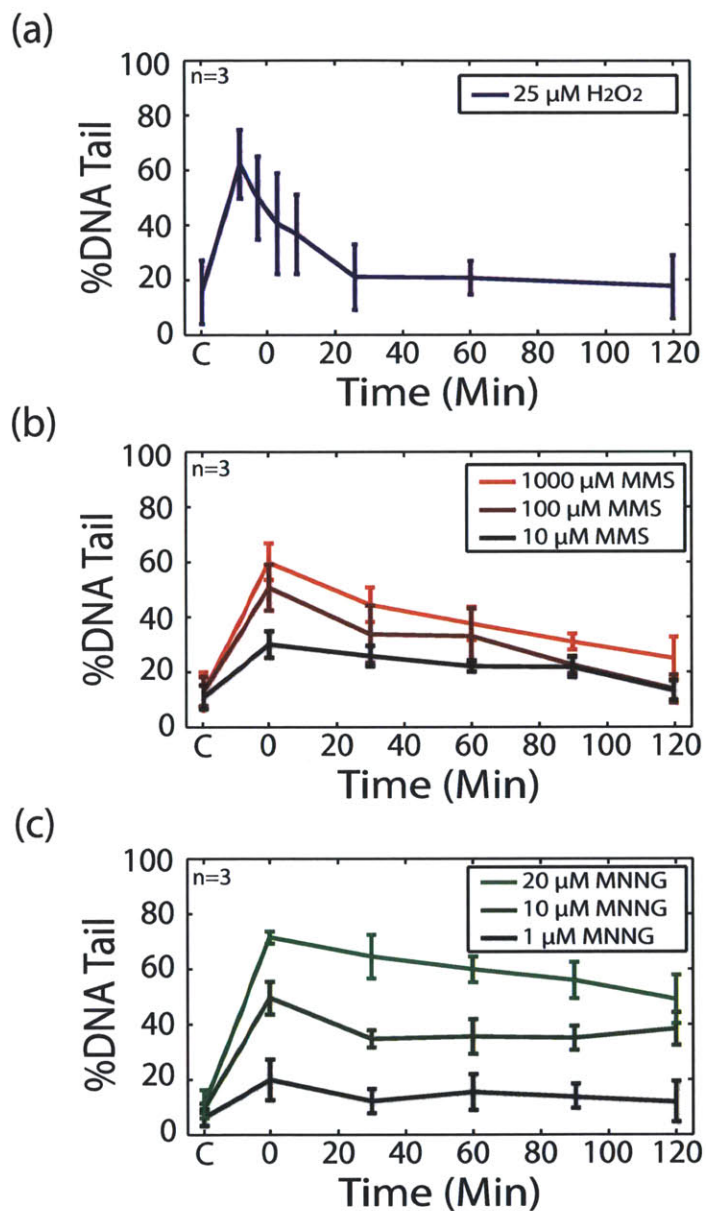
Figure 3-4: **Evaluation of Repair Kinetics of Multiple Chemicals.** For each chemical, all concentrations and repair time points conducted on a single CometChip. **(a)** Repair of damage induced by H_2O_2. **(b)** Repair of damage induced by MMS. **(c)** Repair of damge induced by MNNG.

Figure 3-5: **Comparison of TK6 Repair Kinetics from Damage Induced by MNNG, MMS, and H_2O_2.** 1000 μM MNNG and 25 μM MMS were evaluated on the same CometChip ($t_{1/2} \approx 120$ and 90 min, respectively). H_2O_2 assessment was conducted on a separate CometChip ($t_{1/2} \approx 15$ min).

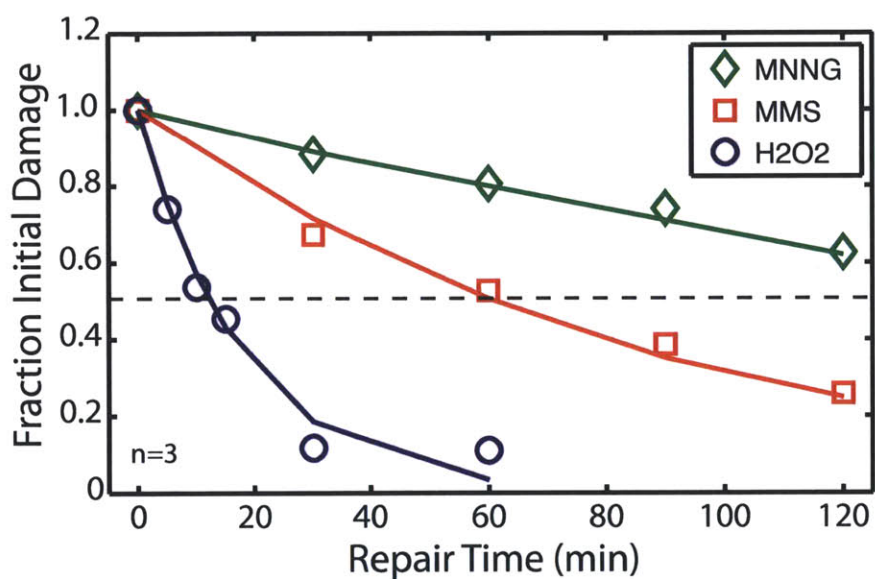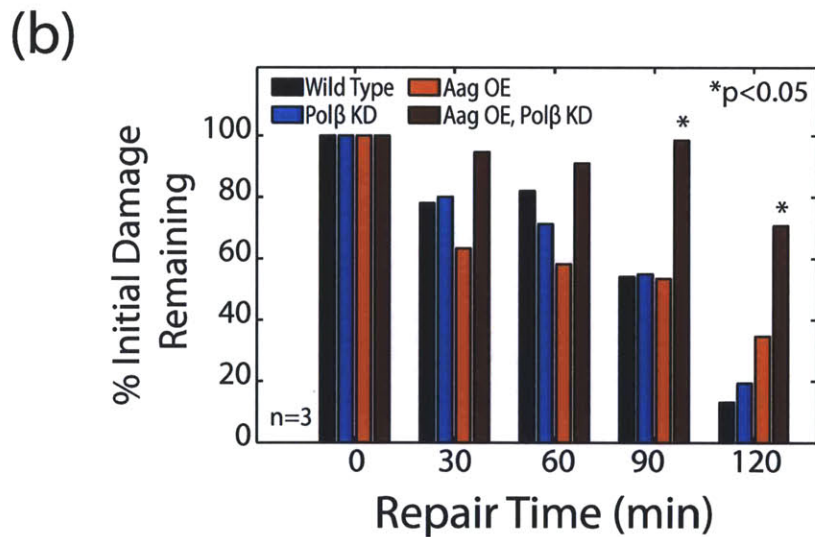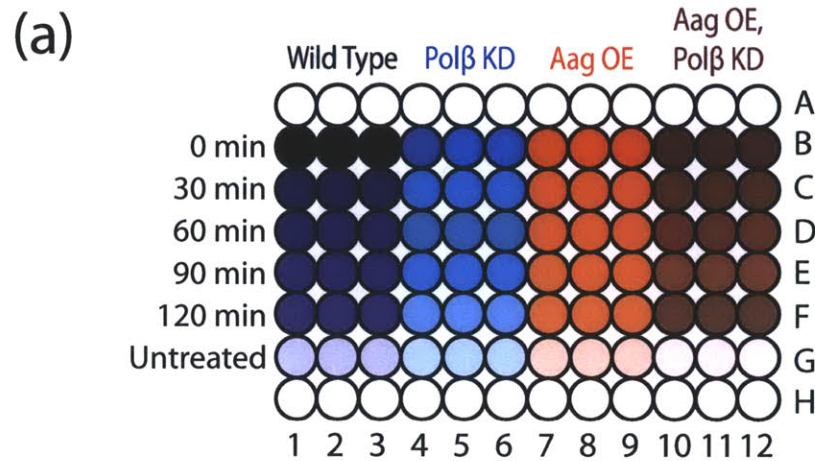Figure 3-6: **Detection of a Base Excision Repair Deficiency using 96-well CometChip.** (a) Repair of all four LN428 glioblastoma genotypes, WT, PolβKD, AAGOE, and AAGOE/PolβKD, evaluated on a single CometChip. Cells were exposed to 1 mM MMS and allowed to repair for 0, 30, 60, 90, 120 min. (b) Damage levels in WT, PolβKD, and AAGOE decreased at similar rates over 120 min, while the AAGOE/PolβKD cells had a persistent damage signal over the entire evaluation period. Significance determined by Student's t-test.

136
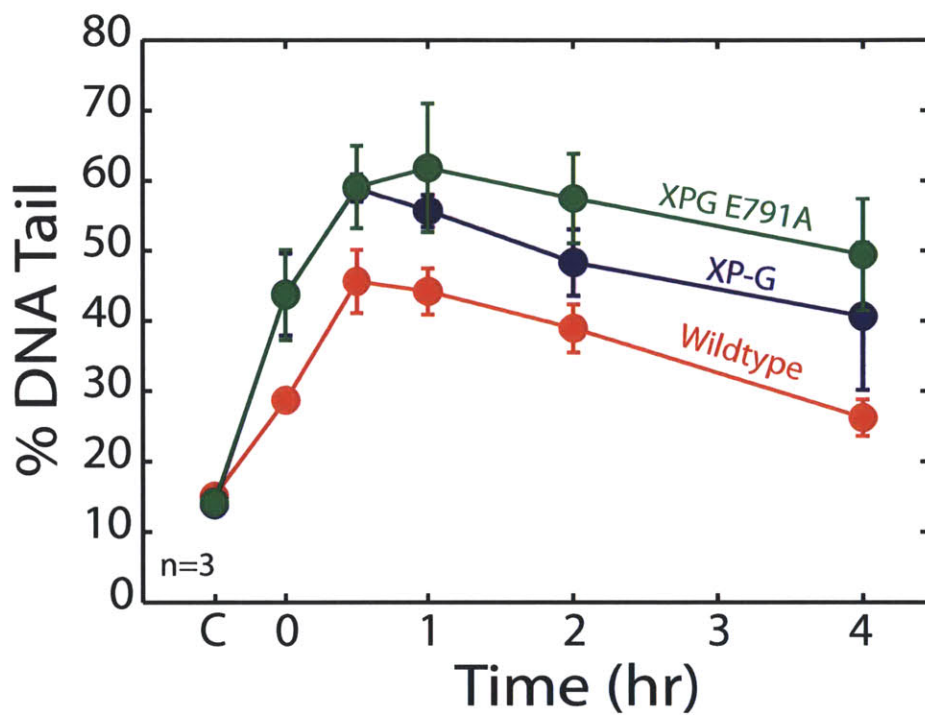
Figure 3-7: **Analysis of Repair Kinetics of XPG Mutants Exposed to 4NQO.** All three human fibroblast cell lines were exposed to 500 nM 4NQO and repair was assessed over a 4 hr period. XPG/E791A (green) cells are catalytically inactive for XPG and XP-G cells (blue) are XPG deficient.

(a) XPG wildtype — Theoretical NER Products

(b) XPG Deficient

(c) XPG Incision Mutant (E791A)
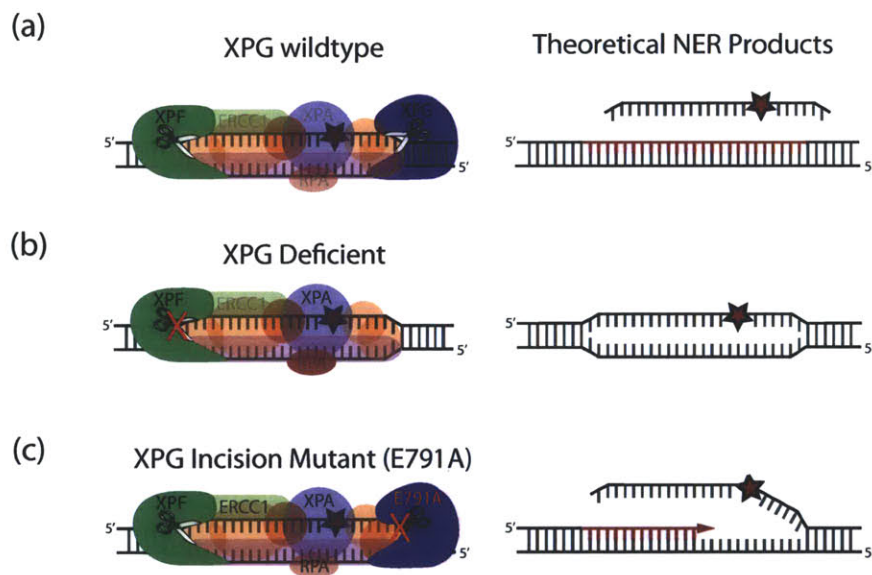
Figure 3-8: **Theoretical Nucleotide Excision Repair Products for XPG Mutants.** **(a)** Wild type cells are expected to completely repair NER damage. **(b)** XP-G cells lack both 3′ and 5′ incision activities and are expected to produce minimal NER intermediates. **(c)** XPG/E791A cells lack 3′ incision activity but have functional 5′ activity and are expected to accumulate intermediates through one-sided NER.
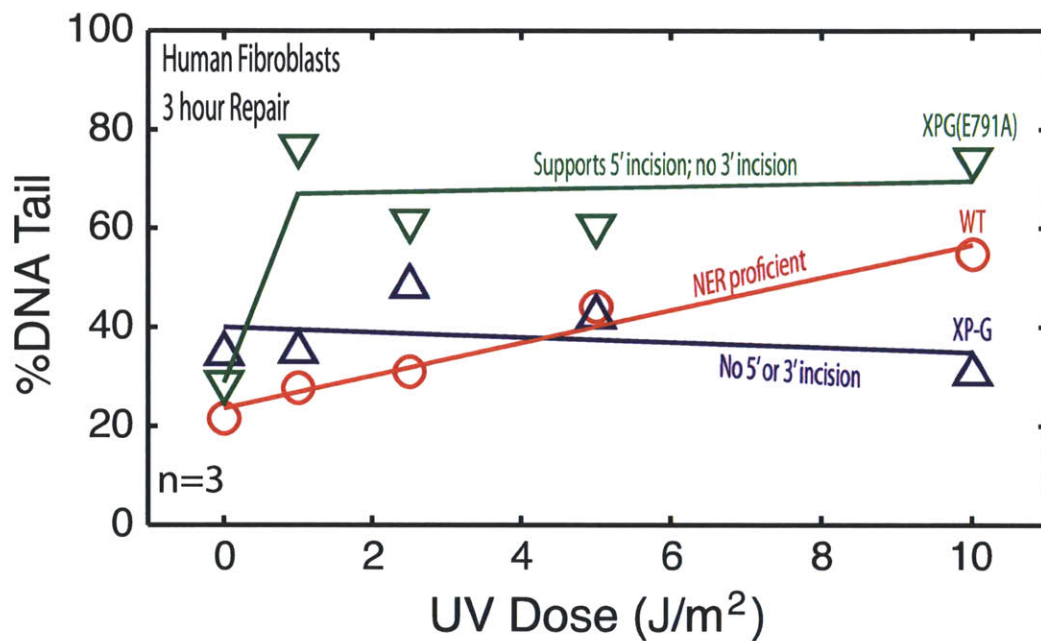
Figure 3-9: **Analysis of Nucleotide Excision Repair Products Formed in XPG Mutants Exposed to UV Radiation.** XPG/E791A (green), WT (red), and XP-G (blue) human fibroblasts were exposed to a range of UVC exposures and allowed to repair for 3 hr before analysis by comet assay. All cell types were evaluated in triplicate on a 3x3 well CometChip at each UV dose.
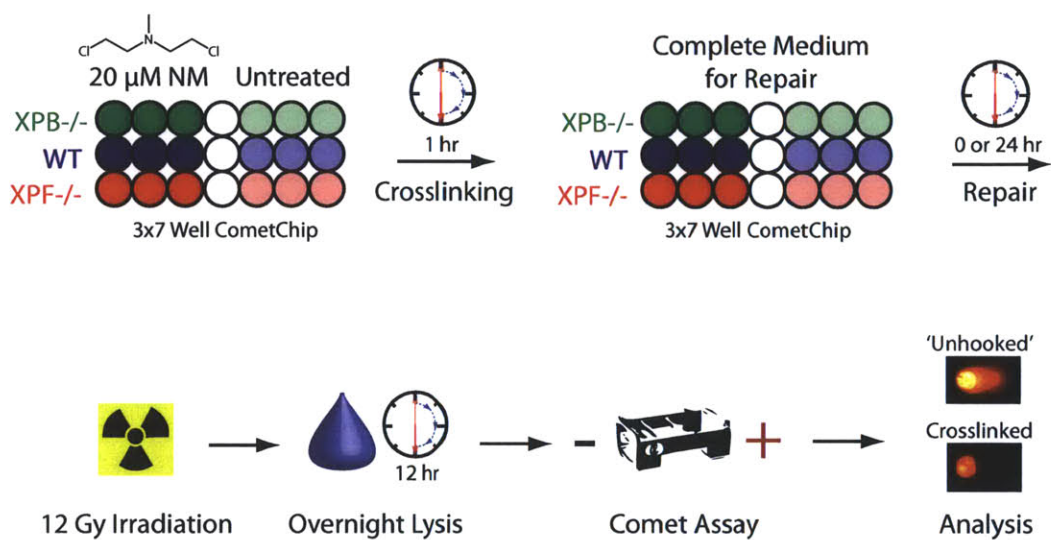
Figure 3-10: **Protocol to Evaluate Crosslinking Repair using the CometChip.** WT, XPB-/-, and XPF-/- CHO cells were exposed to 20 μM NM for 1 hr. Cells were allowed to repair for 0 or 24 hr. Immediately before lysis, cells were exposed to 12 Gy irradiation. The extent of unhooking was determined as the relative increase in comet signal in cells repaired for 24 hr versus 0 hr.
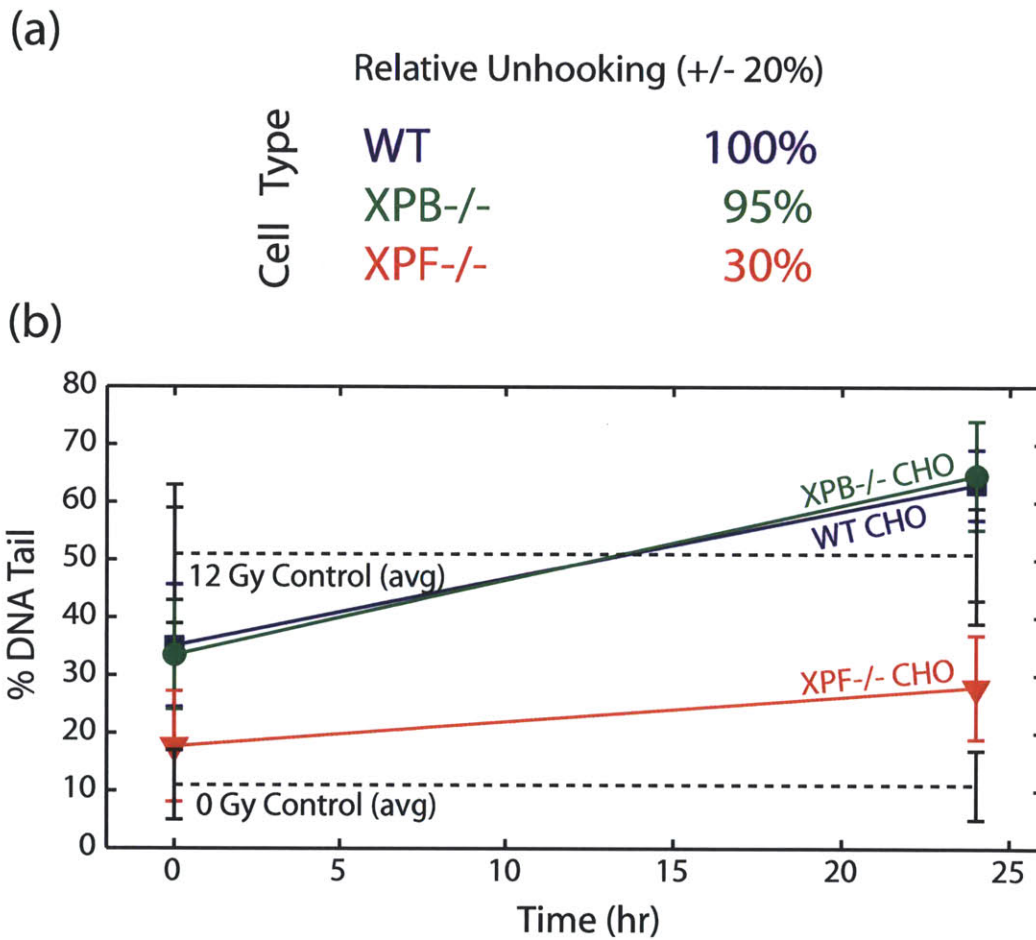
Figure 3-11: **Evaluation of Interstrand Crosslinking Repair in NER Mutants.** (a) Relative unhooking capacity was calculated for WT, XPB-/-, and XPF-/- CHO cells as 100, 95, and 30%, respectively. (b) After 24 hr of repair, WT and XPB-/- cells had significantly greater damage (resulting from unhooking activity) than XPF-/- cells when challenged with a 12 Gy dose.

Chapter 4

Single Cell Microarray Enables High Throughput Evaluation of DNA Double Strand Breaks and DNA Repair Inhibitors

4.1 Abstract

Many cancer chemotherapy agents and radiation therapy act through the formation of DNA double strand breaks (DSBs), which are preferentially toxic to uncontrolled, rapidly dividing cancer cells. DSB repair capacity is therefore a therapeutic target for adjuvant chemotherapy. Currently available assays to detect double strand breaks are limited in throughput and specificity and offer minimal information concerning the kinetics of repair. We present the CometChip, a high throughput (HT) arrayed platform that enables assessment of DNA DSB levels and repair capacity in multiple cell types and assay conditions in parallel and integrates with standard HT screening (HTS) technologies. We confirm the ability to detect multiple genetic deficiencies in DSB repair and evaluate a set of clinically relevant chemical inhibitors of non-homologous end joining. While other repair assays measure residual damage or

143

indirect markers of damage, the CometChip detects physical DSBs in a HT format, and serves as a novel discovery tool for identification of modulators of DNA damage induction and repair capacity.

4.2   Introduction

Mammalian cells have evolved mechanisms of DNA damage repair owing to endogenous processes such as generation of reactive oxygen species and VDJ recombination, and rely predominantly upon two major pathways of DSB repair: non-homologous end joining (NHEJ) and homologous recombination (HR) [1, 2, 3]. Ionizing radiation (IR) and radiomemetic chemicals are frontline tools in cancer management [4, 5]. One of their main mechanisms of action is the formation of toxic DSBs, which act as a signal to promote cell death. DSB repair has been identified as an underlying mechanism of drug resistance and is therefore important in guiding treatment strategies that more selectively target cancerous cells and reduce side-effects [6, 7]. One emerging approach is to sensitize tumors by inhibiting their DNA repair response system, e.g. NHEJ [8, 9, 10, 11]. A major challenge in identifying such inhibitors is that currently available DNA damage assays are limited in throughput, and often provide information about residual damage (e.g. chromosomal aberrations or signaling events), but offer little insight into the actual lesion burden or kinetics of repair. Better methods to measure DSBs are needed to assess DNA repair capacity in tumor cells and to identify novel pharmaceutical compounds that modulate DNA damage repair. Here, we describe a novel HT approach that enables direct physical detection of DSBs.

Currently, one of the most broadly used DSB assays is the gamma-H2AX assay, which relies upon detection of phosphorylated serine 129 of the histone variant H2AX (γ-H2AX), an early signaling event in response to a DSB. Although the γ-H2AX assay is remarkably sensitive [12, 13], H2AX phosphorylation is separable from DSBs, in part due to its dependence on the activity of ATM, DNA-PK and other phosphatidylinositol 3-kinase (PI3K) related kinases (PI3KKs) [14]. Another approach is

to directly measure DSBs based on their physical properties. Physical detection is the basis for alkaline elution and single cell gel electrophoresis (the comet assay), both of which rely upon changes in the mobility of intact versus broken DNA. While the alkaline elution method suffers from being technically difficult and slow, the comet assay is gaining in popularity [15]. When performed at neutral pH, the quantity of DSBs in a cell is proportional to the distance and the amount of DNA that migrates during electrophoresis [16]. Although the neutral comet assay can directly analyze DSBs, the specificity and statistical precision of the assay are limited. Additionally, the standard technique is laborious, making HTS difficult.

To overcome problems in reproducibility and throughput of the comet assay, we recently developed the CometChip [17]. The CometChip exploits single cell patterning using microwell arrays, which enables spatial encoding and increases throughput and consistency. Here, we have adapted the CometChip to accommodate a 96-well device (with microwells at the base of each 96 well; Figure 4-1) that can be integrated with HTS tools, including fully automated imaging and analysis. Furthermore, we show that this new 96-well format suppresses variability among samples. In addition to increasing throughput and reliability, we used established protocols to adapt the CometChip for HT physical detection of DSBs in mammalian cells, wherein DSBs are directly measured via analysis of comet tail length following single cell gel electrophoresis. Using cell lines harboring specific defects in DSB repair and a set of compounds with known effects on DNA repair, we show that the CometChip can be used to detect DSBs and furthermore that is offers a useful screen for DSB repair inhibitors. The neutral CometChip is straightforward to implement, and compatible with HTS, thus providing a valuable tool for researchers, clinicians and epidemiologists.

4.3 Materials and Methods

4.3.1 Cell Culture

TK6 human lymphoblastoid cells were cultured in suspension in RPMI medium 1640 with L-glutamine (Invitrogen) supplemented with 10% horse serum (Invitrogen). Chinese hamster ovary (CHO) cell lines were cultured in Dulbeccos modified Eagles medium (Invitrogen) supplemented with 10% fetal bovine serum (Atlanta Biologicals, Atlanta, GA). All cell culture media were supplemented with 100 units/mL penicillin-streptomycin (Invitrogen). CHO-K1 and xrs-6 CHO cells were kindly supplied by Larry H. Thompson (Lawrence Livermore National Laboratory) and irs-20 CHO cells were a generous gift by Dr. Joel S. Bedford (Colorado State University). All genotypes were confirmed by Western blot (data not shown).

4.3.2 Microwell Fabrication

Negative molds were fabricated from silicon wafers (WaferNet, San Jose, CA) that were lithographically patterned with SU-8 photoresist microwells (SU-8 2025, Microchem, Newton, MA), following a protocol similar to Wood, et al. [17]. Polydimethylsiloxane (PDMS, Dow Corning, Midland, MI) was cast on the negative silicon mold and baked for 1 hr at 50 °C according to the manufacturers instructions. After 1 hr the PDMS was removed to reveal patterned microposts of approximately 50 μm depth and 30 μm width. Molten 1% normal melting point agarose (Omnipur, Invitrogen) was applied to a sheet of GelBond film (Lonza, Basil, Switzerland) and the PDMS mold was allowed to float until the agarose set. The PDMS mold was removed, leaving a 300 μm thick gel with arrayed microwells. The microwell gel was then clamped between a glass plate and a bottomless 96-well titer plate (Greiner BioOne).

4.3.3 Multiwell Preparation

Figure 4-1b illustrates CometChip loading. At least 10,000 cells were added to each multiwell and allowed to settle by gravity in complete growth media at 37°C, 5% CO_2. Excess cells were aspirated after 15 min and the bottomless 96-well plate was removed in order to enclose the arrayed cells in a layer of 1% low melting point agarose. Traditional comet slides were prepared as previously described [16].

4.3.4 Exposure to Ionizing Radiation

Microwell gels were either irradiated all at once in the multiwell format or cut and exposed in smaller pieces. A Cobalt-60 irradiator (Gammacell 220 Excel, MDS Nordion, Canada) was used to deliver 0-100 Gy of IR at an approximate rate of 120 Gy/min. Cells were irradiated in 4 °C phosphate buffered saline (PBS). To evaluate repair kinetics, wells were synchronized by cell lysis after repairing damage in media for varying time intervals. In the evaluation of NHEJ deficient cells, all time points (0, 30, 60, 90, 120 min) were conducted on a single multiwell plate. For the screen of NHEJ repair inhibitors, each condition (nontreated, 0 and 60 min) was run on a separate gel. For the dose response assessment, a single CometChip was divided into six 3x2-well pieces for exposure to varied levels of IR.

4.3.5 Treatment with Chemicals

Bleomycin (Bioworld, Dublin, Ohio) was dissolved in PBS and was exposed to cells for 1 hr at 4 °C. All chemical conditions, controls, and replicates were conducted on a single multiwell plate. All repair inhibitors were purchased from Tocris (Ellisville, Missouri). NU7441, NU7026, and PI103 hydrochloride were prepared in dimethyl sulfoxide (DMSO) and Wortmannin, LY294002, Compound 401, and DMNB were prepared in ethanol. All inhibitors were stored at -20 °C until immediately before use. The inhibitors were diluted to 50 μM in complete growth medium and exposed in triplicate wells of the 96-well plate for 1 hr at 37°C, 5% CO_2. CHO-K1 cells in 1% DMSO and untreated xrs-6 and irs-20 cells were used as controls. The inhibitors

were replaced with 4°C PBS during irradiation and fresh inhibitor was applied during evaluation of repair kinetics.

4.3.6   Neutral Comet Assay

The comet assay was performed using a modified version of the neutral comet protocol as previously described [18]. Briefly, gels were lysed for four hours at 43°C (2.5M NaCl, 100 mM Na_2EDTA, 10 mM Tris, 1% N-Lauroylsarcosine, pH 9.5 with 0.5% Triton X-100 and 10% DMSO added 20 min before use). For evaluation of repair kinetics of NHEJ deficient cells, lysis was synchronized in the multiwell plate at 37°C and then completed at 43°C. After lysis, the slides were washed three times for 30 min with the electrophoresis buffer (90 mM Tris, 90 mM Boric Acid, 2 mM Na_2EDTA, pH 8.5). Electrophoresis was conducted at 4°C for 1 hr at 0.6 V/cm and 6 mA.

4.3.7   Fluorescence Imaging and Comet Analysis

After electrophoresis, gels were neutralized in 0.4 M Tris, pH 7.5 (3x5 min). Slides were then stained with SYBR Gold (Invitrogen). Images were captured automatically using an epifluorescent microscope and analyzed automatically using custom software written in MATLAB (The Mathworks). Traditional comet slides were scored manually using Komet 5.5 (Andor Technology). ANOVA analysis was conducted to determine statistical significance between irradiation doses (Fig. 2) and a Student's t-test was used to evaluate relative repair differences between cells (Fig. 3-5).

4.3.8 γ-H2AX Assay

Wild type (CHO-K1) and DNA-PKcs-/- (irs-20) CHO cells were seeded in 6-well plates and allowed to grow to confluency over night. Media containing 50 μM NU7441 inhibitor was added to wild type cells for 1 hr at 37°C, 5% CO_2. All plates except the untreated control were exposed to 100 Gy in the Cobalt-60 irradiator (Gammacell 220 Excel, MDS Nordion, Canada). Cells were allowed to repair for (0, 1, 2, 4, 8 hr) in either fresh medium or medium supplemented with NU7441. Cell samples were lysed

at each time point (4% SDS, 0.12 M Tris-HCl pH 6.8 with Photostop tab (Roche) and complete Mini tabs (Roche)), scraped from the dish, and stored in eppendorf tubes for γ-H2AX analysis by Western blot. Briefly, samples were sonicated and run in the HT E-Page gel system (Invitrogen) and transferred using the iBlot Blotting System (Invitrogen). γ-H2AX was visualized using anti-γ-H2AX rabbit monoclonal antibody (Cell Signaling Technology) and normalized to actin levels using anti-actin mouse monoclonal antibody (Sigma).

4.4 Results

4.4.1 High Throughput Neutral Comet Assay

Currently available assays for detecting DSBs are limited in throughput and speed of analysis, attributes that are critical for large-scale pharmaceutical discovery projects. The multiwell CometChip enables multiple different cell samples or chemical conditions to be assayed on a single agarose gel (Figure 4-1). Briefly, cells are arrayed in microwells in an agarose gel by gravity, and subsequently cultured, treated, lysed, and electrophoresed using traditional comet protocols [16, 18]. The resulting patterned comets at the base of each 96 well (Figure 4-2a) can be imaged manually on a fluorescent microscope or in an automated fashion using any imaging platform. One advantage of the arrayed microwell approach is that the comets are optimally patterned at the same focal depth with no overlap, enabling ten or more comets to be captured and automatically analyzed in a single image. Images are analyzed using unbiased, fully automated software, increasing the processing rate from a maximum of 50 samples a day to over 400.

Here, we set out to evaluate the sample to sample noise using the CometChip versus the traditional assay. To assess sample to sample variation on the neutral CometChip, TK6 lymphoblastoid cells were exposed to 100 Gy IR and analyzed for DSBs. Images were captured in an automated fashion and automatically analyzed using software described by Wood, et al. [17]. We found a coefficient of variance

149

of approximately 15% between the 96 wells of the CometChip compared to around 20% between ten slides of the traditional assay. Figure 4-6 illustrates the improved throughput and well-to-well variability of the neutral CometChip. It is noteworthy that it was not practical to process 96 slides for a direct comparison; had we done so, the experimental noise for the traditional approach would likely have risen. Taken together, being able to process 96 samples in parallel on a single platform, rather than on separate slides, helps to reduce experimental noise.

To compare the sensitivity and dose response of the CometChip to the traditional neutral comet assay, we performed a dose response analysis following exposure to IR. Extent of damage was evaluated by measuring comet tail length (μm), because among the standard comet parameters, it was found to best correlate with radiation dose (Figure 4-7d). A comparison of the traditional assay and the CometChip revealed that both approaches yield a linear dose response over the 100 Gy range (Figure 4-2b). As expected, the absolute values between the two assays appear to vary somewhat due to differences in experimental protocols. Importantly, the CometChip appears to be more sensitive at higher doses, as reflected by the regression statistics ($R^2 = 0.99$ and $R^2 = 0.85$ for microwell and standard comets, respectively). This increased sensitivity may result from the improved morphology of the microwell comet, since the DNA is constrained by the walls of the microwells, thus providing a more distinct head-to-tail cutoff and thus more reliable assessment of comet tail length (Figure 4-7a).

HT screens are most useful when a very small volume is required per sample, thus minimizing the amount of test agent required. An important feature of the CometChip is the ability to evaluate conservative volumes of multiple chemical conditions in parallel (while approximately 2 ml is generally required for on-slide treatment using the traditional method, only 100 μl is required using the CometChip). Furthermore, all chemical conditions can be conducted on the CometChip, eliminating the need for cell plating and post-exposure centrifugation and trypsinization required by other HT versions of the comet assay [19], [Trevigen, Inc.]. To further assess the efficacy of the neutral CometChip for evaluating chemical exposures, we assayed bleomycin, a glycopeptide antibiotic that efficiently introduces DSBs and is

used in the treatment of numerous cancers [20, 21, 22]. To analyze bleomycin-induced DSBs, more than 300 comets were pooled from six replicate wells and the resulting data fit a linear dose response with $R^2 = 0.999$ (Figure 4-2c). Together, these data show that the CometChip can be used effectively to measure DSBs following multiple chemical exposure conditions in parallel.

4.4.2 Detection of a Repair Deficiency

In order to assess the specificity of the neutral comet assay for DSBs, we set out to compare DSB repair kinetics among cell lines with known genetic deficiencies in NHEJ. An early step in the NHEJ pathway is recognition of the DSB by the Ku70/Ku80 heterodimer. The Ku heterodimer recruits the DNA-PK catalytic subunit (DNA-PKcs) to form the DNA-PK complex, which promotes strand alignment and recruitment of factors involved in end-processing and ligation (Figure 4-3a) [23, 24]. We used mammalian cells specifically mutated in either Ku80 (xrs-6) or DNA-PKcs (irs-20) to see if cells lacking critical genes in NHEJ show a repair deficit when analyzed on the CometChip. Cells were exposed to 100 Gy IR and the multiwells corresponding to the zero min time point were immediately lysed, while the remaining wells were filled with growth medium and allowed to repair over the course of 120 min. Wild type cells demonstrated a fast recovery within the first hour, while both the Ku80 and DNA-PKcs deficient cells showed a severe repair defect, with most of the damage still remaining after two hours (Figure 4-3b). These data show that the assay is effective for detection of DSBs, which is consistent with previously published studies of Ku80 and DNA-PKcs deficient cells using similar methods [24, 25]. Interestingly, even in the absence of DNA-PK activity, there is some residual clearance of DNA damage, which is likely due to alternative DSB repair pathways that are revealed in the absence of NHEJ [1, 26]. Nevertheless, most of the IR-induced comet signal persists in the DNA repair defective cell lines, indicating that most of the IR-induced comet signal is due to DSBs.

4.4.3 Comparison of CometChip and the γ-H2AX assay

One potential advantage of the CometChip is that it enables direct physical measurement of DSBs, rather than detection of a signaling events triggered by DSBs. A potential shortcoming of the latter approach is that conditions that inhibit either phosphorylation or dephosphorylation of γ-H2AX could lead to false negative or false positive results, respectively. To directly compare CometChip and γ-H2AX, we studied repair following exposure to 100 Gy IR using both wild type and DNA-PKcs-/- cell lines. Physical breaks were assessed by CometChip and levels of γ-H2AX were determined by Western blot, as shown in Figure 4-4a and Figure 4-4b, respectively. For the CometChip, there is a significant induction of DSBs followed by rapid clearance to baseline within two hours of exposure in the wild type cells. There is almost no DSB repair capacity in the DNA-PKcs-/- cells, which is consistent with the essential role of DNA-PK in NHEJ [27]. In contrast, for the γ-H2AX assay, there is a clear induction of H2AX phosphorylation reflecting apparent DSBs in wild type cells, but the signal induction is delayed by 30-60 min after appearance of DSBs, and persists for more than six hours after DSBs have been completely repaired according to the CometChip analysis. Thus, disappearance of the γ-H2AX signal clearly lags behind repair of actual physical DSBs, leading to a false positive result. Additionally, the levels of DSBs according to the γ-H2AX assay are significantly reduced in the DNA-PKcs-/- cell line, which is consistent with results showing that DNA-PK contributes to phosphorylation of H2AX [14]. Thus, despite there being equal levels of damage when assessed physically, there is a false negative result when assessed using an indirect measure of DSBs. Taken together, these data demonstrate the value of physical detection of DSBs rather than assessment of a response to the damage, to avoid both false positive and false negative results. Furthermore, they support the use of the CometChip for analysis of small molecule inhibitors of DNA-PK and other DSB repair proteins.

4.4.4   Screen of DNA-PK Inhibitors

Evaluating DNA-PK inhibitors that could be useful in the clinic is a potentially valuable application of CometChip technology, as inhibitors of DSB repair are of particular interest in the clinic as radio- and chemotherapy sensitizers. To test the efficacy of the CometChip, we screened a subset of leading DNA-PK inhibitors, listed in Table 4-1. Wortmannin and LY294002 are benchmark PI3KK inhibitors that have been shown to sensitize cancer cells to DNA damaging agents via inhibition of DNA-PK dependent DSB repair [28, 29]. NU7441, NU7026, and Compound 401 were developed as LY294002-like inhibitors with improved specificity for DNA-PK [30, 31, 32]. DMNB and PI103 represent the range of other DNA-PK inhibitors, with DMNB having high selectivity and relatively low inhibitory efficiency for DNA-PK (i.e. 15000 nM), and PI103 having nanomolar potency for numerous PIKKs.

CHO-K1 (wild type) cells were loaded into a 96-well CometChip and exposed in triplicate wells to 50 μM of each inhibitor. This concentration represents the half maximal effective concentration (EC_{50}) of LY294002, which can be greater than 1000-fold higher than the half maximal inhibitory concentration (IC_{50}) due to cellular penetration, competition with ATP, and the high abundance of cellular DNA-PK [33]. The use of the multi-well plate minimized the volume requirement of each inhibitor to 50 μL and reduced the complexity of the experiment to just three CometChips. All steps including cell loading, repair inhibition, irradiation, and repair took less than three hours to complete. Imaging was greatly reduced in terms of labor requirement through automation.

NU7441 is being pursued as a potential adjuvant in cancer treatment due to its ability to increase efficacy of both chemo- and radio-therapy in tumor-bearing mice through selective inhibition of DNA-PK [34]. Figure 4-5 shows the relative repair 1 hr after exposure compared to wild type for each inhibitor and cell type. All inhibitors except for the less potent, DMNB, displayed inhibition of DSB repair at an efficiency comparable to or greater than the cells with DNA-PK genetic deficiencies. Inhibitors with multiple PI3KK targets had a more pronounced effect on DSB repair. For

example, PI103, which has low specificity but ten-fold greater potency for DNA-PK than NU7441, resulted in complete inhibition of repair. Inhibition of mammalian target of rapamycin (mTOR) has recently been shown to significantly inhibit NHEJ, which might explain the increased efficacy of several of the DNA-PK inhibitors [35]. Most notably, Compound 401 is highly specific to DNA-PK and mTOR, and was found to completely inhibit DSB repair. Thus, the CometChip can be used to both identify inhibitors of DSB and provide information regarding their relative potencies.

4.5 Discussion

Here, we have described a HT method to directly assess DSBs resulting from both radiation and a chemotherapeutic agent and we show the DSB repair kinetics for multiple cell samples analyzed in parallel. In addition to its utility in screening compounds, the CometChip can also potentially be used for personalized medicine. DNA damaging agents are central to non-surgical cancer treatment and as adjuvants to surgery, but their clinical efficacy varies considerably among individuals. The CometChip provides a relatively inexpensive and fast method of measuring DSB repair capacity, which could be used to assess patient sensitivity and tumor resistance in order to design optimal therapeutic strategies that minimize side-effects.

We have shown that the CometChip has a distinct advantage over the γ-H2AX assay, in particular for evaluating DNA-PK or other PI3KK inhibitors, since it directly measures DNA damage. Further, the CometChip readout reflects the integrated response of multiple DNA repair pathways and sub-pathways, as opposed to a biomarker that may otherwise be influenced by the compound being assessed [14, 36]. DNA-PK inhibitors and other drugs that target DNA repair proteins have emerged as promising adjuvants in combinational therapy, and whole-cell screening platforms to characterize such compounds will be increasingly valuable to the pharmaceutical industry as more companies add them to their advanced preclinical pipelines [10].

The morphology of neutral comets differs from that of alkaline comets and is often criticized for reducing the sensitivity and reproducibility of the assay 4-7a. Single

strand breaks relax supercoiled DNA, resulting in a 'halo' that makes it difficult to decipher the head-to-tail threshold [16]. One advantage of the arrayed comet platform is that the DNA conforms to the morphology of the microwell, producing a distinct and reproducible comet head and tail. This feature may explain the increased sensitivity of the CometChip at higher doses compared to the traditional comet assay as determined by ANOVA analysis. Another contributing factor may be the reduced variability in the CometChip. In addition to increased sensitivity, a major advantage of the CometChip is the reduction of labor, and therefore human error, resulting from the ability to conduct all samples and controls on a single device that integrates with HTS technologies and automated imaging and analysis platforms. Additionally, the multiwell format minimizes the required amount of reagent, which is important in terms of cost savings when evaluating expensive chemotherapeutic compounds. This increase in throughput not only has potential applications in drug screening and personalized medicine, but it also can be used to better classify environmental pollutants and understand the risk they represent to exposed populations.

We had previously shown that the CometChip is compatible with multiple cell types. Here, we extended this work, evaluating the DSB repair kinetics of three cell types on a single CometChip and demonstrating detection of two functionally different deficiencies in DNA-PK (Fig. 3). The ability to detect such deficiencies is important in predicting treatment response and managing cancer resistance.

In addition to NHEJ and HR, DSBs can also be repaired by alternative mechanisms, such as single strand annealing (SSA) and microhomology mediated endjoining (MMEJ) [2, 26]. In the case of HR, we do not anticipate detecting a significant impact from this pathway during the early time points, since NHEJ is significantly faster than HR [1]. Likewise, SSA and MMEJ are significantly slower than NHEJ, and are thus kinetically separable. The ability of the CometChip to measure precise end joining kinetics is critical in understanding the integrity of repair, as the deleterious MMEJ pathway masks NHEJ deficiencies at times greater than two hr [26].

The irs-20 CHO cell line contains a defect in the DNA-PKcs that disrupts its kinase domain, while maintaining its DNA-binding activity [36]. Detection of this deficiency

supports the use of the CometChip for screening potential adjuvant therapies known to inhibit the phosphorylation activity of DNA-PK. We found the potent DNA-PK inhibitor, NU7441, to induce equivalent levels of repair inhibition as the irs-20 mutant (Fig. 4). Compounds with lower specificity for DNA-PK demonstrated stronger inhibition profiles, revealing the importance of other PI3KKs in DSB repair mediation. This is best exemplified by LY290042, which has relatively less potency for DNA-PK than the other inhibitors (Table 4-1), but had a dramatic effect on DSB repair capacity. The increased efficacy of LY290042 over Wortmannin may also result from its ability to competitively inhibit the active site of DNA-PKcs, as opposed to the non-competitive nature of Wortmannin [37]. Further differences in efficacies may be due to off-target interactions with mTOR, as previously discussed [35], or PI3K, which has recently been shown to influence DSB repair through interaction with other PI3KKs (e.g. ataxia telangiectasia mutated (ATM)) [38]. In support of this hypothesis, NU7026, a highly selective inhibitor, has significantly less potency for mTOR and negligible affinity for PI3K, and did not have as profound of an effect as NU7441 (Fig. 5). It will be interesting to further explore this concept through evaluation of specific inhibitors of mTOR, such as PP242 and PP30 [35]. There are limited tools to investigate the direct effect of the PI3KK signaling cascade and other chromatin remodeling processes on DSB repair. Chromatin modifications are gaining attention for their role in carcinogenesis and for their potential as targets for pharmaceutical intervention [39, 40]. CometChip studies are currently underway to assess other PI3KK-targeting compounds, such as ATM (i.e. KU55933), as well as histone deacetylase (HDAC) inhibitors, a promising new class of small molecules in cancer treatment [41].

In conclusion, the CometChip is an effective tool for directly measuring the induction of DSBs. The 96-well format enables multiple cell types and chemical conditions to be assayed in parallel with improved processing speed to that of the traditional comet assay. Using both a genetic approach and a chemical inhibitor of DNA repair, we demonstrated that the assay is sensitive for DSB detection and showed that the assay improves reproducibility and enhances throughput by nearly an order of magni-

tude compared to the traditional assay according to [16]. Furthermore, the platform directly measures DSB repair kinetics, enabling the detection of end joining deficiencies and the evaluation of inhibitors of DSB repair. The CometChip may therefore be useful in a variety of clinical settings.

References

[1] G. Iliakis, H. Wang, A. R. Perrault, W. Boecker, B. Rosidi, F. Windhofer, W. Wu, J. Guan, G. Terzoudi, and G. Pantelias, "Mechanisms of dna double strand break repair and chromosome aberration formation," *Cytogenet Genome Res*, vol. 104, pp. 14–20, Jan 2004.

[2] T. Helleday, J. Lo, D. Vangent, and B. Engelward, "Dna double-strand break repair: From mechanistic understanding to cancer treatment," *DNA Repair*, vol. 6, pp. 923–935, Jul 2007.

[3] M. Shrivastav, L. P. D. Haro, and J. A. Nickoloff, "Regulation of dna double-strand break repair pathway choice," *Cell Res*, vol. 18, pp. 134–147, Jan 2008.

[4] L. H. Hurley, "Dna and its associated processes as targets for cancer therapy," *Nat Rev Cancer*, vol. 2, pp. 188–200, Mar 2002.

[5] J. Bernier, E. J. Hall, and A. Giaccia, "Radiation oncology: a century of achievements," *Nat Rev Cancer*, vol. 4, pp. 737–47, Sep 2004.

[6] E. Dikomey, J. Dahm-Daphi, I. Brammer, R. Martensen, and B. Kaina, "Correlation between cellular radiosensitivity and non-repaired double-strand breaks studied in nine mammalian cell lines," *International Journal of Radiation Biology*, vol. 73, pp. 269–78, Mar 1998.

[7] D. S.-W. Tan, M. Gerlinger, B.-T. Teh, and C. Swanton, "Anti-cancer drug resistance: understanding the mechanisms through the use of integrative genomics and functional rna interference," *Eur J Cancer*, vol. 46, pp. 2166–77, Aug 2010.

[8] S. Madhusudan and I. Hickson, "Dna repair inhibition: a selective tumour targeting strategy," *Trends in Molecular Medicine*, vol. 11, pp. 503–511, Nov 2005.

[9] J. Ding, Z. Miao, L. Meng, and M. Geng, "Emerging cancer therapeutic opportunities target dna-repair systems," *Trends in Pharmacological Sciences*, vol. 27, pp. 338–344, Jun 2006.

[10] N. Curtin, "Therapeutic potential of drugs to modulate dna repair in cancer," *Expert Opin Ther Targets*, vol. 11, pp. 783–99, Jun 2007.

[11] T. Helleday, E. Petermann, C. Lundin, B. Hodgson, and R. A. Sharma, "Dna repair pathways as targets for cancer therapy," *Nat Rev Cancer*, vol. 8, pp. 193–204, Mar 2008.

[12] A. Kinner, W. Wu, C. Staudt, and G. Iliakis, "Gamma-h2ax in recognition and signaling of dna double-strand breaks in the context of chromatin," *Nucleic Acids Research*, vol. 36, pp. 5678–94, Oct 2008.

[13] I. Revet, L. Feeney, S. Bruguera, W. Wilson, T. K. Dong, D. H. Oh, D. Dankort, and J. E. Cleaver, "Functional relevance of the histone h2ax in the response to dna damaging agents," *Proceedings of the National Academy of Sciences*, pp. 1–5, May 2011.

[14] J. An, Y.-C. Huang, Q.-Z. Xu, L.-J. Zhou, Z.-F. Shang, B. Huang, Y. Wang, X.-D. Liu, D.-C. Wu, and P.-K. Zhou, "Dna-pkcs plays a dominant role in the regulation of h2ax phosphorylation in response to dna damage and cell cycle progression," *BMC Mol Biol*, vol. 11, p. 18, Jan 2010.

[15] S. M. Piperakis, "Comet assay: A brief history," *Cell Biol Toxicol*, vol. 25, pp. 1–3, Feb 2009.

[16] P. Olive and J. Banáth, "The comet assay: a method to measure dna damage in individual cells," *Nat Meth*, vol. 1, no. 1, pp. 23–29, 2006.

[17] D. K. Wood, D. M. Weingeist, S. N. Bhatia, and B. P. Engelward, "Single cell trapping and dna damage analysis using microwell arrays," *Proc Natl Acad Sci USA*, vol. 107, pp. 10008–13, Jun 2010.

[18] M. Wojewódzka, I. Buraczewska, and M. Kruszewski, "A modified neutral comet assay: elimination of lysis at high temperature and validation of the assay with anti-single-stranded dna antibody," *Mutat Res*, vol. 518, pp. 9–20, Jun 2002.

[19] E. Kiskinis, W. Suter, and A. Hartmann, "High throughput comet assay using 96-well plates," *Mutagenesis*, vol. 17, pp. 37–43, Jan 2002.

[20] C. Nichols and C. Kollmannsberger, "First-line chemotherapy of disseminated germ cell tumors," *Hematol Oncol Clin North Am*, vol. 25, pp. 543–56, viii, Jun 2011.

[21] S. E. Richardson and C. McNamara, "The management of classical hodgkin's lymphoma: Past, present, and future," *Adv Hematol*, vol. 2011, p. 865870, Jan 2011.

[22] M. Linnert and J. Gehl, "Bleomycin treatment of brain tumors: an evaluation," *Anticancer Drugs*, vol. 20, pp. 157–64, Mar 2009.

[23] E. Feldmann, V. Schmiemann, W. Goedecke, S. Reichenberger, and P. Pfeiffer, "Dna double-strand break repair in cell-free extracts from ku80-deficient cells: implications for ku serving as an alignment factor in non-homologous dna end joining," *Nucleic Acids Research*, vol. 28, pp. 2585–96, Jul 2000.

[24] I. H. Ismail, S. Mårtensson, D. Moshinsky, A. Rice, C. Tang, A. Howlett, G. McMahon, and O. Hammarsten, "Su11752 inhibits the dna-dependent protein kinase and dna double-strand break repair resulting in ionizing radiation sensitization," *Oncogene*, vol. 23, pp. 873–82, Jan 2004.

[25] R. Losada, M. T. Rivero, P. Slijepcevic, V. Goyanes, and J. L. Fernández, "Effect of wortmannin on the repair profiles of dna double-strand breaks in the whole

genome and in interstitial telomeric sequences of chinese hamster cells," *Mutat Res*, vol. 570, pp. 119–28, Feb 2005.

[26] R. Perrault, H. Wang, M. Wang, B. Rosidi, and G. Iliakis, "Backup pathways of nhej are suppressed by dna-pk," *J Cell Biochem*, vol. 92, pp. 781–94, Jul 2004.

[27] S. J. Collis, T. L. DeWeese, P. A. Jeggo, and A. R. Parker, "The life and death of dna-pk," *Oncogene*, vol. 24, pp. 949–61, Feb 2005.

[28] C. J. Vlahos, W. F. Matter, K. Y. Hui, and R. F. Brown, "A specific inhibitor of phosphatidylinositol 3-kinase, 2-(4-morpholinyl)-8-phenyl-4h-1-benzopyran-4-one (ly294002)," *The Journal of biological chemistry*, vol. 269, pp. 5241–8, Feb 1994.

[29] Y. Hosoi, H. Miyachi, Y. Matsumoto, H. Ikehata, J. Komura, K. Ishii, H. J. Zhao, M. Yoshida, Y. Takai, S. Yamada, N. Suzuki, and T. Ono, "A phosphatidylinositol 3-kinase inhibitor wortmannin induces radioresistant dna synthesis and sensitizes cells to bleomycin and ionizing radiation," *Int J Cancer*, vol. 78, pp. 642–7, Nov 1998.

[30] J. J. Hollick, B. T. Golding, I. R. Hardcastle, N. Martin, C. Richardson, L. J. M. Rigoreau, G. C. M. Smith, and R. J. Griffin, "2,6-disubstituted pyran-4-one and thiopyran-4-one inhibitors of dna-dependent protein kinase (dna-pk)," *Bioorg Med Chem Lett*, vol. 13, pp. 3083–6, Sep 2003.

[31] J. J. J. Leahy, B. T. Golding, R. J. Griffin, I. R. Hardcastle, C. Richardson, L. Rigoreau, and G. C. M. Smith, "Identification of a highly potent and selective dna-dependent protein kinase (dna-pk) inhibitor (nu7441) by screening of chromenone libraries," *Bioorg Med Chem Lett*, vol. 14, pp. 6083–7, Dec 2004.

[32] R. J. Griffin, G. Fontana, B. T. Golding, S. Guiard, I. R. Hardcastle, J. J. J. Leahy, N. Martin, C. Richardson, L. Rigoreau, M. Stockley, and G. C. M. Smith, "Selective benzopyranone and pyrimido[2,1-a]isoquinolin-4-one inhibitors of dna-dependent protein kinase: synthesis, structure-activity studies, and radiosensiti-

zation of a human tumor cell line in vitro," *J Med Chem*, vol. 48, pp. 569–85, Jan 2005.

[33] A. Kashishian, H. Douangpanya, D. Clark, S. T. Schlachter, C. T. Eary, J. G. Schiro, H. Huang, L. E. Burgess, E. A. Kesicki, and J. Halbrook, "Dna-dependent protein kinase inhibitors as drug candidates for the treatment of cancer," *Molecular Cancer Therapeutics*, vol. 2, pp. 1257–64, Dec 2003.

[34] Y. Zhao, H. D. Thomas, M. A. Batey, I. G. Cowell, C. J. Richardson, R. J. Griffin, A. H. Calvert, D. R. Newell, G. C. M. Smith, and N. J. Curtin, "Preclinical evaluation of a potent novel dna-dependent protein kinase inhibitor nu7441," *Cancer Research*, vol. 66, pp. 5354–62, May 2006.

[35] H. Chen, Z. Ma, R. P. Vanderwaal, Z. Feng, I. Gonzalez-Suarez, S. Wang, J. Zhang, J. L. R. Roti, S. Gonzalo, and J. Zhang, "The mtor inhibitor rapamycin suppresses dna double-strand break repair," *Radiat Res*, vol. 175, pp. 214–24, Feb 2011.

[36] A. Priestley, H. J. Beamish, D. Gell, A. G. Amatucci, M. C. Muhlmann-Diaz, B. K. Singleton, G. C. Smith, T. Blunt, L. C. Schalkwyk, J. S. Bedford, S. P. Jackson, P. A. Jeggo, and G. E. Taccioli, "Molecular and biochemical characterisation of dna-dependent protein kinase-defective rodent mutant irs-20," *Nucleic Acids Research*, vol. 26, pp. 1965–73, Apr 1998.

[37] R. A. Izzard, S. P. Jackson, and G. C. Smith, "Competitive and noncompetitive inhibition of the dna-dependent protein kinase," *Cancer Research*, vol. 59, pp. 2581–6, Jun 1999.

[38] A. Kumar, O. Fernandez-Capetillo, O. Fernadez-Capetillo, and A. C. Carrera, "Nuclear phosphoinositide 3-kinase beta controls double-strand break dna repair," *Proc Natl Acad Sci USA*, vol. 107, pp. 7491–6, Apr 2010.

[39] T. L. Yuan and L. C. Cantley, "Pi3k pathway alterations in cancer: variations on a theme," *Oncogene*, vol. 27, pp. 5497–510, Sep 2008.

[40] M. Mazzoletti, F. Bortolin, L. Brunelli, R. Pastorelli, S. D. Giandomenico, E. Erba, P. Ubezio, and M. Broggini, "Combination of pi3k/mtor inhibitors: Antitumor activity and molecular correlates," *Cancer Research*, vol. 71, pp. 4573–84, Jul 2011.

[41] M. Dokmanovic, C. Clarke, and P. A. Marks, "Histone deacetylase inhibitors: overview and perspectives," *Mol Cancer Res*, vol. 5, pp. 981–9, Oct 2007.

(a)

Bottomless Plate

Agarose
Microwells

GelBond Film

Glass Plate

~300 Microwells
per 96-well

(b)

Excess Cells

Patterned Cells

Load Cell
Samples

Aspirate
Excess Cells
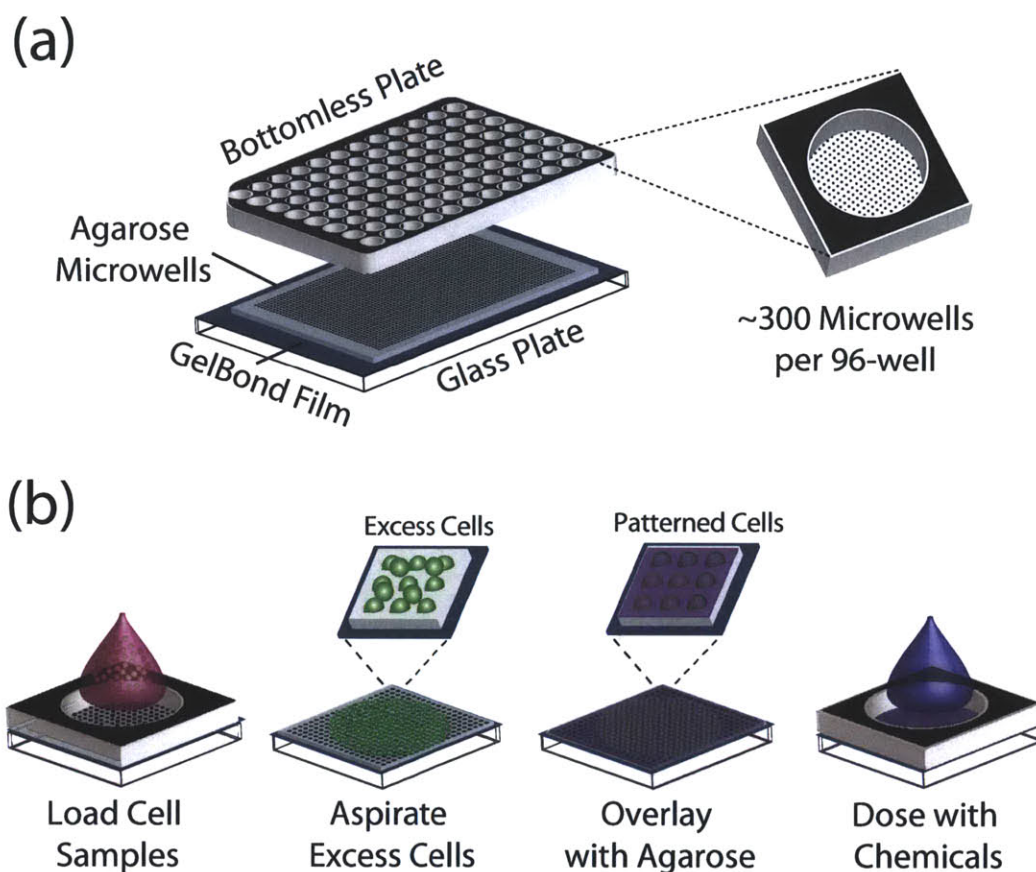
Overlay
with Agarose

Dose with
Chemicals

Figure 4-1: **96-well CometChip: Single Cell Microarray Platform.** (a) Assembly of multiwell comet array. Agarose gel with microwells is sandwiched between a glass substrate and a bottomless multiwell plate and sealed with mechanical force. Approximately 300 arrayed microwells comprise the bottom of each multiwell. (b) Loading and chemical dosing of cell samples in multiwell. One cell sample is loaded in each multiwell and cells settle by gravity into the arrayed microwells. The bottomless plate is removed in order to aspirate excess cells and enclose the cells in agarose. The bottomless plate is replaced in order to treat each multiwell with a chemical condition.
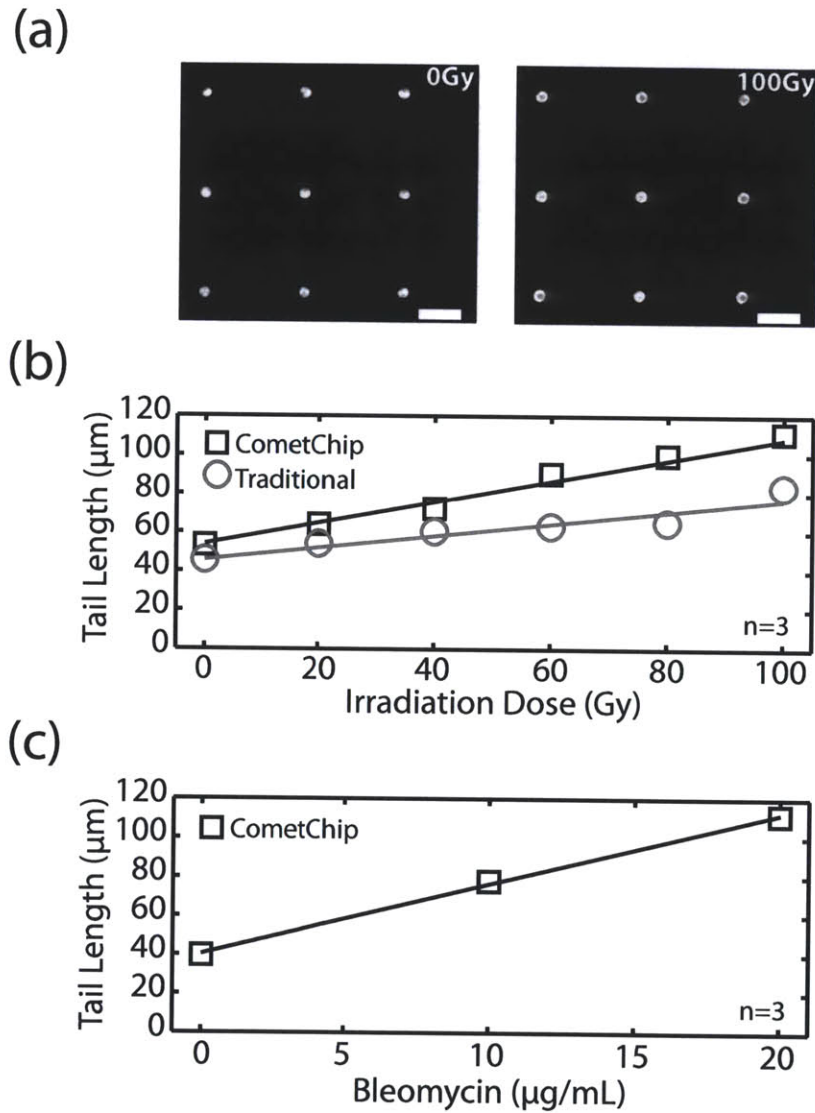
Figure 4-2: **Arrayed Microwell Comet Assay for Detection of Double Strand Breaks.** (a) Arrayed microwell comets from untreated TK6 human lymphoblasts and TK6 cells exposed to 100 Gy gamma irradiation. Scale bar is 100 μm. (b) Comparison of irradiation dose response between traditional comet slides scored using commercial software and microwell comets scored using automated software. Each data point is the average of three independent experiments, where the median tail length (μm) of 100 individual comets was used to represent the extent of DNA damage. (c) Bleomycin dose response conducted on multiwell platform with each data point representing the median tail length (μm) of at least 300 comets pooled from six multiwells.
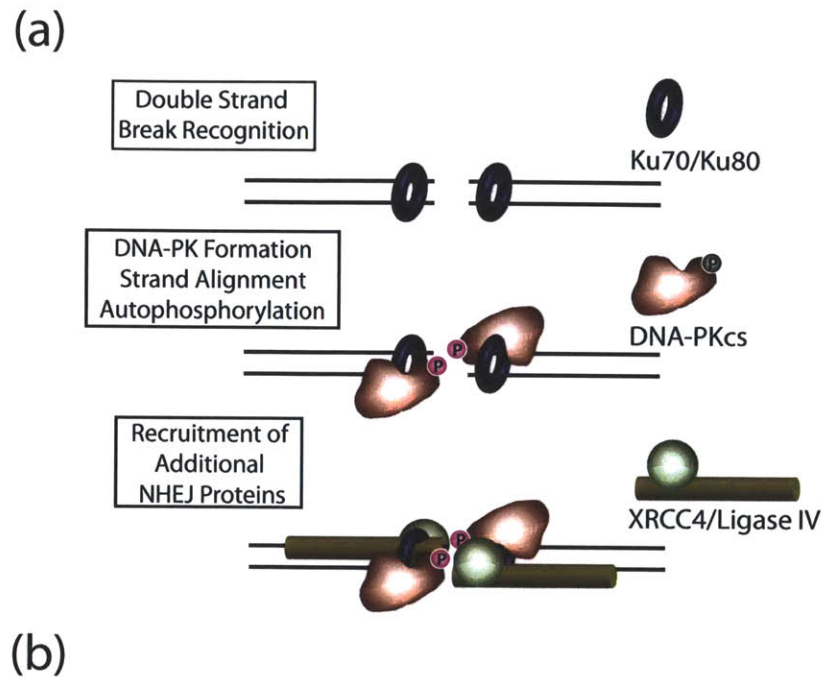
Figure 4-3: **Detection of NHEJ Deficiencies.** **(a)** Simplified model of non-homologous endjoining. The Ku70/Ku80 heterodimer binds to the DNA ends formed by a DSB and recruits DNA-PKcs to form DNA-PK. DNA-PK autophosphorylates to signal further recruitment and processing of the DSB as well as its subsequent release. **(b)** Evaluation of DNA repair kinetics of CHO-K1 (wild type), xrs-6 (Ku80-/-), and irs-20 (DNA-PKcs-/-) exposed to 100 Gy IR. All cell types and repair times conducted on a single CometChip with data representing median comet tail lengths (μm) from at least 50 comets. Error bars represent standard deviations of three independent experiments. Symbols indicate a significant difference compared to wild type according to Student's t-test: *$p < 0.05$, **$p < 0.005$.
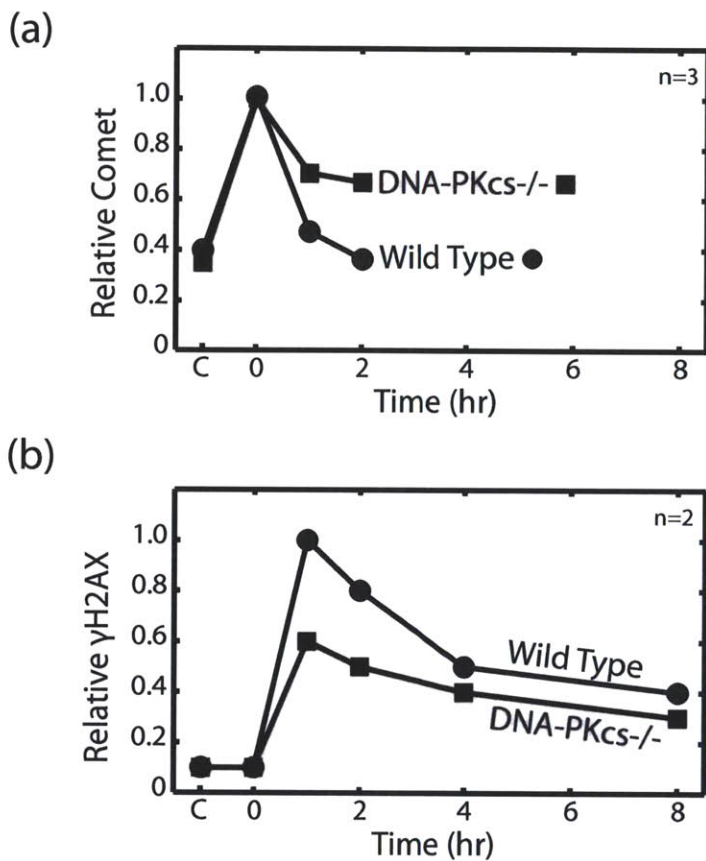
Figure 4-4: **Comparison of Neutral CometChip to γ-H2AX Assay.** Wild type (circles) and DNA-PKcs-/- (squares) were exposed to 100 Gy IR. **(a)** All cell conditions and repair time points were conducted in triplicate wells of a single CometChip. Comet tail length (μm) values were normalized to peak wild type damage. Irs-20 cells displayed significantly different repair kinetics from CHO-K1 ($P < 0.005$). **(b)** Repair kinetics were measured in triplicate over eight hours using a Western blot version of the γ-H2AX assay.
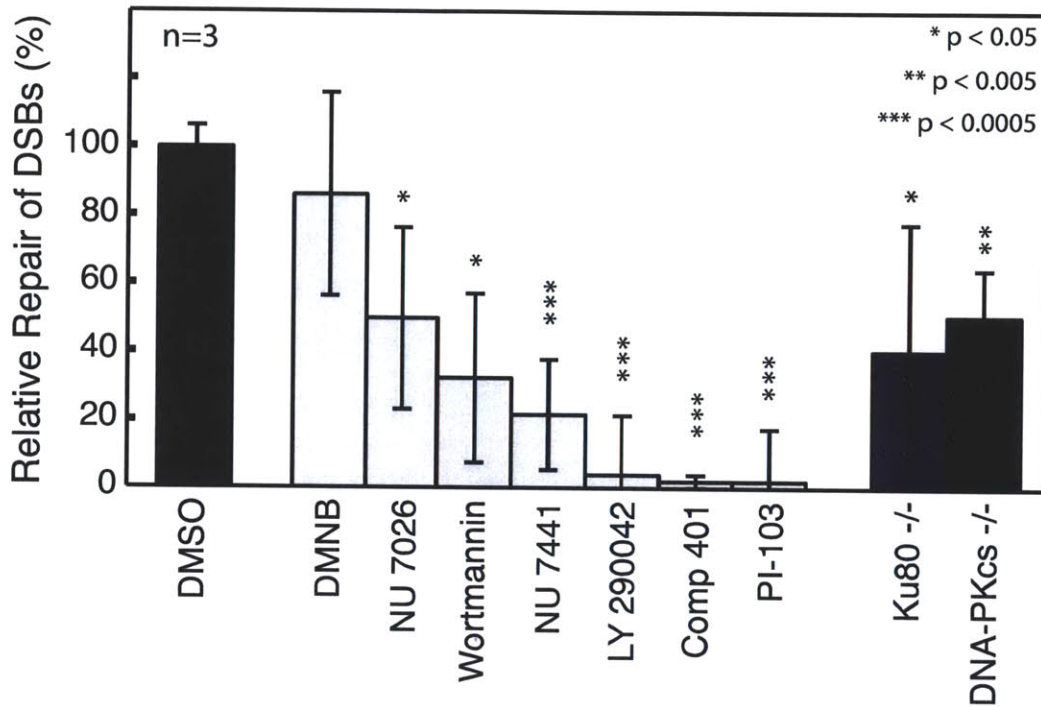
Figure 4-5: **Evaluation of Relative Repair from 100 Gy IR after 1 hr Exposure to DNA-PK Inhibitor Library.** CHO-K1 (wild type) cells pre-incubated for 1 hr in 50 μM of each inhibitor. All conditions and controls, xrs-6 (Ku80-/-) and irs-20 (DNA-PKcs-/-) assayed in triplicate wells. Data and error bars represent averages and standard deviations of three independent experiments. Symbols indicate significance compared to wild type (DMSO) according to Student's t-test: *p < 0.05, **p < 0.005, ***p < 0.0005.
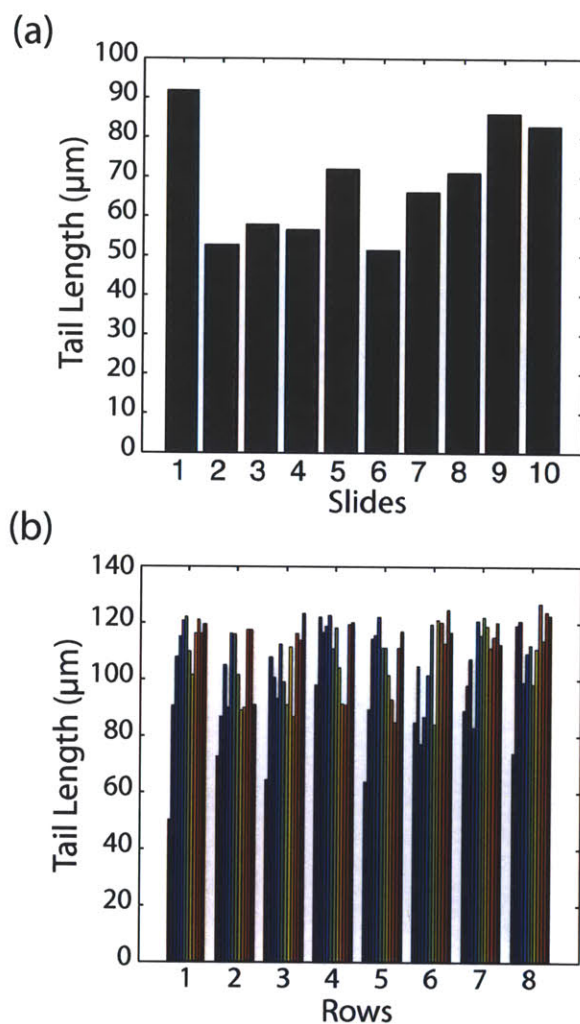
Figure 4-6: **Well-to-well Variability of Traditional Comet Assay and Arrayed Cell CometChip using TK6 Cells Exposed to 100 Gy IR.** (a) Median of 30 traditional neutral comets from ten slides. Median comet length: 70 μm; Coefficient of variance: $\sim$20% (b) Median of at least 30 microwell comets from 96 wells of CometChip. Median: 105 μm; Coefficient of variance: $\sim$15%.
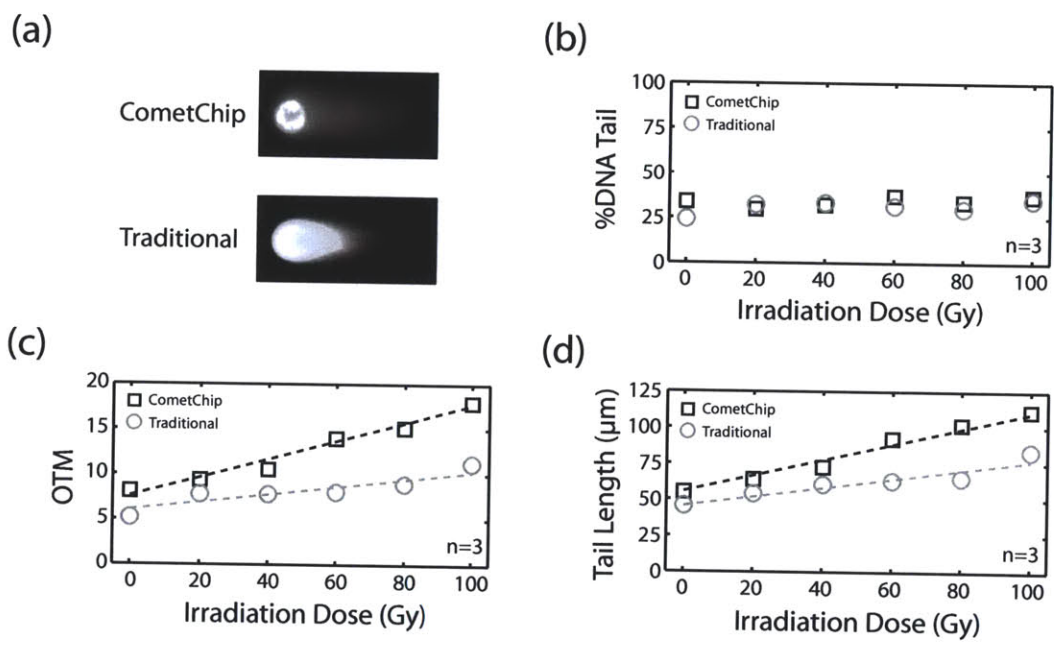
Figure 4-7: **Comparison of CometChip to Traditional Neutral Comet Assay.**
(a) Comparison of comet morphologies resulting from 100 Gy IR. (b) Percent total
DNA in tail: $R^2 = 0.30$ (CometChip) and $R^2 = 0.42$ (Traditional). (c) Olive tail
moment: $R^2 = 0.88$ (CometChip) and $R^2 = 0.63$ (Traditional). (d) Tail length (μm):
$R^2 = 0.99$ (CometChip) and $R^2 = 0.85$ (Traditional).

Table 4-1. DNA-PK inhibitors

Compound	Other Major Targets [a]	IC$_{50}$ (nM) [b]			Relative [d]
		DNA-PK	PI3K	mTOR	Inhibition (%)
PI-103	ATR, ATM, PI3K, P110β/γ, PI3KC2α/β, mTORC1/2, hsVP534	2	8	20	100
Compound 401	mTOR	280	>100000	5300	100
LY290042 [c]	PI3K, P110β/γ, CKII, mTOR	360	1.4	2500	100
NU7441 [c]	PI3K, mTOR	14	5000	1700	79
Wortmannin	PI3K, PLK1, mTOR	150	2-5	1000	68
NU7026 [c]		230	>100000	13000	50
DMNB		15000			14

[a,b] Data compiled from manufacturer (Tocris)   [c] (Leahy, 2004)   [d] Relative inhibition values calculated from Fig.4-5

Chapter 5

Conclusions

This thesis represents the foundational work surrounding the engineering and characterization of the CometChip, a method to pattern single cells in agarose for high throughput analysis of DNA damage and repair using the well-established comet assay protocol. The CometChip was shown to have equivalent sensitivity compared to the standard comet assay, while increasing throughput by at least an order of magnitude and reducing experimental noise. Furthermore, the CometChip can be imaged automatically and continuously without the requirement of a slide feeder and the number of analyzable comets in each image is improved by the spacing of the microwell array. We developed an automated software suite that exploits the defined spacing of the array to objectively select comets and utilizes the fixed head size, provided by the microwell geometry, to accurately determine comet parameters. Additionally, the microwell array provides the ability to evaluate DNA damage in cell aggregates and the potential to include multiplexed labeling for parallel analysis of multiple single cell endpoints (e.g. viability). The 96-well version of the assay can be integrated with standard high throughput screening (HTS) and imaging technologies for automated analysis of multiple cell types, chemical conditions, and repair time points on a single device. The CometChip has applications in both epidemiology, such as determining the consequences of harmful exposures and identifying susceptible populations, and clinical practice, such as determining tumor sensitivities and guiding treatment strategies.

We used the CometChip to compare repair kinetics of damage induced by a range of chemical agents, each revealing a distinct repair profile. By using model agents with known spectra of lesion induction, we calculated the kinetic half lives for four major DNA repair pathways, which varied considerably from as fast as 15 min for base excision repair (BER) of oxidized damage, 1 hr for non-homologous end joining (NHEJ), 4 hr for nucleotide excision repair (NER), to more than 10 hours for interstrand crosslink repair (ICLR). We used these repair profiles as standards for evaluation with deficiencies in repair from a specific chemical exposure being detected as deviations from the corresponding standard repair curve.

We evaluated glioblastoma cell lines with known deficiencies in alkyladenine glycosylase (AAG) and polymerase beta (Polβ) and found that only when cells were both over-expressed (OE) in AAG and knocked-down (KD) in Polβ did an accumulation of BER intermediates result in response to alkylation damage. This emphasizes that it is the coordinated effort of multiple repair proteins that is important to maintaining balance in the BER pathway. It would be interesting to probe the system further with a range of MMS concentrations to determine whether imbalances might be concentration dependent. For example, at higher doses, cells overexpressing AAG may saturate Polβ activity. Understanding such thresholds may be important for optimizing therapeutic dosing regimens.

We successfully employed the CometChip for detection of XPG deficiencies in NER, however, the mechanistically rich repair profiles expected for XPG deficient and catalytically inactive XPG mutant cells were not revealed. This is likely because not all lesions in the 4-Nitroquinoline 1-oxide (4NQO) spectrum are substrates for NER and the resulting 4NQO repair profile is therefore dictated by multiple repair processes. By using a dose range of ultraviolet (UV) radiation, which is known to produce mostly single strand breaks (SSBs) and pyrimidine dimers, and evaluating repair after three hours, when BER can be expected to be complete, the theoretical repair profiles predicted by the Dual Incision Hypothesis emerged. This is an example of how the increased throughput and improved reproducibility provided by the CometChip can enable an informed user to exploit the versatility of the comet assay

for detection of numerous lesions and repair profiles. We plan to evaluate a set of more than ten other transgenic human fibroblast cell lines with mutations in other key NER enzymes (e.g. XPF and XPA). The data may provide further details of the NER mechanism.

In another modality of the comet assay, cells can be exposed to ionizing radiation (IR) in order to determine the extent of interstrand crosslinking. We adapted this protocol to the CometChip and identified the critical role of a NER deficiency (XPF-/-) in interstrand crosslink repair (ICLR). In addition, we showed that a deficiency in XPB, the NER helicase associated with XPF, did not have an effect on ICLR. It would be interesting to similarly evaluate the NER deficient human fibroblast cell lines from the Laboratory of Dr. Orlando Schärer, in order to determine the roles of other NER proteins and protein functions in human ICLR. The CometChip can also be used to evaluate efficacies of ICL agents or evaluate sensitivities of tumor cells.

Lastly, we evaluated double strand break (DSB) repair through adaption of the neutral comet assay on the CometChip. The use of a Cobalt-60 gamma irradiator (120 Gy/min) and ability to assess repair of multiple cell types on a single CometChip enabled the efficient detection of deficiencies in two critical NHEJ proteins, confirming the specificity of the assay for DSBs. The CometChip represents one of the only platforms available for direct measurement of DSBs and DSB repair kinetics, providing a relatively inexpensive and fast method of measuring DSB repair capacity, which could be used to assess patient sensitivity and tumor resistance.

It is conceivable that a specific DNA repair profile can be obtained for numerous other genotoxic agents. A cell sample could then be challenged with an established set of chemicals in order to produce a DNA repair signature that could reveal biological insights such as lesion sensitivities and repair deficiencies. Similarly, an uncharacterized genotoxic compound could be screened against a small set of transgenic cells in order to better understand its chemical mode of action. We demonstrated that even with a limited number of model cell lines and DNA damaging agents, mechanistically rich repair profiles can be obtained, providing insight into multiple pathways of repair, revealing a range of genetic deficiencies.

The use of the CometChip in detecting DNA repair deficiencies serves as proof of principle for its use in evaluating small molecule inhibitors of DNA repair proteins, which have emerged as a promising new target in cancer management. We used the CometChip to assess potential inhibitors of AP Endonuclease (APE). The screen of three inhibitors provided results that were consistent with the literature, supporting this approach as a secondary measure of the efficacy of APE inhibition. However, this application of the assay was not ideal, because inhibitor efficacy was detected as a dose dependent comet signal assumed to be formed by an accumulation of spontaneous abasic sites. In contrast, the use of the neutral CometChip provides a more direct application for screening DNA repair inhibitors. We screened seven inhibitors of DNA-PK and two control cell lines with deficiencies in DNA-PK on a single CometChip in triplicate. We found a range of DSB inhibition efficiencies that appeared to correlate with known inhibition parameters. The detection of such deficiencies is a niche application for the CometChip, as the γ-H2AX assay, which has become a standard in DSB detection, measures a signal that is dependent on DNA-PK and other proteins and is therefore limited in its ability to measure DSB repair kinetics. That is not to say that the γ-H2AX assay does not provide useful information. In fact, the marriage of the two assays may provide a wealth of new information in screens of other PI3KKs or HDAC inhibitors or studies involving the effects of chromatin structure on DSB repair kinetics.

The studies described in this thesis support the use of the CometChip in many settings ranging from the straight forward application of genotoxicity testing to more elaborate investigations into the biological mechanisms of DNA repair. In addition, many of the experiments were conducted partially as a technical proof of principle and therefore have uncovered numerous avenues for deeper analysis, which in turn may require additional technical advancements. For example, one reoccurring theme is how to best interpret repair profiles of BER in experiments such as the screen of glioblastoma lines in Chapter III. Without knowledge of relative enzyme activities, the WT, AAGOE, and PolβKD cells would be interpreted as having identical repair capacities, which we know is not the case due to the accumulation of repair intermedi-

176

ates in AAGOE/PolβKD cells. One way to fully realize the alkylation damage burden and true extent of repair is through the implementation of post-lysis enzymes (i.e. AlkA, FPG, T4EndoV) to convert base lesions (Collins, *et al.*, 1997). The CometChip may be favorable for such applications, as enzyme treatment could be applied using the 96-well format. This addition to the CometChip tool set would enable increased sensitivity of DNA damage quantification and provide another layer of analysis into DNA repair capacity.

Ultimately, we want to provide an assay that is useful in both a variety of clinical and population studies. It will therefore be necessary to develop protocols for analysis of primary cells. We have successfully assayed human lymphocytes and nasal epithelial cells for baseline levels of damage. We have also conducted proof of principle experiments using a variety of murine tissues, including thymus, spleen, hepatocytes, etc. Most recently, we demonstrated an ability to detect MMS induced damage in freshly harvested thymus cells. These results are encourgaging, however, in most cases it will be important to freeze samples and store them before conducting experiments. The effects of such freezing protocols must therefore be explored. Another barrier to the use of primary cells is potential contamination of the comet signal by dead or apoptotic cells, which may represent a large fraction of the sample population in some tissues. One strategy we are pursuing is to develop microwell registration algorithms in order to multiplex viability endpoints with comet analysis, such as fluorescent live/dead stains. The CometChip could then be imaged before analysis and comets resulting from dead/apoptotic cells could be eliminated during analysis. These algorithms may also be applied for selection of fluorescently labeled cells (e.g. with a fluorescent antibody), which could be an important method for analyzing heterogeneous cell popluations. Together, these technological improvements may enable DNA damage measurements of primary samples with improved resolution that have the potential to become a new standard in DNA damage analysis.

This thesis work sits at the interface of engineering and biology, demonstrating the ability of engineering approaches to significantly improve existing biological assays. So while we initiated the project with a tool that resembled the standard comet

assay, the current version of the CometChip enables analysis of multiple cell samples, multiple chemical conditions, and multiple repair time points on a single device, and integrates with standard high throughput screening technologies, providing a platform for drug discovery and genotoxicity screening. Furthermore, the CometChip is the first device to enable simultaneous evaluation of multiple DNA repair pathways, which is important both in characterizing chemical exposures and also for detection of repair deficiencies. The use of microwells not only improves throughput and reproducibility, but may also permit new applications, such as multiplexing endpoints and including internal standards for further reduction of variability between experiments. Other technological improvements can also be envisioned, such as the use of materials with greater stability and more uniform consistency than agarose or the application of various electrophoresis techniques to enhance signal resolution. Lastly, improvements to the analysis software may reveal new parameters that provide more information, such as about cell cycle, or the distribution of damage levels among a sample population. At the heart of the CometChip technology lies the microwell array, an approach whose elegance will enable the continued evolution of the CometChip as a high throughput platform for DNA damage and repair analysis.

Appendix A

Protocols

A.1   Photolithography

TRL SU-8 (Purple) Process on 4" Silicon

1) Dehydrate wafer at 180C for 5m on hotplate 1

2) Spin SU-8 2050 @ 3500 rpm for 30s on SU8spinner

3) Prebake wafer @ 65C for 2m on hotplate 2

4) Softbake wafer @ 95C for 7.5m on hotplate 1

5) Expose wafer for 20s on EV1 with transparency mask using 5s intervals and 15s delay

6) Prebake wafer @ 65C for 2m on hotplate 2

7) Postbake @ 95C for 5m on hotplate 1

8) Develop SU-8 using PM Acetate

A.2 CometChip
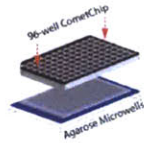
Table of Contents:

2

Creating a CometChip

Materials:

Normal Melting Point (NMP) Agarose (Invitrogen; Catalog No. 15510-027)
Low Melting Point (LMP) Agarose
Dulbecco's Phosphate Buffered Saline 1X (GIBCO)

GelBond® Film (Lonza; Size: 85 x 100 mm, Catalog No. 53734)
PDMS Stamp (Provided by Engelward Lab)
Square petri dish (VWR: Catalog No. 25378-047)
Bottomless 96-well plate (Greiner Bio-One: Reference 655000)
1.5" Binder Clips
Glass plate

3

Boil agarose and Place gelbond

- Prepare molten 1% NMP agarose in PBS by bringing solution to a boil
- Cut and place GelBond® paper hydrophilic side facing up in petri dish

TIPS: 1) Use ~2mL of 1% agarose to seal the gelbond to the dish surface
2) Water will bead on surface of hydrophobic side

4

Pour agarose and set PDMS mold

- See chart to determine amount of NMP agarose
- Add molten 1% NMP agarose
- Immediately set PDMS mold on top of agarose

Alkaline HTA	Neutral HTA
20 mL	5 mL
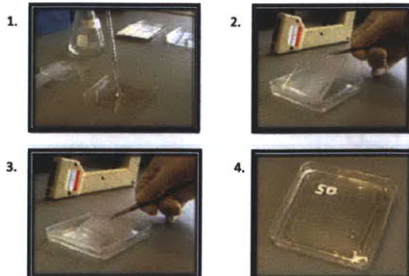
5

Remove PDMS mold

- Allow agarose to gel (3-5min), then add 10mL PBS on top of gel/mold
- **Carefully** remove PDMS stamp from gel using tweezers to peel from the corner
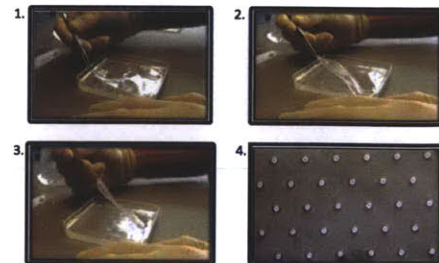
Inspect microwells for quality control

6

Remove Gel

- Remove gelbond with gel from dish and discard excess gel
- Label back of gelbond using permanent chemical resistant marker (VWR)

7

Clamp 96-well Plate

- Set gel on glass plate and press bottomless 96-well plate upside-down into it
- Clamp all four sides of 96-well plate to glass using 1.5" binder clips
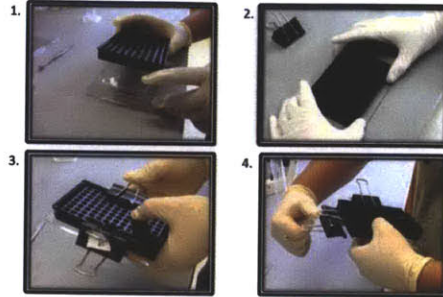
8

Load Cells

- Add 100uL of each single cell suspension (>100,000 cell/mL) to each well of plate
- Cover plate with gelbond to prevent evaporation of media during incubation
- Allow microwells to load for at least 30min in 37C incubator

9

Remove Excess Cells

- Remove plate from incubator* and aspirate media from each well
- Remove 96-well plate and gently rinse with PBS to remove excess cells

*Tip: Use microscope to ensure that >70% wells contain cells.

10

Apply Overlay

- Overlay gel with 37C 1% Low Melting Point Agarose
- Allow to gel in refrigerator for five minutes
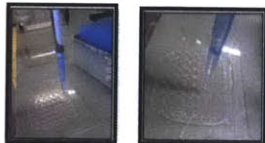
11

Dosing and Repair

- If multiple chemical conditions or repair time points are to be conducted, replace the 96-well plate by carefully aligning the wells to exact location.
- Use a marker to circle the backside of 2-3 wells to help with realignment
- 96-well plate should slip back into position with minimal force.

12

Alkaline Assay

Materials:

Buffers
  Lysis Buffer
  Electrophoresis Buffer
  Neutralizing Buffer
  TE Buffer
Electrophoresis chamber and Power Supply
SYBR Gold Stain (Invitrogen: Catalog Number S11494)

13

Alkaline Lysis Buffer

Alkaline Lysis Stock Solution		Total Volume of Lysis Buffer			
Chemical and final concentration in solution	MW (g/mol)	0.5 L	1.0 L	2.0 L	4.0 L
2.5 M NaCl	58.4	73.1 g	146.1 g	292.2 g	584.4 g
100 mM Na₂EDTA	372.2	18.6 g	37.22 g	74.5 g	148.9 g
10 mM Tris (Base)*	121.1	0.606 g	1.211 g	2.442 g	4.844 g
Distilled H₂O	* use analytical scale				

<u>Working solution: 1% Triton X-100</u>
1% Triton X-100: Directly before use add 1mL Triton X-100 per 100mL buffer

Stock Solution Preparation:

1) Dissolve crystalline substances half of the desired end volume

2) Adjust the pH to 10: add NaOH until cloudy solution becomes clearer (~pH 9.8)

3) Fill with distilled water to final volume

14

Electrophoresis Buffer

5M NaOH Stock Solution		Total volume in water			
Sodium Hydroxide	MW (g/mol)	0.5L	1L	2L	4L
Crystalline NaOH	40	99.8g	199.5g	399.9g	799.8g

NOTE: Dissolving NaOH is exothermic - add small amounts to water carefully!

0.2M Na₂EDTA Stock Solution		Total volume in water			
Ethylenediaminetetraacetic acid	MW (g/mol)	0.5L	1L	2L	4L
Crystalline Na₂EDTA	372	37.2g	74.5g	148.9g	297.8g

<u>Working solution: Prepare 1hr before use</u>

0.3M NaOH, 1mM Na₂EDTA	Total Volume of Working Solution				
Chemical and stock solution concentration	1L	2L	2.5L	3.5L	4L
5M NaOH	60 mL	120 mL	150 mL	210 mL	240 mL
0.2M Na₂EDTA	5 mL	10 mL	12.5 mL	17.5 mL	20 mL
Distilled H₂O					

15

Neutralization Buffer

1M Tris Stock Solution (pH 7.5)		Total volume in water			
Tris-base	MW (g/mol)	0.5L	1L	2L	4L
Crystalline Tris	121.14	60.6g	121.1g	242.3g	484.57g
Tris-acid may be used in place of tris-base					
Tris-acid	MW (g/mol)	0.5L	1L	2L	4L
Crystalline Tris	157.59	78.8g	157.6g	315.2g	630.4g

Adjust the pH to 7.5 with either HCl (35%) or 1M NaOH

<u>Working solution: Prepare directly before use</u>

0.4M Tris (pH 7.5)	Total Volume of Final Buffer			
Chemical and stock solution concentration	100mL	250mL	500mL	1000mL
1M Tris	40mL	100mL	200mL	400mL
Distilled H₂O				

16

Alkaline Comet Assay

• Remove 96-well plate and submerge gel in 4C alkaline **lysis buffer** for 1hr or overnight

• Tape each gel in electrophoresis chamber with double-sided tape
• Fill chamber with 4C alkaline **electrophoresis buffer** to volume that covers gels
• Allow 40min for alkaline unwinding

• Run electrophoresis at 1V/cm and 300 mA for 30 min at 4C
  • Adjust level of electrophoresis buffer in chamber to achieve 300 mA current

17

Neutral Assay

Materials:

Buffers
- Lysis Buffer
- Electrophoresis Buffer
- Neutralizing Buffer
- TE Buffer

Electrophoresis chamber and Power Supply

SYBR Gold Stain (Invitrogen: Catalog Number S11494)

18

Neutral Lysis Buffer

Neutral Lysis Stock Solution (pH 9.5)		Total Volume of Lysis Buffer			
Chemical and final concentration in solution	MW (g/mol)	0.5 L	1.0 L	2.0 L	4.0 L
2.5 M NaCl	58.4	73.1 g	146.1 g	292.2 g	584.4 g
100 mM Na$_2$EDTA	372.2	18.6 g	37.22 g	74.5 g	148.9 g
10 mM Tris (Base)	121.1	0.606 g	1.211 g	2.442 g	4.844 g
1% N-Lauroylsarcosine	N/A	5 g	10 g	20 g	40 g
Distilled H$_2$O	*use analytical scale				

Stock Solution Preparation:

1) Dissolve crystalline substances half of the desired end volume

2) Adjust the pH to 9.5

3) Fill with distilled water to final volume

Working solution: 0.5% Triton X-100 and 10% DMSO

Directly before use add: - 0.5mL Triton X-100 per 100mL buffer
                 - 10mL DMSO per 100mL buffer

19

Neutral Electrophoresis Buffer

Neutral Assay Electrophoresis Buffer is TBE at pH 8.5

TBE Solution (pH 8.5)		Total Volume of Lysis Buffer			
Chemical and final concentration in solution	MW (g/mol)	0.5 L	1.0 L	2.0 L	4.0 L
2 mM Na$_2$EDTA	372.2	0.372 g	0.744 g	1.488 g	2.976 g
90 mM Tris (Base)	121.1	5.45 g	10.9 g	21.8 g	43.6 g
90 mM Boric Acid	61.83	2.78 g	5.56 g	11.13 g	22.26 g

Stock Solution Preparation:

1) Dissolve crystalline substances half of the desired end volume

2) Adjust the pH to 8.5

3) Fill with distilled water to final volume

20

Neutralization Buffer

1M Tris Stock Solution (pH 7.5)		Total volume in water			
Tris-base	MW (g/mol)	0.5L	1L	2L	4L
Crystalline Tris	121.14	60.6g	121.1g	242.3g	484.57g
Tris-acid may be used in place of tris-base					
Tris-acid	MW (g/mol)	0.5L	1L	2L	4L
Crystalline Tris	157.59	78.8g	157.6g	315.2g	630.4g

Adjust the pH to 7.5 with either HCl (35%) or 1M NaOH

Working solution: Prepare directly before use

0.4M Tris (pH 7.5)	Total Volume of Final Buffer			
Chemical and stock solution concentration	100mL	250mL	500mL	1000mL
1M Tris	40mL	100mL	200mL	400mL
Distilled H$_2$O				

21

Neutral Comet Assay

- Remove 96-well plate and submerge gel in 43C **neutral lysis buffer** for 3 hours
  - Can refrigerate overnight in lysis solution after 3 hours
- Remove lysis buffer and rinse with **neutral electrophoresis buffer** (TBE) for 2 x 1 hour at room temperature

- Tape each gel in electrophoresis chamber with double-sided tape
- Fill chamber with 4C TBE to volume that just covers gels
- Allow gel to sit in chamber at 4C for 30 minutes

- Run electrophoresis at 0.6 V/cm and 6mA for 1 hour at 4C
  - Adjust level of electrophoresis buffer in chamber to achieve 6 mA current

22

Fluorescent Imaging

- Neutralize gels in **neutralization buffer** for 3 x 5min at 4°C
- Store gels hydrated in TE buffer at 4°C until imaging

- Stain gels with DNA stain of choice (i.e.SYBR Gold, Ethidium Bromide, etc.)
- Image using fluorescent microscope and 10X objective

H2O2 Dose Response

23

Data Analysis with MATLab:

(1) Stack images as .tiff using ImageJ (http://rsbweb.nih.gov/ij/)
(2) Open Matlab
(3) Type "guicometanalyzer.m" into the Command Window
(4) Click Browse and select the folder containing your .tiff images
(5) Select image files to analyze
(6) Set parameters (Default is for 40um PDMS stamp)
- Head diameter: 40   Array spacing: 240
- Image rotation: 0 (tail to the right)
(7) ANALYZE

Data output as text files in directory folder

getcometdata.m can be used to extract data (median/std) from text files
Type "getcometdata([])" into Command Window and select directory

24

ImageJ

Microscope images (.tiff) must be converted to stacks for MatLAB analysis

Download for free: http://rsbweb.nih.gov/ij/

1) Open all .tiff images for a single analysis condition

2) Convert Images to Stack
3) Save as .tiff (in directory to be analyzed)

25

Screenshot of GUIcometanalyzer.m
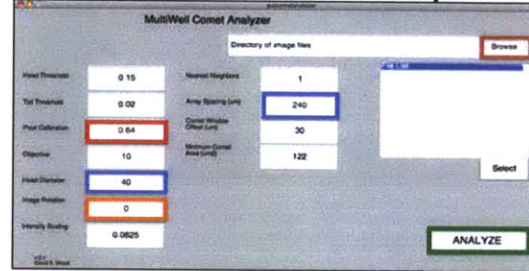
26

Screenshot of Output Textfile

Data exported as .txt files
Import .txt files into excel or MATLab for analysis

27

Credits

Design of CometChip: David Wood and David Weingeist
Oversight of protocol development: David Weingeist
Photodocumentation: Kelly Schulte

Questions and Concerns:
Contact David Weingeist (dmw555@mit.edu)

Appendix B

MatLAB Code

B.1 guicometanalyzer.m

```matlab
1  function varargout = guicometanalyzer(varargin)
2  % GUICOMETANALYZER M-file for guicometanalyzer.fig
3  % GUICOMETANALYZER, by itself, creates a new GUICOMETANALYZER or ...
      raises the existing singleton*.
4  %
5  % H = GUICOMETANALYZER returns the handle to a new ...
      GUICOMETANALYZER or the handle to the existing singleton*.
6  %
7  % GUICOMETANALYZER('CALLBACK',hObject,eventData,handles,...) ...
      calls the local function named CALLBACK in GUICOMETANALYZER.M ...
      with the given input arguments.
8  %
9  % GUICOMETANALYZER('Property','Value',...) creates a new
10 % GUICOMETANALYZER or raises the existing singleton*.  Starting ...
      from the left, property value pairs are applied to the GUI ...
      before guicometanalyzer_OpeningFcn gets called.  An ...
      unrecognized property name or invalid value makes property ...
      application stop.  All inputs are passed to ...
      guicometanalyzer_OpeningFcn via varargin.
11 %
```

185

```matlab
12 % *See GUI Options on GUIDE's Tools menu.  Choose "GUI allows ...
       only one instance to run (singleton)".
13 %
14 % See also: GUIDE, GUIDATA, GUIHANDLES

15

16 % Edit the above text to modify the response to help guicometanalyzer

17

18 % Last Modified by GUIDE v2.5 29-Sep-2009 10:28:21

19

20 % Begin initialization code - DO NOT EDIT
21 gui_Singleton = 1;
22 gui_State = struct('gui_Name',       mfilename, ...
23                    'gui_Singleton',  gui_Singleton, ...
24                    'gui_OpeningFcn', ...
                         @guicometanalyzer_OpeningFcn, ...
25                    'gui_OutputFcn',  @guicometanalyzer_OutputFcn, ...
26                    'gui_LayoutFcn',  [] , ...
27                    'gui_Callback',   []);
28 if nargin && ischar(varargin{1})
29     gui_State.gui_Callback = str2func(varargin{1});
30 end

31

32 if nargout
33     [varargout{1:nargout}] = gui_mainfcn(gui_State, varargin{:});
34 else
35     gui_mainfcn(gui_State, varargin{:});
36 end
37 % End initialization code - DO NOT EDIT
38 end

39

40 % —— Executes just before guicometanalyzer is made visible.
41 function guicometanalyzer_OpeningFcn(hObject, eventdata, handles, ...
       varargin)

42

43 handles.output = hObject;

44
```

```matlab
45  % Initialize handle objects
46  handles.SelectedFiles = 1;
47
48  % Update handles structure
49  guidata(hObject, handles);
50
51  end
52
53  % —— Outputs from this function are returned to the command line.
54  function varargout =guicometanalyzer_OutputFcn(hObject, ...
        eventdata, handles)
55
56  % Get default command line output from handles structure
57  varargout{1} = handles.output;
58  end
59
60  % —— Executes on button press in pushbutton1.
61  function pushbutton1_Callback(hObject, eventdata, handles)
62
63  analysisok = mwcometanalyzer(handles);
64
65  guidata(hObject,handles)
66  end
67
68  function edit1_Callback(hObject, eventdata, handles)
69  end
70
71  % —— Executes during object creation, after setting all properties.
72  function edit1_CreateFcn(hObject, eventdata, handles)
73  if ispc && isequal(get(hObject,'BackgroundColor'),
74      get(0,'defaultUicontrolBackgroundColor'))
75      set(hObject,'BackgroundColor','white');
76  end
77  end
78
79
```

```matlab
80  function edit2_Callback(hObject, eventdata, handles)
81  end
82
83  % ── Executes during object creation, after setting all properties.
84  function edit2_CreateFcn(hObject, eventdata, handles)
85
86  if ispc && isequal(get(hObject,'BackgroundColor'),
87      get(0,'defaultUicontrolBackgroundColor'))
88      set(hObject,'BackgroundColor','white');
89  end
90  end
91
92  function edit3_Callback(hObject, eventdata, handles)
93  end
94
95  % ── Executes during object creation, after setting all properties.
96  function edit3_CreateFcn(hObject, eventdata, handles)
97  % Hint: edit controls usually have a white background on Windows. ...
        See ISPC and COMPUTER.
98  if ispc && isequal(get(hObject,'BackgroundColor'),
99      get(0,'defaultUicontrolBackgroundColor'))
100     set(hObject,'BackgroundColor','white');
101 end
102 end
103
104 function edit4_Callback(hObject, eventdata, handles)
105 end
106
107 % ── Executes during object creation, after setting all properties.
108 function edit4_CreateFcn(hObject, eventdata, handles)
109 if ispc && isequal(get(hObject,'BackgroundColor'),
110     get(0,'defaultUicontrolBackgroundColor'))
111     set(hObject,'BackgroundColor','white');
112 end
113 end
114
```

```matlab
115  function edit5_Callback(hObject, eventdata, handles)
116  end
117
118  % —— Executes during object creation, after setting all properties.
119  function edit5_CreateFcn(hObject, eventdata, handles)
120
121  if ispc && isequal(get(hObject,'BackgroundColor'),
122      get(0,'defaultUicontrolBackgroundColor'))
123      set(hObject,'BackgroundColor','white');
124  end
125  end
126
127  % —— Executes on button press in pushbutton2.
128  function pushbutton2_Callback(hObject, eventdata, handles)
129
130  FileDirectory = uigetdir('C:\Documents and Settings\');
131  set(handles.edit6,'String',FileDirectory);
132  dirlist = dir(fullfile(FileDirectory,'*.tif'));
133  [filenames,dummyvar] = sortrows({dirlist.name}');
134  set(handles.listbox1,'String',filenames);
135  handles.FileDirectory = FileDirectory;
136  guidata(hObject,handles)
137  end
138
139  % —— Executes on selection change in listbox1.
140  function listbox1_Callback(hObject, eventdata, handles)
141
142  handles.SelectedFiles = get(hObject,'Value');
143  guidata(hObject,handles);
144  end
145
146  % —— Executes during object creation, after setting all properties.
147  function listbox1_CreateFcn(hObject, eventdata, handles)
148
149  if ispc && isequal(get(hObject,'BackgroundColor'),
150      get(0,'defaultUicontrolBackgroundColor'))
```

```matlab
151        set(hObject,'BackgroundColor','white');
152    end
153    end
154
155    function edit6_Callback(hObject, eventdata, handles)
156    end
157
158    % ─── Executes during object creation, after setting all properties.
159    function edit6_CreateFcn(hObject, eventdata, handles)
160    if ispc && isequal(get(hObject,'BackgroundColor'),
161        get(0,'defaultUicontrolBackgroundColor'))
162        set(hObject,'BackgroundColor','white');
163    end
164    end
165
166    % ─── Executes on button press in pushbutton3.
167    function pushbutton3_Callback(hObject, eventdata, handles)
168
169    FileNames = get(handles.listbox1,'String');
170    handles.SelectedFilenames = FileNames(handles.SelectedFiles);
171    set(handles.listbox1,'String',handles.SelectedFilenames);
172    set(handles.listbox1,'Value',1:length(handles.SelectedFiles));
173    guidata(hObject,handles);
174    end
175
176    function edit7_Callback(hObject, eventdata, handles)
177    end
178
179    % ─── Executes during object creation, after setting all properties.
180    function edit7_CreateFcn(hObject, eventdata, handles)
181    if ispc && isequal(get(hObject,'BackgroundColor'),
182        get(0,'defaultUicontrolBackgroundColor'))
183        set(hObject,'BackgroundColor','white');
184    end
185    end
186
```

```matlab
187  %%%%%%%%%%%%%%%%%%%%%%%%%%%%%%%%%%%%%%%%%%%%%%%%%%%%%%%%%%%%%%%%%%%%%%%%%%
188  function analysisok = mwcometanalyzer(handles)
189  % Function mwcometanalyzer This function analyzes images of ...
        microwell comets that are in a grid.
190  %
191  % David K. Wood and Drew Regitsky Modified 2/19/09
192  %
193  % Inputs:
194  %
195  % FileDirectory []  — tells the program where to look for comet ...
        images. If no directory is set, the program will allow the ...
        user to browse for the appropriate folder.
196  % convfac [0.64]    — sets the pixel to distance conversion ...
        factor for the imaging microscope and is used to calculate ...
        comet parameters. Units are microns/pixel. Default is for a ...
        10X objective.
197  % objective [10]    — sets the magnification of imaging for ...
        writing to output file.
198  % hdthresh [0.15]   — sets the threshold used to detect the ...
        beginning of a comet in the analysis routine.
199  % tailthresh [0.02] — sets the threshold used to detect the end ...
        of a comet in the analysis routine
200  % headdia [40]      — approximate size of microwells. Units are ...
        pixels.
201
202  %% Assign parameters from handles structure
203
204  tempvar = get(handles.edit2,'String');
205  hdthresh = str2double(tempvar);
206
207  tempvar = get(handles.edit3,'String');
208  tailthresh = str2double(tempvar);
209
210  tempvar = get(handles.edit4,'String');
211  convfac = str2double(tempvar);
212
```

```matlab
213  tempvar = get(handles.edit5,'String');
214  objective = str2double(tempvar);
215
216  tempvar = get(handles.edit7,'String');
217  headdia = str2double(tempvar);
218
219  tempvar = get(handles.edit9,'String');
220  imagerot = str2double(tempvar);
221
222  tempvar = get(handles.edit10,'String');
223  scale_intensity = str2double(tempvar);
224
225  tempvar = get(handles.edit12,'String');
226  PIXEL_SPACING = round(str2double(tempvar)/convfac);
227  %Spacing between comets in array
228
229  tempvar = get(handles.edit11,'String');
230  CROPOFFSET = round(str2double(tempvar)/convfac);
231  %X-offset for cropped comet picture to include tail (positive = ...
         to the left)
232
233  tempvar = get(handles.edit13,'String');
234  MINCOMETAREA = round(str2double(tempvar)/convfac^2);
235  %Minimum number of pixels in object for it to be a comet
236
237  tempvar = get(handles.edit14,'String');
238  NearestNeighbors = str2double(tempvar);
239
240
241  FileDirectory = handles.FileDirectory;
242  filenames = handles.SelectedFilenames;
243
244
245  %% Select files for analysis
246
247      if isempty(FileDirectory) % if no directory is specified open gui
```

192

```matlab
248        FileDirectory = uigetdir;
249     end
250
251     NumFiles = length(filenames); % total number of selected files
252
253     %% Analysis Loop
254
255     h = waitbar(0,'Analyzing File 0 of 0 (0%)'); % initialize waitbar
256     % Begin looping through files
257     for fileID = 1:NumFiles
258
259         % Set Parameters for finding comets in images
260         CROPWIDTH = round(PIXEL_SPACING*0.9);
261         %Width of cropped comet picture to output
262         CROPHEIGHT = round(CROPWIDTH/2);
263         %Height of cropped comet picture to output
264
265         %Set default values for comet analysis parameters
266         if isempty(convfac)
267             convfac = 0.64; % 0.64 microns/pixel for 10X objective
268         end
269         if isempty(objective)
270             objective = 10; % 10X objective
271         end
272         if isempty(hdthresh)
273             hdthresh = 0.15; % 15% of peak intensity
274         end
275         if isempty(tailthresh)
276             tailthresh = 0.02; % 2% of peak intensity
277         end
278         if isempty(headdia)
279             headdia=40; % 40 pixels
280         end
281
282         % File housekeeping
283         filename = fullfile(FileDirectory,filenames{fileID});
```

```matlab
284            % assign placeholder variable
285            display(filename); % Show user what file is being analyzed
286            fileinfo = imfinfo(filename);
287            Nimages = length(fileinfo); % how many frames in tif
288            clear fileinfo % clear unused variable
289
290    %Open file for comet data and write initial info to it
291    fid0 = fopen([filename(1:length(filename)-4),'.txt'],'wt');
292    fprintf(fid0,'%s \n',['Size Calibration: ',num2str(convfac),' ...
           micron/Px']);
293    fprintf(fid0,'%s \n',['Objective: ',num2str(objective),'X']);
294    fprintf(fid0,'\n');
295    fprintf(fid0,'%s \t %s \t %s \t %s \t %s\n',...
296                '%Head DNA','%Tail DNA','OTM (um)','Tail Len. (um)',...
297                'Comet Len. (um)');
298
299            % Initialize number of comets in file
300            cometsInFile = 0;
301
302            % Update wait bar to include number of frames in file
303            waitbar(0,h,['Analyzing File 'num2str(fileID)
304                        ' of 'num2str(NumFiles) ' (0%)']);
305            % Begin looping through image frames in tif
306            for nimage = 1:Nimages
307                % Update waitbar at each frame
308                waitbar(nimage/Nimages,h,['Analyzing File ...
                    ',num2str(fileID),
309                            ' of ',num2str(NumFiles),...
310                    ' (',num2str(round(nimage/Nimages*100)),'%)']);
311                % Read in image from file
312                cometimage = imread(filename,nimage)/scale_intensity;
313                cometimage = imrotate(cometimage,imagerot); %rotate image
314                % Find comet in images using findcomets function
315                [temp_objs,NumComets] = ...
                        findcomets(cometimage,MINCOMETAREA,
316                                    PIXEL_SPACING,NearestNeighbors);
```

194

```matlab
317                                         % Analyze identified comets ...
                                                using runcometanlaysis ...
                                                function and save data to fid0
318             if NumComets == 0
319                 NumAnalyzed = 0;
320             else
321 NumAnalyzed = ...
        runcometanalysis(cometimage,temp_objs,NumComets,CROPWIDTH,...
322         CROPHEIGHT,CROPOFFSET,convfac,hdthresh,tailthresh,headdia,fid0);
323             end
324             clear cometimage % clear comet image
325             cometsInFile = cometsInFile + NumAnalyzed; % update ...
                    num. comets
326         end
327
328         % Housekeeping and cleanup
329         fclose(fid0); % close data file
330         clear fid0 I % clear file I/O and image
331         display(['Total number of ANALYZED comets in images: '
332                     ,num2str(cometsInFile)]);
333     end
334     close(h) % close waitbar
335     analysisok = 'Analysis OK'; % assign dummy output
336 end
337
338 function [ObjectsInfo,NumComets] = findcomets(I,MINCOMETAREA,
339                                     PIXEL_SPACING,NearestNeighbors)
340
341     bwim = im2bw(I,graythresh(I));
342     % Create bw image using otsu thresholding method
343     labmat = bwlabel(bwim); % Create label matrix from bw image
344     labdata = regionprops(labmat);
345     % Get area and location of objects in label matrix
346
347     %% Sort Objects by size
348     ObjectsInfo = zeros(length(labdata),2); % initialize matrix
```

```matlab
349     NumComets = 0; % initialize number of comets
350     % Loope through objects, keeping only objects that are larger ...
            than the
351     % minimum allowed area
352     for nobjects = 1:length(labdata)
353         if labdata(nobjects).Area ≥ MINCOMETAREA && ...
                labdata(nobjects).Centroid(1) > 20 && ...
                labdata(nobjects).Centroid(2) > 20 && ...
                labdata(nobjects).Centroid(2) < size(bwim,1)-20 && ...
                labdata(nobjects).Centroid(1) < size(bwim,2)-20
354             NumComets = NumComets +1;
355             ObjectsInfo(NumComets,:) = labdata(nobjects).Centroid;
356         else
357             ObjectsInfo(end,:) = [];
358         end
359     end
360
361     if NumComets > 1
362     %% Sort objects by nearest neighbor distance
363     % Calculate distances between objects and create square ...
            matrix of distances
364     distances = pdist(ObjectsInfo);
365     ObjDist = squareform(distances);
366     clear distances
367
368     % filter objects based on distance relative to PIXEL_SPACING ...
            parameter
369     uniquekeepers = [];
370     for nmult = 1:NearestNeighbors
371         [keepers{nmult}(:,1),keepers{nmult}(:,2)] =
372     find(ObjDist < nmult*PIXEL_SPACING+25 & ObjDist > ...
            nmult*PIXEL_SPACING-25);
373         uniquekeepers = [uniquekeepers;unique(keepers{nmult})];
374         % only keep unique objects
375     end
376     uniquekeepers = unique(uniquekeepers);
```

```matlab
377     NumComets = length(uniquekeepers);
378     temp_objects = ObjectsInfo(uniquekeepers,:);
379     clear ObjectsInfo
380     ObjectsInfo = round(temp_objects); % round to intgr values ...
            for indexing
381     else
382         NumComets = 0;
383         ObjectsInfo = [];
384     end

385

386 end

387

388 function NumAnalyzed = runcometanalysis(OrigCometImage,
389         ObjectsInfo,NumComets,CROPWIDTH,CROPHEIGHT,
390         CROPOFFSET,convfac,hdthresh,tailthresh,headdia,fid0)

391

392     cometdata = -ones(NumComets,5);
393     XCENT = 1;
394     YCENT = 2;
395     NumAnalyzed = 0;
396       for numcomet = 1:NumComets
397       cropRect = ...
              [ObjectsInfo(numcomet,XCENT)-CROPWIDTH/2+CROPOFFSET,...
398       ObjectsInfo(numcomet,YCENT)-CROPHEIGHT/2,CROPWIDTH,CROPHEIGHT];
399       CropCometImage = imcrop(OrigCometImage,cropRect);
400             if ...
                  size(CropCometImage,1)*size(CropCometImage,2) ...
                  ==
401               (CROPWIDTH+1)*(CROPHEIGHT+1)
402 [cometdata(numcomet,1),cometdata(numcomet,2),cometdata(numcomet,3),
403 cometdata(numcomet,4),cometdata(numcomet,5)]=
404 analyzecomet(CropCometImage,convfac,hdthresh,tailthresh,headdia);
405             end
406         if cometdata(numcomet,4) > 0
407       fprintf(fid0,'%7.4f \t %7.4f \t %7.4f \t %7.4f \t %7.4f \n',
408               cometdata(numcomet,:));
```

```matlab
409                     NumAnalyzed = NumAnalyzed+1;
410                 end
411                 clear CropCometImage
412             end
413 end
414
415 function [headdna,taildna,otm,taillength,cometlength] =
416 analyzecomet(cometim,convfactor,hdthresh,tailthresh,headdiameter)
417
418 % Funtion analyzecomet is used to calculate various comet ...
        parameters from
419 % an image of a comet.
420 %
421 % David K. Wood May 2008
422 %
423 % inputs: cometim - image of comet convfactor - pixel to distance ...
        conversion for objective/camera combination used for imaging ...
        (pixels/micron)
424 % hdthresh - % of peak intensity where comet begins tailthresh - ...
        % of peak intensity where comet ends headdiameter - diameter ...
        of head in pixels
425 %
426 % outpus: headdna - % dna in comet head taildna - % dna in comet ...
        tail otm - olive tail moment in microns taillength - length of ...
        comet tail in microns cometlength - total length of comet in ...
        microns
427
428
429 %% Calculate Background
430 backgndwidth = round(0.1*length(cometim(:,1)));
431 % make background 10% of total image width
432
433 background = sum(cometim(1:backgndwidth,:))/backgndwidth;
434 % background is the total average intensity in each column from ...
        the top 10% of the image
435 cometsum = sum(cometim)/length(cometim(:,1))-background;
```

```matlab
436  % cometsum is the average intensity in each column minus the ...
         background
437  % Reverse polarity of comet image cometsum = cometsum([end:-1:1]);
438
439  %Default comet params to -1: this will indicate that these comets ...
         have not been analyzed and should not be written to data file
440  headdna = -1;
441  taildna = -1;
442  otm = -1;
443  taillength = -1;
444  cometlength = -1;
445
446  %% Define Comet Head and Tail
447  indices = find(cometsum > hdthresh*max(cometsum)); %col. where ...
         comet begins
448
449  if numel(indices) > 0 && indices(1) < 0.5*length(cometsum)
450      % if beginning found, assign location to startx
451
452      startx = indices(1);
453      indices = find(cometsum(startx:end) < tailthresh*max(cometsum));
454      % find column where comet ends
455
456      if numel(indices) > 0 % if end found, assign location to endx
457
458          endx = indices(1)+startx-1;
459
460          clear indices % clear unused variable
461
462          %Find head/tail division
463          temp_htx = startx + headdiameter; % approximate with head ...
                 diameter
464
465          % Search for division by looking for minimum of first ...
                 derivative around approximate head diameter
466          startsearch = round(temp_htx*0.9);
```

199

```
467      endsearch = round(temp_htx*1.1);
468      [trash,headtailx] = ...
              min(diff(cometsum(startsearch:endsearch)));
469      headtailx = startsearch+headtailx; % assign value to ...
            headtailx
470      clear trash temp_htx startsearch endsearch
471
472      if headtailx ≤ endx
473          % if head is not longer than tail, calculate comet ...
                parameters
474
475          %Round indices to nearest integer
476          headtailx=round(headtailx);
477          endx=round(endx);
478          startx=round(startx);
479
480          % tail center—of—mass
481          tailcom = ...
                sum(cometsum(headtailx+1:endx).*(headtailx+1:1:endx))
482                  /sum(cometsum(headtailx+1:endx))*convfactor;
483          % head center—of—mass
484          headcom = ...
                sum(cometsum(startx:headtailx).*(startx:1:headtailx))
485                  /sum(cometsum(startx:headtailx))*convfactor;
486          % percentage dna in comet head
487          headdna = sum(cometsum(startx:headtailx))
488                  /sum(cometsum(startx:endx))*100;
489          % percentage dna in comet tail
490          taildna = sum(cometsum(headtailx:endx))
491                  /sum(cometsum(startx:endx))*100;
492          otm = (tailcom—headcom)*taildna/100; % olive tail ...
                moment (um)
493          taillength = (endx—headtailx)*convfactor; % tail ...
                length (um)
494          cometlength = (endx—startx)*convfactor; %comet length ...
                (um)
```

```matlab
495
496                  %% This code is for debugging
497       %{
498       figure subplot(2,1,1) imshow(cometim) line([startx startx],[1
499       length(cometim(:,1))],'Color','w') line([headtailx headtailx],[1
500       length(cometim(:,1))],'Color','r') line([endx endx],[1
501       length(cometim(:,1))],'Color','b') subplot(2,1,2)
502       plot((cometsum)/max(cometsum))
503       %}
504             end
505         end
506   end
507   end
508
509   function edit14_Callback(hObject, eventdata, handles)
510   end
511
512   % ── Executes during object creation, after setting all properties.
513   function edit14_CreateFcn(hObject, eventdata, handles)
514   if ispc && isequal(get(hObject,'BackgroundColor'),
515       get(0,'defaultUicontrolBackgroundColor'))
516       set(hObject,'BackgroundColor','white');
517   end
518   end
519
520   function edit9_Callback(hObject, eventdata, handles)
521   end
522
523   % ── Executes during object creation, after setting all properties.
524   function edit9_CreateFcn(hObject, eventdata, handles)
525
526   if ispc && isequal(get(hObject,'BackgroundColor'),
527       get(0,'defaultUicontrolBackgroundColor'))
528       set(hObject,'BackgroundColor','white');
529   end
530   end
```

```matlab
function edit11_Callback(hObject, eventdata, handles)
end


% —— Executes during object creation, after setting all properties.
function edit11_CreateFcn(hObject, eventdata, handles)

if ispc && isequal(get(hObject,'BackgroundColor'),
    get(0,'defaultUicontrolBackgroundColor'))
    set(hObject,'BackgroundColor','white');
end
end


% —— Executes during object creation, after setting all properties.
function edit10_CreateFcn(hObject, eventdata, handles)
if ispc && isequal(get(hObject,'BackgroundColor'),
    get(0,'defaultUicontrolBackgroundColor'))
    set(hObject,'BackgroundColor','white');
end
end


function edit12_Callback(hObject, eventdata, handles)
end


% —— Executes during object creation, after setting all properties.
function edit12_CreateFcn(hObject, eventdata, handles)

if ispc && isequal(get(hObject,'BackgroundColor'),
    get(0,'defaultUicontrolBackgroundColor'))
    set(hObject,'BackgroundColor','white');
end
end


function edit13_Callback(hObject, eventdata, handles)
end
```

```matlab
567  % —— Executes during object creation, after setting all properties.
568  function edit13_CreateFcn(hObject, eventdata, handles)
569
570  if ispc && isequal(get(hObject,'BackgroundColor'),
571      get(0,'defaultUicontrolBackgroundColor'))
572      set(hObject,'BackgroundColor','white');
573  end
574  end
```